UNIVERSITEIT VAN PRETORIA
UNIVERSITY OF PRETORIA
YUNIBESITHI YA PRETORIA

Study of the early stages of carbonisation of some pitch materials of different composition

By

Segaula Isaac Manabile

Submitted in partial fulfilment of the requirements for the degree of

Master of Science

In the Department of Chemistry
Faculty of Natural and Agricultural Sciences
University of Pretoria
Pretoria

July, 2009

DECLARATION

I, **Segaula Isaac Manabile,** declare that the dissertation that I hereby submit for the degree in Chemistry at the University of Pretoria has not previously been submitted by me for degree purposes at any other University.

SIGNED ON THIS ------- DAY OF JULY 2009

---------- ----------

Segaula I. Manabile (Author) **Prof. Brian Rand (Supervisor)**

SYNOPSIS

The formation and development of mesophase from different pitches under carbonisation conditions was investigated. Members of the pyrolysis series were prepared from four pitches. A temperature range between 380 and 500 °C was used to follow mesophase development for each pitch. As-received pitches and their green cokes were characterised by thermomechanical analysis (glass transition temperature and softening point temperature), elemental analysis, Fourier transform infrared spectroscopy, thermogravimetry or differential thermogravimetry, and optical microscopy (mesophase content). Additional data about the evolution of different volatile products and about possible chemical reactions occurring during thermal decomposition were obtained from thermogravimetric mass spectrometric analysis. The effect of heating rate on the behaviour and carbon yield was also studied.

The results showed that the two anthracene oil pitches do not develop mesophase, whereas the medium-temperature and high-temperature pitches do. However, their textures are completely different. The medium-temperature pitch shows an improvement in texture from the mosaic to the coarse domain at 500 °C, whereas the high-temperature pitch shows flow domains. It was further shown that the process of preparing mesophase, i.e. the heat-treatment process, increases the aromaticity and carbon yield. Thermogravimetric mass spectrometric analysis showed that the dominant reaction for all the pitches is the condensation reaction, which is accompanied by the evolution of H_2 and CO. The heating rate affects the behaviour of the pyrolysing pitches in that a lower heating rate lowers the carbon yield. This study gave insight into the influence of the nature and composition of the precursor on the formation of mesophase.

KEYWORDS: Pitch, mesophase, chemical composition, heat treatment, green coke.

ACKNOWLEDGEMENTS

I express my sincere gratitude to my supervisors, Professors Brian Rand and Walter Focke, for providing me with the opportunity to work with them and for their invaluable guidance and encouragement, which made this work possible. I believe it is a rare privilege to be able to pursue research under the guidance of such academics. Special thanks go to Department of Science and Technology (DST) and the University of Pretoria for their financial support which enabled me to complete this work. Lastly, I would like to thank Luxolo Holo for preparing the Anthracene Oil Pitches.

Ke leboga lerato le thekgo ya baithuti le bašomi ka moka ba Institute of Applied Materials.

La mafelelo, Ke leboga tlhotlholetšo le thekgo ya batswadi (Lesetja le Setlhodi Manabile) le bana bešo kamoka. Ke re go lena Bakone: Modimo a le šegofatše ka moka ga lena.

CONTENTS

LIST OF FIGURES

LIST OF TABLES

LIST OF ABBREVIATIONS

amu	Atomic mass units
AO	Anthracene oil
AOP	Anthracene oil pitch
AR	As-received material
ATR	Attenuated total reflectance
CY	Carbon yield
DRIFT	Diffuse reflectance infrared Fourier transform
DSC	Differential scanning calorimetry
DTA	Differential thermal analysis
DTG	Differential thermogravimetry
EA	Elemental analysis
EGA	Evolved gas analysis
FT-IR	Fourier transform infrared spectroscopy
GC	Gas chromatography
H_{al}	Aliphatic hydrogen
H_{ar}	Aromatic hydrogen
HTT	Heat-treatment temperature
IR	Infrared spectroscopy
K	Kelvin
IRE	Internal reflection element
IRS	Internal reflection spectroscopy
LC	Liquid crystal
LMO	Local molecular orientation
MIR	Multiple internal reflectance
MS	Mass spectroscopy
MP	Mittal pitch
NMR	Nuclear magnetic resonance
OM	Optical microscopy
QI	Quinoline insolubles
PAH	Polyaromatic hydrocarbons
PNA	Polynuclear aromatic

SP	Sasol pitch
TI	Toluene insoluble
TA	Thermal analysis
T_{endset}	Mass loss endset temperature
Tg	Glass transition temperature
TGA	Thermogravimetric analysis
TG/MS	Thermogravimetric mass spectrometric analysis
T_{onset}	Mass loss onset temperature
T_m	Temperature of formation of mesophase
Ts	Softening point temperature
TMA	Thermomechanical analysis
T_{max}	Temperature of maximum rate of mass loss
°C	Degree Celsius
µm	Micrometre
nA	Nano amperes
Å	Ångström

CHAPTER 1: INTRODUCTION

Pitches are a valuable source of aromatic compounds and carbonaceous materials. They are used because they can be transformed into a graphitisable carbon, when heat treated to sufficiently high temperatures in an inert atmosphere. The main field of their use is industrial electrode production, but preparation of carbon fibres, graphite and composites is also possible.

The process of converting a pitch material to graphite and other high-performance carbons involves an intermediate phase called *mesophase*. It is a unique liquid-crystal, obtained by controlling the pyrolysis of coal and petroleum pitches (carbonaceous precursors) at an early stage of carbonisation. Mesophase is an excellent precursor of carbon materials with advanced properties. It is an anisotropic phase and initially has a spherical morphology. Depending on the experimental conditions, the spheres grow and coalescence to form bulk-mesophase.

In the formation of this liquid crystal phase, large aromatic disc-like (discotic) molecules align with each other in an approximately parallel order ('nematic order') to form a discotic nematic liquid crystal. Large molecules are formed due to thermal decomposition and condensation reactions, which occur concurrently with the removal of volatiles. The mesophase defines the degree of preorder and further graphitisation of the residue. However, its formation is a difficult process to control. Both the nature of the pitch (chemical composition) and the process conditions affect the generation and properties of the mesophase. The thermal reactivity of the molecules present in the pitch structure (aromatic condensation, fragmentation reactions with volatile matter release, etc.) constitutes the chemical backstage of mesophase formation.

Several factors influence the formation and final characteristics of the mesophase, for instance: temperature used, time of treatment and pressure, use of solvents and subsequent thermal treatment. This study concentrates on the impact of temperature on the early stages of carbonisation, i.e. on mesophase development in pitches of different compositions.

1.1 Aims and Objectives of the Study

Pitch is the basis of both the filler and binder phases in polygranular materials, such as electrodes, nuclear graphite and mechanical carbons. It must form mesophase spherules to acquire the special properties desirable for material of high value. Although the literature indicates that mesophase has been prepared from various pitches, the mesophase of the pitches used in this study were not known.

The aim of this research was to compare the influence of mesophase development, growth, coalescence and solidification on controlling the texture of the resultant cokes in pitch materials of different compositions. The study also sought to evaluate the dependence of the cokes on the chemical composition of the starting materials and how this chemical composition changes during thermal processing.

The procedure involved the preparation of a pyrolysis series by heat treating the pitches to different final temperatures in an inert atmosphere. The behaviour of the pitches on pyrolysis was monitored by thermogravimetric analysis (TG) and optical microscopy (OM). Fourier transform infrared spectroscopy (FT-IR) would give information about the kinds of functional group present and how they changed during heat treatment. Further information on the composition of the pitches would be provided by elemental analysis. From a combination of thermogravimetric analysis and mass spectrometry it would be possible to deduce the reaction mechanism that might be involved during the transition of pitch to the mesophase. The glass transition temperature and softening point were determined by thermomechanical analysis (TMA).

CHAPTER 2: LITERATURE SURVEY

2.1 Pitch

Pitch is a residue from the pyrolysis of organic material or tar distillation. It is solid at room temperature. Chemically, it consists of a complex mixture of numerous aromatic hydrocarbons and heterocyclic compounds. It exhibits a broad softening range instead of a defined melting temperature. When cooled from the melt, pitches solidify without crystallisation (Fitzer *et al.*, 1995). Another suitable technical description of pitch is that it is a complex mixture of hundreds or thousands of predominantly aromatic organic compounds with an average molecular mass of several hundreds (Singer, 1985). Pitches and mesophase-like polymers are thermoplastic systems (having a glass transition temperature and a softening point temperature) and are generally glass-like at room temperature (Mochida *et al.,* 2000). During processing, binder pitch should be highly thermoplastic to form a homogeneous mixture with the filler (Metzinger & Hüttinger, 1997).

The main source of pitch is coal tar and petroleum. Synthetic pitches are also available and they also exhibit essentially the same degree of diversity in molecular mass and structure as the coal tar and petroleum pitches (Singer, 1985). Coal tar and petroleum pitches are residues from coal tar and crude oil distillation respectively. They are useful and valuable materials in the manufacture of carbon artifacts and synthetic graphite. The key feature that makes pitches attractive and practical to the carbon industry is their polyaromatic nature. They have a wide range of molecular distributions, with the average range being between 180 and 600 amu. Pitch constituents are basically classified into four groups: saturates, naphthene aromatics, polar aromatics and asphaltenes. The saturates are aliphatic compounds of low molecular mass. The naphthene aromatics are aromatics with low molecular mass. The polar aromatics have a higher molecular mass and more heterocyclic rings. The asphaltene fraction has the highest average molecular mass (Bartle & Özel, 2002). However, the coal tar pitch produced by vacuum distillation of tar contains dispersed carbonaceous particles, which are formed mainly by cracking of the volatiles in the upper part of the coke oven (Machnikoski *et al.* 2002a; Romovacek *et al.,* 1983). The higher the extent of cracking, the higher the concentration of pyrolytic particles (Romovacek *et al.*, 1983). They are in the form of chains and clusters that are uniformly dispersed within the pitch matrix. Impurities such as coal and coke dust are

also present in contaminated tars. Their concentration in pitches is determined by dissolving the pitch in quinoline. The dispersed carbonaceous particles are insoluble in quinoline, hence they are called quinoline insolubles (QI) (Romovacek *et al.*, 1983). The specific composition of a coal tar pitch determines its capability of inducing a thermal reaction resulting in a high yield of solid carbon of suitable morphology and structural ordering (Machnikoski *et al.*, 2002a). The behaviour of pitches differs when their composition in terms of α-resins and β-resins changes. α-resins are the part of the pitch that is insoluble in quinoline. The fraction of the whole pitch that is insoluble in toluene is known as β-resins. The part of the pitch that is soluble in quinoline and also soluble in toluene is known as the γ-resins (De Castro, 2006). The β-resins are a fraction of great interest because they enhance the binding capability and improve the carbon yield of the pitch (Pérez *et al.,* 2002).

Pitches containing abundant QI particles or α-resins produce numerous and smaller mesophase spheres than those with no QI. The QI particles locate predominantly around the surfaces of any mesophase spheres present and they inhibit their regular growth and their coalescence (Machnikoski *et al.*, 2002b; de Castro, 2006). The presence of QI material makes the system complicated. On the other hand, Tillmans *et al.,* (1978) found that QI particles in pitch accelerate mesophase formation by nucleating the mesophase.

The QI content of pitch is one factor that determines its suitability for industrial use. QI can also reduce the wettability of the filler by the binder pitch. The binder pitch for the manufacture of carbon artefacts should have QI content within a defined range of about 10-16%wt. There are five main groups of QI: primary, secondary, isotropic, foreign inclusions and material of unusual shape. Isotropic QI are considered to consist of asphaltene-like molecules dispersed in the pitch. They are found in air and acid-treated pitches and increase the coke yield compared with untreated feedstock (Marsh *et al.*, 1985). Primary QI are often described as carbon-black like. They originate from the coke oven by cracking of volatiles in the upper regions of the oven. Secondary QI are spheres of mesophase present only in heat-treated pitches. Foreign particles include the collected dirt and small pieces of coke.

2.2 Characterisation of Pitch

The qualitative and quantitative analysis of pitch provides deeper understanding of pitch structure and behaviour. It is also important in connection with the requirements of environmental legislation and occupational medicine. Pitches can be characterised by using different approaches:

1. *Characterisation by material properties*. These include rheological properties, coking value, ash content, softening point and solubility in organic solvents, etc.
2. *Description of the materials in terms of structural features*. Structural features are average molecular mass, molecular mass distribution, average structural analysis (mostly done by nuclear magnetic resonance and infrared studies), preparative pitch fractionation methods (solvent extraction), preparative size exclusion chromatography, extrography and charge-transfer fractionation (Marsh & Rodríguez-Reinoso, 2000).
3. *Analysis of the materials with regard to the individual compounds.* For example, analysis with regard to benzo[a]pyrene and other carcinogenic hydrocarbons.

All the approaches are complementary and for a complete characterisation all three must be applied. Generally, it is appropriate to understand the material properties of a pitch on the basis of its structural features (Marsh & Rodríguez-Reinoso, 2000).

2.3 Pyrolysis of Pitch: Mesophase Formation

When an isotropic pitch is pyrolysed between 300 and 500 °C in an inert atmosphere, an anisotropic liquid crystalline phase, which is known as 'carbonaceous mesophase' develops (Bartle & Özel, 2002). The first observations of mesophase spheres were made by Brooks & Taylor (1965) who discovered them by heating vitrinite to temperatures between 465 and 490 °C. It was later discovered that the same process occurs on heating bitumen, pitches, some polymers and certain polynuclear aromatic compounds. Mesophase consists of disc-like molecules that lie approximately parallel to each other, which are large enough to self-assemble into a liquid-crystal phase, or mesophase (Marsh *et al.*, 1999). This liquid crystalline system is created by mesogenic molecules (mesogens) with a molecular mass of about 1 000 amu. They are large planar molecules that result from carbonisation reactions (Machnikowski *et al*., 2002a).

Mesophase formation is the key in manufacturing carbon materials with regard to their properties and microstructures (De Castro, 2006). Mesophase can be prepared from a variety of precursors such as petroleum, coal tar residues and polynuclear aromatic compounds (Chang & Lewis, 1998). The first step in mesophase production involves the removal of species with low molecular mass (Bermejo *et al.*, 1995; Bartle & Özel, 2002). This is accompanied by polymerisation, condensation or dealkylation of the more reactive species (De Castro, 2006). Components with low molecular mass play an important role in the pyrolysis process. They can be either removed from or partly retained in the pitch systems, depending on the experimental conditions. A general process for transforming these precursors into mesophase is by heat treatment, coupled with sparging with inert gas to effect chemical polymerisation and the condensation and removal of volatiles respectively (Chang & Lewis, 1998). However, the precursors can be retained in pitch systems by using pressure. If retained in the system, they act as solvents for the system or as hydrogen donors. They therefore modify the pyrolysis process. Therefore the construction of the pyrolysis system controls the chemical composition of the feedstock as it is pyrolysed, i.e. whether or not the volatile material is lost or retained in the system (De Castro, 2006). In some industrial applications the release of volatiles during pyrolysis seems to have a deleterious effect on the mechanical properties of the resulting carbon, green coke or coke. “Green coke is defined as the primary solid carbonisation product from high boiling hydrocarbon fractions obtained at temperatures below 627 °C” (Marsh *et al.*, 1999). The diffusion of the volatile compounds to the atmosphere is a critical step and must occur slowly to avoid disruption and rupture of the carbon network (Pierson, 1993). The influence of light fractions on the chemistry involved in the process and the subsequent coke characteristics are not comprehensively understood.

The chemical and physical properties of pitch systems on pyrolysis are controlled by the reactivity, size and structure of the pitch molecules. They also have an impact on the formation, growth and development of mesophase and subsequently on the structure of the resulting coke (Bermejo *et al.,* 1995). During carbonisation the final size of anisotropic domains, i.e. local molecular orientation (LMO), occurs concurrently with resolidification, further affecting the properties of carbons (Bonnamy, 1999). The morphology established in the carbonaceous mesophase is locked as the pyrolysis reactions result in hardening of the system, thus providing the basic framework for the microstructure of carbonaceous materials (Zimmer & White, 1982).

The green-coke properties are also affected by the physico-chemical behaviour of coking; this includes flow movements or turbulence within the liquid carbonisation system, which are caused by thermal flow and gas evolution from the system (Martínez-Escandell *et al.*, 1999).

The property changes of pitches during pyrolysis have been described by Whitehouse & Rand (1982) using the transformation diagram shown in Figure 2.1 below.

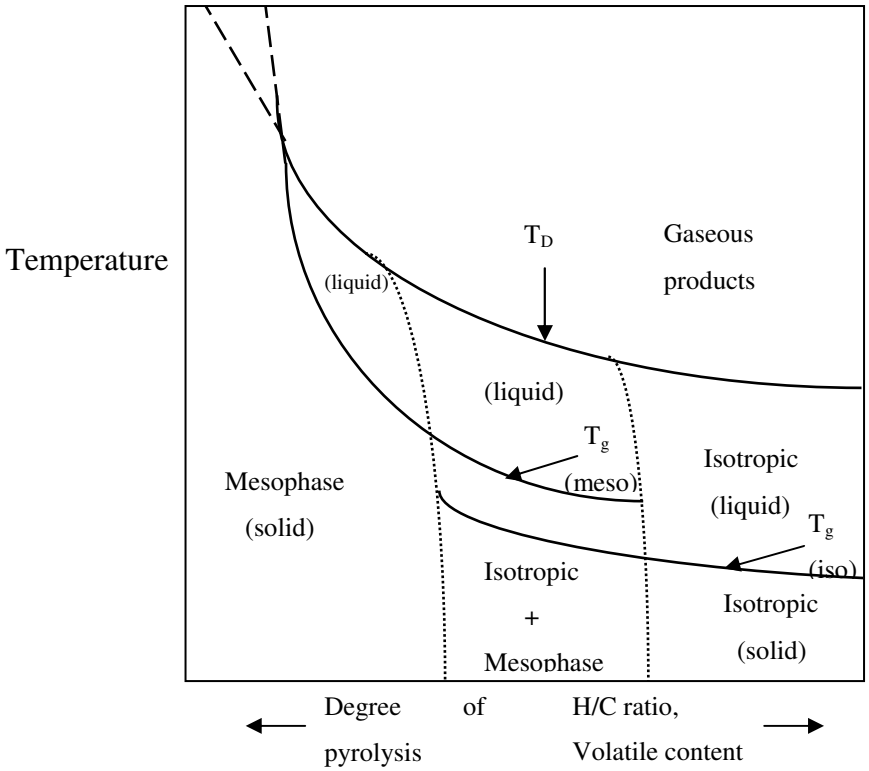

Figure 2.1: Transformation diagram for the pitch–mesophase-carbon transformation (Whitehouse & Rand, 1982)

The degree of pyrolysis and the C/H ratio or volatile content was used to measure the extent of transformation towards carbon. As pyrolysis proceeds, the volatile content decreases and the values of the respective glass transition temperatures increase. In this way the changes in the structure and properties of the pyrolysing residue can be related to the extent of volatilisation. A measure of thermal stability is related to parameters that reflect the composition and temperature dependence of the physical properties of the precursor.

Mesophase in the pyrolysing system is established only if:

1. the intermolecular reactivity or the constituent molecules in the system grow to a limited extent; the molecular growth of polynuclear aromatic (PNA) molecules must not exceed 900 amu on average, or
2. the system remains fluid to temperatures between 400 and 500 °C. This allows the PNA to have sufficient mobility to establish the liquid crystal (Marsh, 1988).

There are a few examples of carbonising systems that pass through the fluid phase without giving mesophase. One example is the pyrolysis of sucrose (Marsh *et al.,* 1999). During the pyrolysis of sucrose, depolymerisation reactions occur. Recombination reactions from within the fluid phase occur subsequently during the process. The temperatures necessary for self-assembly of mesogens is never reached. This is because such molecular systems are too reactive and do not follow the mechanism for the establishment of an ordered structure.

2.3.1 Mesogens: shape and size

The mesogen is the fundamental unit of a liquid crystal that induces structural order in the crystals (wikipedia.org/wiki/Mesogen). They are formed by covalent bonds and non-covalent bonds such as hydrogen bonds, ionic interaction and metal co-ordination.

Pitch contains a mixture of different mesogens. The clusters of mesogen molecules form micro-domains (Mochida *et al.*, 2000). These mesogens occur in a discotic or rodic (linear) shape. Mesogens with a discotic shape are the most efficient ones for self-assembly. However, the discotic shape occurs alongside the rodic shape during the process of condensation reactions. Due to this, a variety of shapes of mesogens of about the same molecular mass is possible. The number is over 1 000 species. Some mesogens are more aliphatic than aromatic, making it difficult to relate the molecular size distribution to mesophase development and to elucidate how they change during pyrolysis.

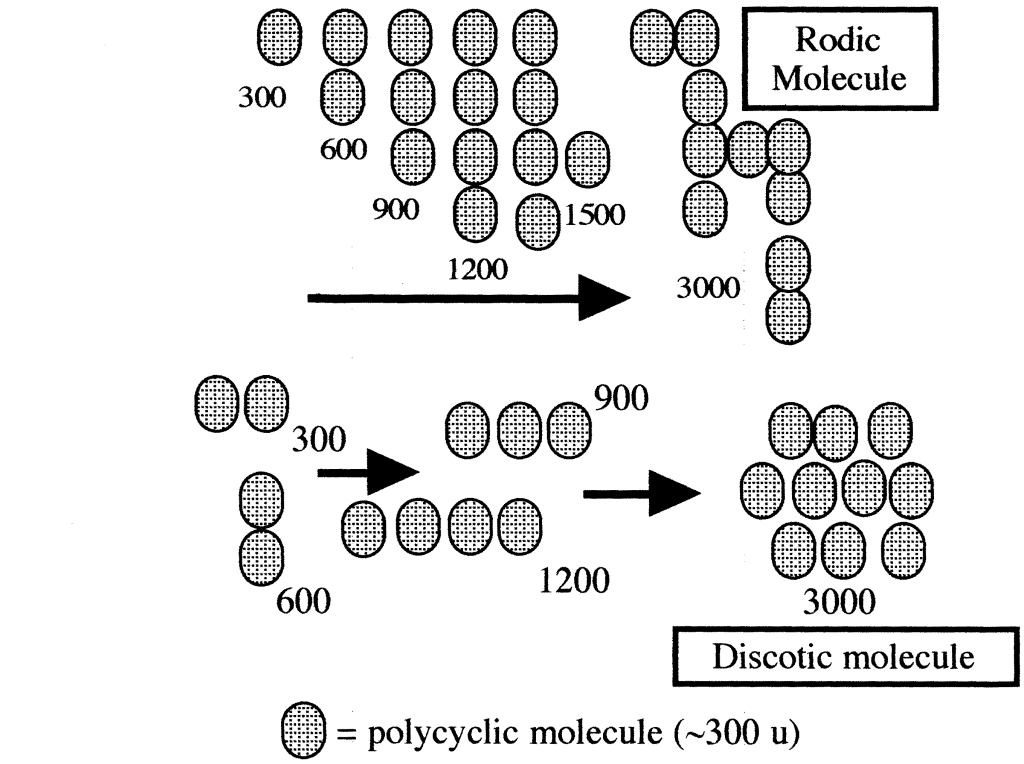

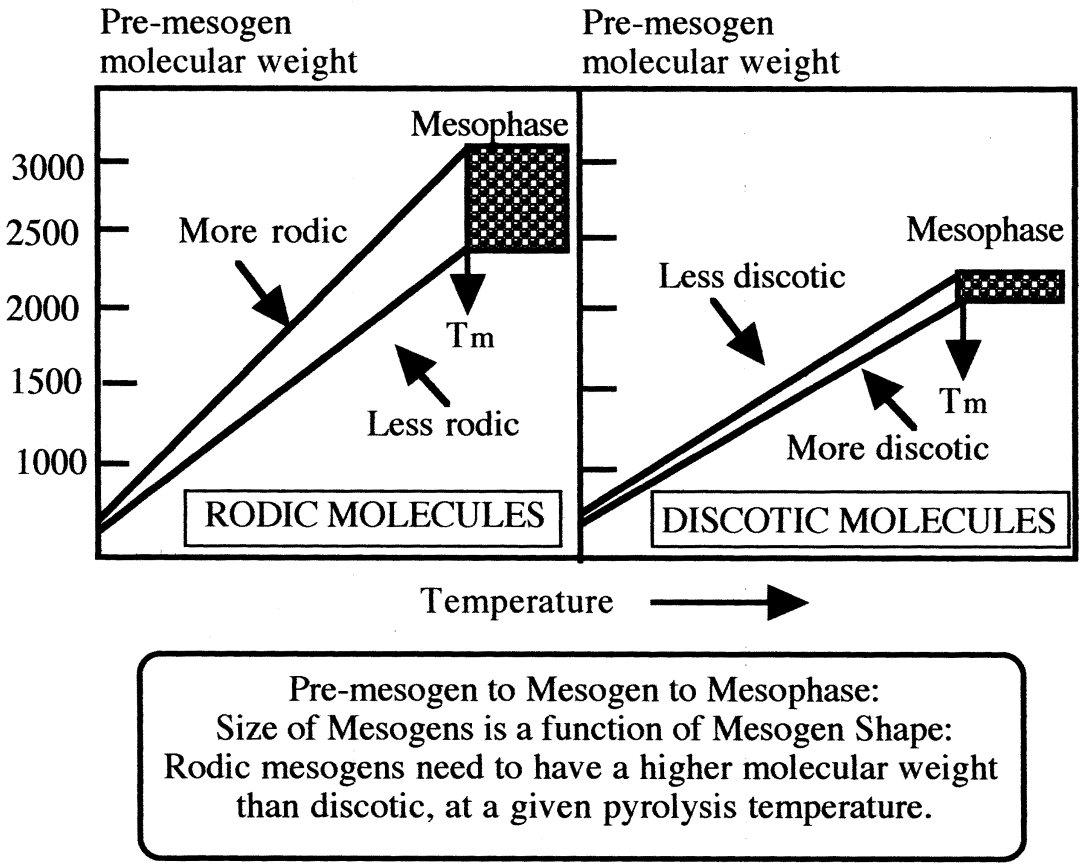

Figure 2.2: **Relationships between rodic and discotic shapes of mesogens in terms of temperature of formation of mesophase (Marsh *et al.*, 1999)**

Figure 2.2 shows how the rodic and discotic shapes of mesogens form. It also illustrates how the shape (rodic or discotic) influences the temperature of mesophase formation (T_m). It appears that the rodic molecules are more likely to form mesophase than the discotic molecules. It can be seen that molecules of rodic shape are more likely to need higher molecular mass than molecules of discotic shape.

2.3.2 Structure of mesophase pitch

Chemical analysis of mesophase spheres was performed by Mochida *et al.* (1977). The spheres were extracted as a quinoline-insoluble fraction from the carbonised pitch. The fraction was hydrogenated or alkylated to be soluble in organic solvents for the structural analyses.

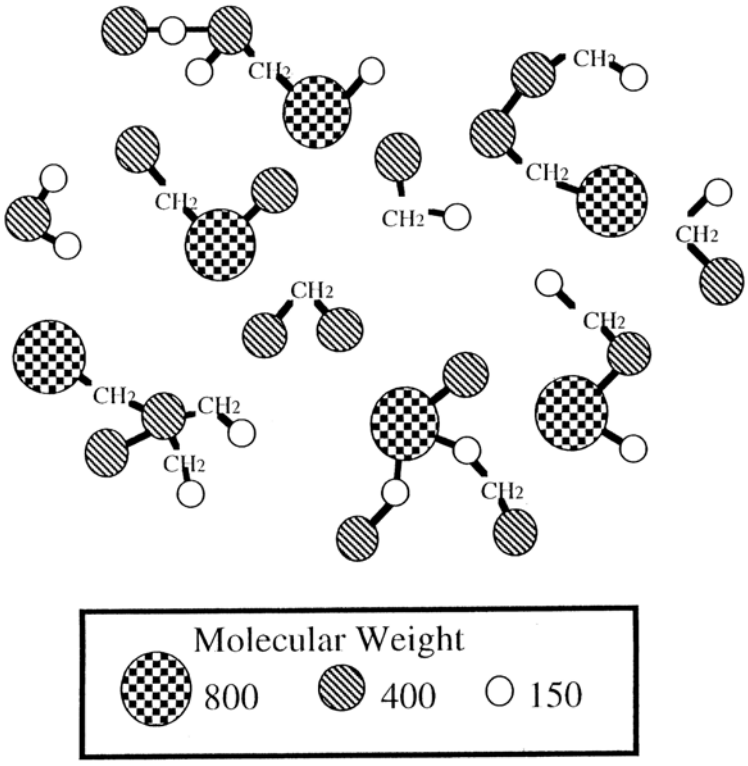

Figure 2.3: Spider Wedge model of mesophase constituent molecules (Mochida *et al.*, 1977)

Figure 2.3 shows the proposed structure, which was called a Spider Wedge model. The authors found that the aromatic units of 0.6 to 1.5 nm in diameter are linked by phenyl–phenyl or methylene bridges to give a molecular mass in the range of 400 to 4 000 amu.

The aromatic planes carry some alkyl and naphthenic groups that are favourable for solubility and fusibility.

A wide molecular mass distribution of the mesophase constituents is important to show the liquid crystal nature. Both ordered stacking of smaller molecules through π–π interaction among larger molecules and the fusibility of the whole mesophase pitch must be satisfied. Therefore an averaged structure of the component molecules is often proposed because of the complexity. However, it is rather useless as there is a broad distribution (Mochida *et al.,* 1977, 2000).

Another model for molecules in the mesophase spheres, which were produced at an early stage of carbonisation, is illustrated by Zimmer & White (1982) (Figure 2.4).

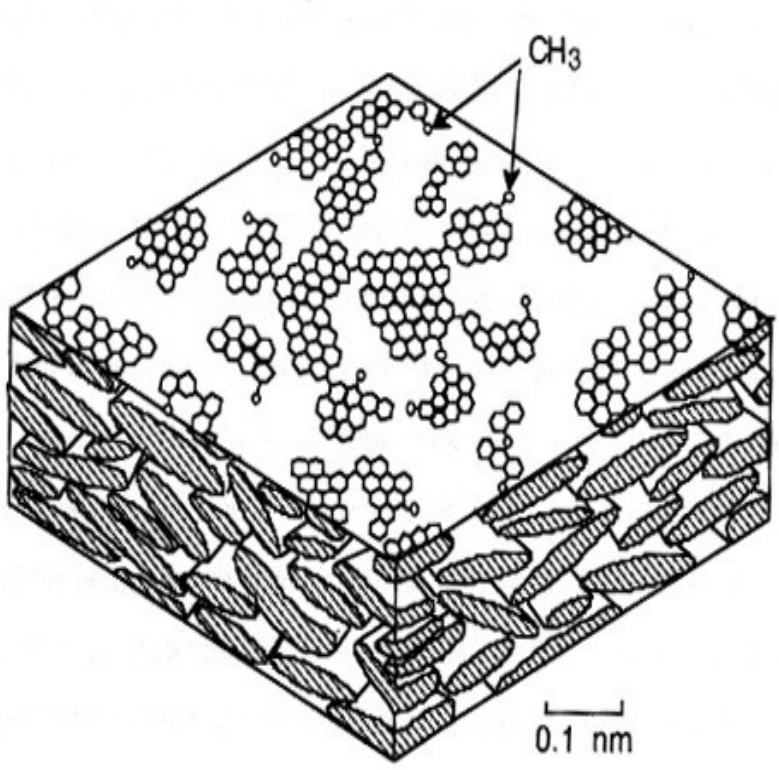

Figure 2.4: Schematic model of carbonaceous mesophase, a discotic nematic liquid crystal (Zimmer & White, 1982)

These authors showed that: (a) mesophase consists of a series of molecules whose molecular mass distribution is from 400 to 10 000 amu; (b) the molecules are oligomeric, have a skeleton of aromatic nuclei that are connected by aryl-aryl and methylene linkages

and the size of the nuclei varies between two and ten rings; and (c) each nucleus carries a restricted number of methyl and naphthenic groups.

Larger molecules are stacked to exhibit discotic anisotropy, whereas smaller molecules may cause thermotropic fluidity, located between the discotic layers. In short, this model shows the stacking, various sizes and possible shapes of the disc-like molecules, which may be quite irregular and contain vacant sites or holes.

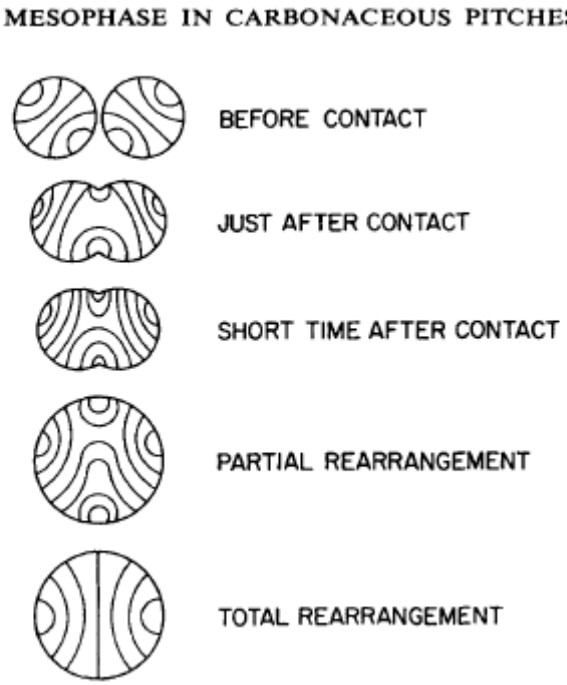

Figure 2.5: Schematic representation of the collision and coalescence of the mesophase spheres (Singer, 1985)

Figure 2.5 shows the process of mesophase formation and development. Mesophase initially appears in a spherical form. The spheres grow and as the viscosity of the system changes, the spheres coalesce – this is called 'bulk-mesophase'.

2.3.3 Viscosity changes during the pyrolysis of pitch

The viscosity of the system controls, to a major extent, the properties of resultant cokes.

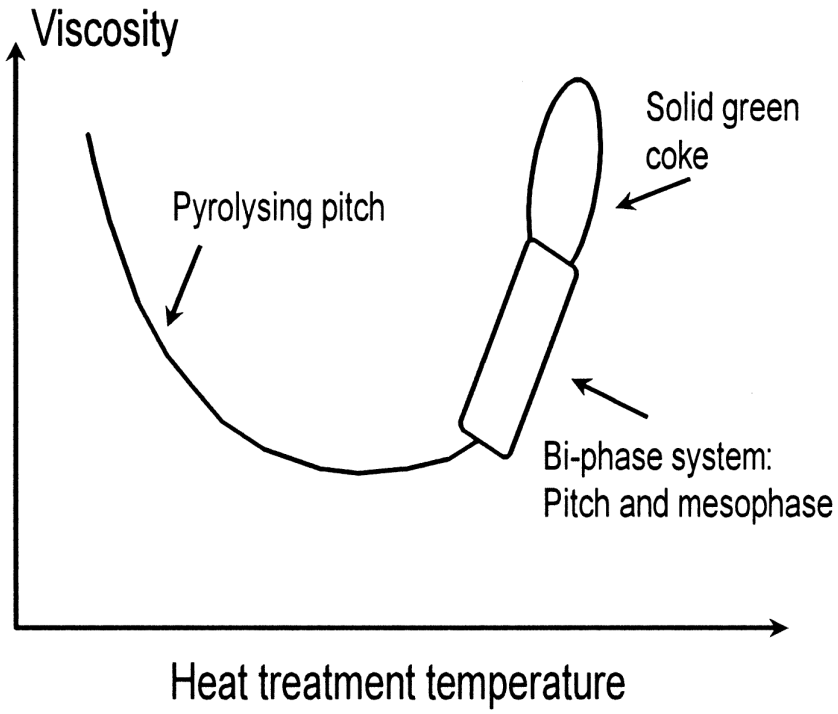

Figure 2.6: **The variation of viscosity with temperature, for pitch pyrolysis systems (Marsh *et al*., 1999)**

Figure 2.6 shows the curve of viscosity vs temperature. Initially, the viscosity decreases with increasing heat-treatment temperature, like all liquids. After reaching a minimum, the viscosity of the system increases until the solid green-coke stage is reached. The increase in viscosity is the result of molecular growth processes of the liquid phase into the green-coke phase.

2.4 Hypothetical Mechanisms of Mesophase Formation

Chang & Lewis (1998) used a simple chemical scheme to present the general nature of mesophase pitch formation. The pitch was considered to be composed of types of molecules designated as A, B, B-S and C:

A – These molecules inhibit mesophase formation because they are low-molecular-mass molecules which do not have the size and the structural requirements to exhibit mesophase.

B – These are aromatic molecules with higher molecular mass aromatic and with the proper size and shape to exhibit mesophase.

B-S – These aromatic molecules can exhibit mesophase but have excessive side chains which interfere with mesophase development.

C – These are very large molecules formed by thermal polymerisation of B-type molecules.

Furthermore, Chang & Lewis (1998) considered that the conversion of the pitch to mesophase occurred in four general reactions:

1. Volatilisation:	$A \rightarrow A\ (vapour)^{\uparrow}$
2. Polymerisation:	(a) $A + A \rightarrow B$
	(b) $A\text{-}S + A\text{-}S \rightarrow B + 2S^{\uparrow}$
3. Side-chain removal	$B\text{-}S \rightarrow B + S^{\uparrow}$
4. Advanced polymerisation	(a) $B + B \rightarrow C$
	(b) $A + B \rightarrow C$

Reaction 1: The volatile fraction represents the portion with the lowest molecular mass, with an average molecular mass of 300 amu.

Reaction 2: Some low-molecular-mass molecules polymerise. The extent of polymerisation is related to the residence time and temperature.

Reaction 3: Side-chains can convert non-mesophase-forming molecules to mesophase-forming molecules without any further polymerisation.

Reaction 4: This makes a minimal contribution to the mesophase-development process since the reacting species are already sufficient to exhibit mesophase.

A more detailed explanation of the mechanism of mesophase formation was given by Marsh *et al.* (1999). They suggested that mesophase formation could involve a series of four reactions.

Three possible consecutive reactions are proposed in Table 2.1 below. The initial mass of 600 amu was an average molecular mass of the molecules in the pitch they used.

Table 2.1: Consecutive reactions detailing the mechanism of mesophase formation

First reaction
600 amu + 600 amu → 1 200 amu
1 200 amu + 600 amu → 1 800 amu
1 800 amu + 1 800 amu → 3 600 amu
3 600 amu → Mesogen
Second reaction
600 amu + 600 amu → 900 amu + 300 amu
900 amu + 600 amu → 1 500 amu
1 500 amu + 600 amu → 2 100 amu
2 100 amu → Mesogen
Third reaction
600 amu + 600 amu → 900 amu + 30 amu
900 amu + 600 amu → 1 500 amu
1 500 amu + 900 amu → 2 400 amu
2 400 amu → Mesogen
Mesogens → Mesophase

The mechanistic scheme for the transition process of pitch to green-coke is as follows (Table 2.2 from Marsh *et al.*, 1999):

Table 2.2: Mechanistic scheme for transition from pitch to coke

$m_a \rightarrow m_a^*$ (free radical)	Reaction A_a
$m_b \rightarrow m_b^*$ (free radical)	Reaction A_b
$m_a^* + m_b^* \rightarrow m_a - m_b^*$ $(=M_p)$	Reaction B
$^1M_p + {}^2M_p \rightarrow M_m$	Reaction C
$M_m \rightarrow$ Mesophase	Reaction D

In this scheme

m_a and m_b are feedstock constituent molecules

m_a* and m_b* are pre-mesogen free radicals

M_p is a pre-mesogen molecule

M_m is a mesogen molecule.

The scheme shows how the transition from pitch to green coke proceeds via radical formation. All reactions (Reactions $A_{a\ \&\ b}$, B, C and D) are irreversible. At a reaction temperature of >400 ^oC, the pitch constituent molecules form radicals. It is not certain whether this occurs by a mono-molecular or bi-molecular process. All of the molecular constituents of the pitch are believed to undergo very similar, but different, types of mono-molecular reaction. Hydrogen and small-molecular-mass hydrocarbons, e.g. CH_4 and C_2H_6, are generated by these reactions – hydrogen by a dehydrogenation process and small-molecular-mass hydrocarbons by a process of dealkylation. Intra-molecular rearrangements and fragmentation are possible. New molecular species are created. A broad range of molecules react to form a broad range of high-molecular-mass molecules (Reaction B). The process continues until the molecules are large enough to be classified as mesogens (Reaction C). At this point the isotropic phase enters the mesophase (Reaction D).

Pierson (1993) used model compounds to deduce the mechanism of pitch carbonisation. Polyaromatic hydrocarbons (PAH) were used because they are contained in pitches as complex mixtures. The mechanism included the following steps:

1. Two PAH molecules disproportionate into one hydroaromatic molecule and one free-radical molecule.
2. The free-radical molecules condense into larger-molecular-mass aromatics.
3. The hydroaromatic molecules cleave to produce liquid and gas-phase species.

On the other hand, Lewis & Kovac (1977) were of the opinion that although aromatic hydrocarbons are important in the mechanism of carbonisation, they are not necessary for the formation of mesophase in pitch. They showed that the melting of a typical aromatic hydrocarbon, containing as many as ten condensed rings, did not involve a liquid crystal transition. They concluded that a condensed ring size of ten is not a sufficient condition

for the formation of mesophase. Molecular size was then believed to be the key prerequisite for obtaining a liquid crystalline state.

2.5 Other Factors Influencing Carbonisation

2.5.1 The influence of additives on carbonisation

The thermal reactions of carbonisation can be changed considerably through the use of certain additives, which enhance the complexity of the pitch system. Machnikoski *et al.* (2002a) found that the polymer thermal degradation product with pitch constituents affects mesophase development. In another study done by Brzozowska *et al.* (1998), a mixture of pitch with 10% of various polymers was prepared. Among the nine polymers they used, poly(vinyl chloride) was the only polymer that showed improved development of anisotropy on carbonisation. Addition of some polymers increased the carbon yield by 5 to 3%, but they gave the green coke a less homogeneous optical texture compared with the parent pitch. This means that segregation of the constituents of the pitch-polymer system can occur to some extent during carbonisation or that the polymers act as agents, promoting the concentration of primary QI to give agglomerations which subsequently carbonise to isotropic material.

Another possibility is the nucleation of mesophase by additives (Marsh & Thrower., 1979). Lim *et al*., (1993) enhanced the mesophase yield by adding anthracene and acenaphthylene as nucleating agents. Upon using nucleating agents they discovered that using 1 wt % increased the mesophase yield, but this decreased at 3 wt % addition.

The addition of iron oxide (Fe_2O_3) was also examined by Wang *et al.* (2001). Fe_2O_3 was found to increase the insoluble fraction yield through the aromatic condensation reactions. It enhanced the reactivity of the molecules in the pitch, thus producing cokes of mosaic texture, whereas the parent pitch without additives produced flow domain texture.

2.5.2 The influence of sulphur on carbonisation

Sulphur in pitch constituent molecules reacts with hydrogen to produce H_2S. Two principal effects are observed on addition of sulphur:

1. Addition of sulphur of less than 5% atom relative to the hydrogen content results in a drastic increase in the coke yield. However, that does not affect the graphisability of the resultant coke significantly.
2. With increasing quantities of sulphur – up to 10% atom – a non-graphitisable isotropic glassy carbon results. Larger quantities of sulphur are believed to form thiobridges. As a result of this, sulphur is retained in a non-fluid carbonising system. These thiobridges occur extensively and randomly to create an isotropic carbon (Marsh & Thrower., 1979).

2.5.3 The influence of oxygen on carbonisation

Mild oxidation of pitch has attracted considerable attention as a potential way of preparing modified isotropic pitches. However, there should be a balance between the oxygen-induced polymerisation and cross-linking reactions as it is crucial for mesophase development during subsequent heat treatment. Oxygen induces molecular cross-linking at low temperatures. It increases both the molecular mass of pitch constituents and the viscosity of the system, resulting in more disordered orientation of the lamellar aromatic molecules, thus limiting the growth and coalescence of mesophase spheres (Menendes *et al*., 1997; Mokoena *et al.,* 2008). The mechanism is thought to involve the formation of new cross-linkages between molecules by hydrogen abstraction to form H_2O and new C-C bonds (Mokoena *et al.,* 2008).

Dumont *et al.* (2005) studied oxidative stabilisation or the addition of oxygen-containing aromatic compounds to pitches. After addition of quinones to pitches, the carbon yield increased.

Carbonisation of an aromatic hydrocarbon in the presence of oxygen was found to lead to the formation of a quinone intermediate (Ruland, 1965). Heat treatment of an aromatic quinone at 3 000 °C leads to carbon with higher interplanar spacing than the corresponding hydrocarbon treated at 3 000 °C. Carbonisation of the quinone results in the degradation of the aromatic ring system through the elimination of carbon dioxide. This degradation leads, in general, to non-planar free radicals which polymerise to give a cross-linked disordered carbon, although in certain cases a rearrangement to give planar aromatic structures was possible (Ruland, 1965).

2.6 Morphology of QI

QI are divided into five types:

Type 1 consists of the primary QI of <1 µm in diameter and these are too small for anisotropy or shape to be monitored by optical microscopy (Marsh, 1985). The SEM micrograph of this type of QI shows that the particles are smooth and spherical. Their diameter ranges from 0.1 to 1.0 µm. The range depends on the QI contents. In pitch with high primary QI, the proportion of smooth spherical particles is much greater (~1.0 µm diameter). In pitch with low primary QI, smooth spherical particles are present in comparable amounts (~1.0 µm diameter). The particles are mainly ~0.1 µm in diameter.

Type 2. They consist of secondary QI or particles of mesophase and are found in heat-treated pitches only. The spheres are 1 to 60 µm in diameter and optically anisotropic. When they come into contact, they coalesce to form large bodies of irregular shape. Coalescence can be prevented if the primary QI come into contact with the growing sphere of mesophase. The primary QI adhere to the surface of the spheres.

Type 3. This consists of the isotropic QI, which are further subdivided into two types. The first type consists of discrete isotropic bodies, irregular or spherical in shape (~20 µm). The isotropic spheres exist either singly or in clusters and chains. The second type is insoluble in quinoline on the basis of its molecular size rather than the existence of discrete particles. These QI are contained in the pitch materials and do not occur as discrete particles.

Type 4. This consists of mainly anisotropic fragments of coke together with the foreign inclusions. These QI also contain irregular, fragmented anisotropic particles with the appearance of pyrolytic carbon and occur in some feedstock pitches.

Type 5. These QI are lemon-shaped mesophase particles. There are some agglomerates between the particles and many particles have deep cracks (Marsh, 1985).

2.7 Different Types of Mesophase Spherule

The first observations of mesophase spherules were made by Brooks & Taylor (1965). Since then two additional mesophase spherules have been reported (Figure 2.7). Mesophase spherules with different optical properties from the Brooks & Taylor ones have also been observed.

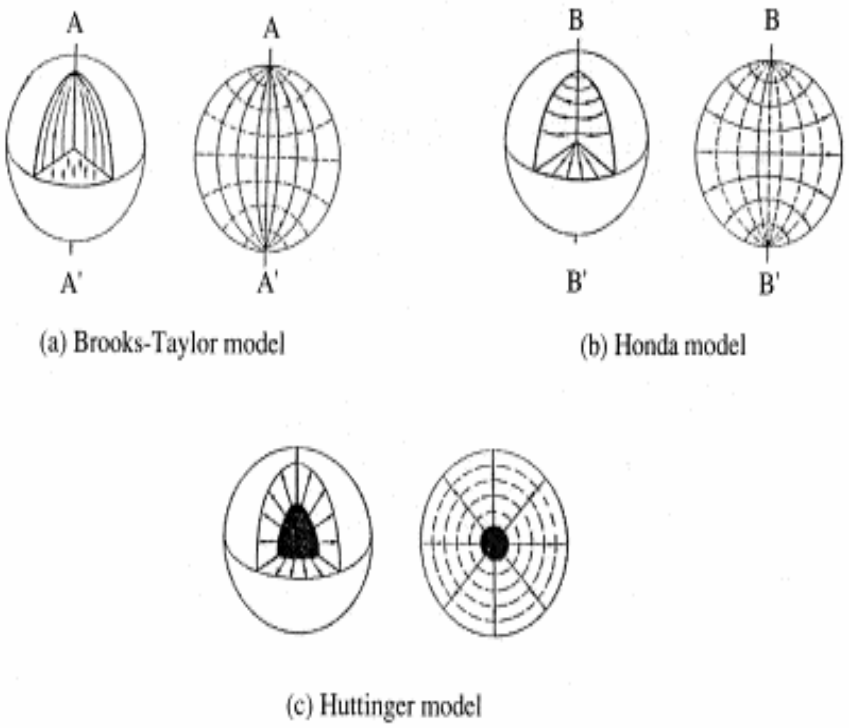

Figure 2.7: Structural model of mesophase spherules; (b) is the second type and (c) is the third type (Imamura *et al.*, 1978)

Below the spheres are the names of the people after whom the models were named.

The structural model for the spherules was proposed to have outer layers lying parallel to the spherule surface. The second type of spherule (b) was found to have a similar layer alignment to the Brooks & Taylor-type spherules around the central region of the spherule. The third type of spherule (c) has all the layers lying in concentric circles about the centre of the spherule. Imamura *et al.,* (1978) proposed the fourth type of spherule from microscopic observation and from its orientational behaviour in a magnetic field. They believed that the fourth type is a metastable phase of the Brooks & Taylor type. Spherules of the fourth type were found in pitch at carbonisation temperatures up 330 °C. They exist together with other mesophase spherules having a petaloid texture.

2.8 Variety of Mesophase Pitches

2.8.1 Homo-oligomeric mesophase pitches

The oligomerisation of aromatic hydrocarbons produces homo-oligomeric mesophase pitches, in which the properties are controlled by the structure of the starting monomer, as well as by the extent of the condensation and dehydrogenation, e.g. oligomerisation of naphthalene using HF–BF_3 (Mochida *et al.,* 2000).

2.8.2 Co-oligomerisation

Co-oligomeric mesophase pitch results from the mixing of aromatic hydrocarbons. This kind of pitch has been prepared from naphthalene and methylnaphthalene at a mixing ratio of 7 (naphthalene) to 3 (methylnaphthalene). The product exhibited different features and fibre properties from those of both the single oligomers (Mochida *et al.,* 2000).

2.8.3 Pitch blends or alloys

Mesophase pitches derived from different aromatic hydrocarbons can be mixed to produce pitch alloys or blends. Once again a blend of methylnaphthalene and naphthalene-derived mesophase pitches showed better properties than the fibre precursor (Mochida *et al.,* 2000).

2.8.4 Mesophase spheres-containing pitch

A pitch that contains both isotropic and anisotropic portions is called a ‘mesophase spheres-containing pitch’. These pitches can also be referred to as isotropic–mesophase pitch alloys (Mochida *et al.,* 2000).

2.9 Structure of Cokes and their Formation

Coke is a solid product of the carbonisation of organic materials, of which at least parts have passed through a liquid crystal stage, and which consist of non-graphitic carbon. “Non-graphitic carbons are all varieties of substances consisting mainly of the element carbon with two-dimensional long-range order of the carbon atoms in planar hexagonal networks but without any measurable crystallographic order in the third direction (c-direction) apart from more or less parallel stacking” (Fitzer et al., 1995). The organic

starting materials are commonly petroleum pitch, coal tar pitch, aromatic model compounds and coking coals (Marsh, 1989).

However, all materials that carbonise in a plastic, visco-elastic or solid state follow a similar trend when pyrolysed under an inert atmosphere at a fixed heating rate. They are composed mainly of carbon, nitrogen, oxygen and, in some cases, nitrogen and sulphur. At first oxygenated functional groups are released, along with their sulphur and nitrogen equivalents, forming CO_2, H_2O, SH_2, etc. The aliphatic groups are removed, forming tars. These two processes lead to the green-coke stage, followed by the coke stage. After the carbonisation stage, the materials may or may not graphitise on further heat treatment (Oberlin, 1984).

2.9.1 Soft and hard carbons

Soft carbons are formed from organic materials which melt on heating and then solidify at temperatures above 400 °C, whereas the hard ones are a broad class covering all the substances formed from organic materials which do not melt or which solidify at low temperatures (Mrozowski, 1954). Soft carbon results from carbon materials that are able to pass through the temporary fluid phase during carbonisation (Mochida *et al*., 2006). A schematic presentation of how soft and hard carbons form during carbonisation is given in Figure 2.8 below.

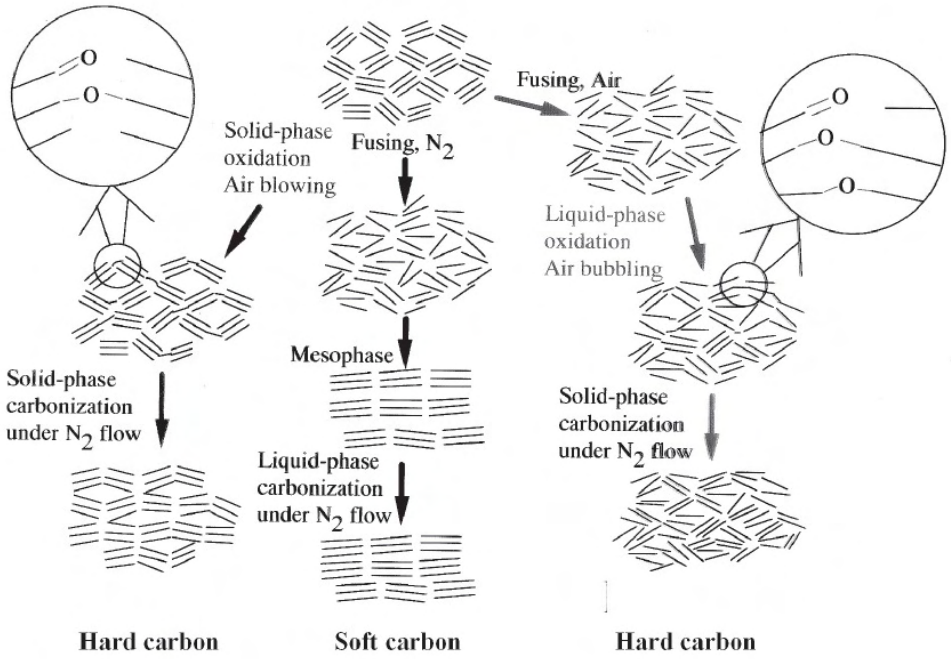

Figure 2.8: **Soft and hard carbons from as-received (AR) pitch by modifying the carbonisation stages (Mochida *et al*., 2006)**

Precursors that develop a fluid phase during the early stage of carbonisation are graphitisable (soft carbon), which means that they transform into graphite by heat treatment to 2 800 ºC under atmospheric or lower pressures. Most of petroleum pitch, coking coals, coal tar and molecular compounds (such as poly(vinyl chloride)) or synthetics (such as aromatic resins obtained from naphthalene), etc. are precursors used to give graphitisable carbons. Soft carbons formed from polymeric solids are composed of organic molecules cross-linked in a complicated pattern; a great portion of these molecules is made up of large condensed ring systems. The remaining portion comprises different types of organic molecule interspersed between the systems, forming the disorganised phase. At temperatures around or above 800 °C these substances gradually lose most of their atoms, other than carbon, by evolution of gases. At this stage these carbons are composed of small turbostratic crystallites of about 30 Å in diameter, built of disorganised stacks of parallel, equidistant planes of condensed benzene rings, with the disorganised carbon phase forming a matrix which surrounds these crystallites. The crystallites grow with increased temperature, at first mainly at the expense of the disorganised phase. When this (the disorganised phase) is exhausted, further growth

continues at the expense of the smaller and less advantageously located crystallites (Mrozowski, 1954).

Most condensed materials that do not have a fluid phase during carbonisation form non-graphitisable (hard carbons) even after heat treatment to 2 800 ºC. Non-graphitisable carbons generally contain cross-linking functional groups (e.g. oxygen, sulphur or nitrogen-based groups) and a low concentration of hydrogen donors. Coconuts, brown coals, most anthracites, etc. are good examples of non-graphitisable carbons (Marsh & Rodriquez-Reinoso, 2000). In hard carbons the stabilisation of the structure by intermolecular bonding hampers the condensation process, hence such carbons show a slower increase in the size of carbon crystallites. However, hard carbons also lose the light fractions in the same temperature range as the soft ones (Mrozowski, 1954).

Soft and hard carbons have distinctive characteristics. On a microscopic scale, soft cokes possess the regular structure which forms as the substance solidifies, i.e. swarms or stacks of flat molecules or crystallites all well packed into a thin layer. In hard cokes, the criss-cross bonding makes the system rigid, creating conditions under which such structures could not develop (Mrozowski, 1954).

CHAPTER 3: EXPERIMENTAL AND ANALYTICAL TECHNIQUES

3.1 Materials Used

Four pitches were used in these investigations. They are: a medium-temperature pitch, which looks very much like a tar (here referred to as SP); a high-temperature pitch (90MP); and two pitches derived from anthracene oil (AOP9 and AOP10). The SP and 90MP were supplied from two different sources, whereas the AOPs were prepared in our laboratory (by a co-worker) by air-blowing at different conditions. All the above pitches were then modified as outlined in the Section 3.3. The pitches were selected on the basis of their differences in origin or their preparation route, and more importantly because of their differences in chemical composition. The SP has high oxygen and low aromaticity, the 90MP has low oxygen and high aromaticity, and both the AOPs have high oxygen and high aromaticity. However, they differ in quantity of oxygen.

3.2 Preparation of Anthracene Oil Pitches

Anthracene oil pitches were prepared by air-blowing anthracene oil (AO) in a stainless steel reactor at atmospheric pressure. 100 g of AO was placed in the reactor and heated to 296 and 310 °C for periods of three and five hours under an air flow of 175 and 185 $ml.min^{-1}$ respectively. The temperature was monitored via a thermocouple inserted into the reactor. Stirring was applied throughout the entire treatment to achieve a better interaction between the AO and the air. The pitch obtained at 296 °C was named AOP9 and the one obtained at 310 °C was named AOP10.

3.3 Thermal Treatment of Pitches

Pitch samples were weighed into an alumina crucible and put into a Carbolite Eurotherm twin horizontal tube furnace. The inert atmosphere was created prior to thermal treatment by purging with nitrogen gas for 30 minutes. A pyrolysis series was prepared from each pitch by heat treating the starting pitches to various final temperatures. The temperature range of 380 to 500 °C was employed at a heating rate of 10 $°C.min^{-1}$. The holding time for each final temperature was one hour. The samples were allowed to cool naturally after heat treatment. These samples are referred to as the ‘green cokes’.

3.4 Sample Analysis

3.4.1 Thermal analysis (TA)

There is a range of thermal analytical techniques that monitor the differences in some physical properties of a sample as a function of temperature (Wendlandt, 1986).

3.4.1.1 Thermogravimetric analysis (TGA)

Thermogravimetry (TG) is a technique by which the mass of a substance is continuously measured as a function of time or temperature. Measurements are normally carried out under a controlled atmosphere, which can be air, a vacuum or an inert gas, such as nitrogen, helium or argon. They can also occur in a self-generated atmosphere, normally observed when the sample is heated in a small container with a restricted opening. The resulting curve of mass change vs temperature gives information about thermal stability, the composition of the original sample, the intermediate compounds and the residue (Brown, 1988; Wendlandt, 1986). The maximum temperature and heating rate to which the sample can be subjected are selected depending on the properties of the sample or the experimental intentions.

Thermogravimetric analysis can be coupled with other analytical techniques, such as chromatography, mass spectrometry and Fourier transform infrared spectrometry (FT-IR) to analyse the evolved gas(es). These combinations with other techniques can be used for qualitative and quantitative purposes.

3.4.1.2 Differential thermogravimetry (DTG)

Differential thermogravimetry is the first derivative of the TGA curve. The differential mass change with respect to time is recorded as a function of temperature. The area under the peak is proportional to the total mass change of the sample (Wendlandt, 1986).

TG/DTG was carried out in a Mettler Toledo TGA/sDTA 831 thermal analyser. This thermogravimetric analyser is equipped with an additional sensor to record the difference between the temperature measured directly at the sample and the model's reference temperature. The signal obtained indicates whether a transition is exothermic or endothermic, analogous to differential scanning calorimetry (DSC). About 20 mg of sample was placed in an alumina crucible with a capacity of 70 µl and heated to 1 000 °C

at 10 °C.min^{-1} or 1 °C.min^{-1} in a nitrogen flow of 50 ml.min^{-1}. Thermogravimetric parameters such as the mass loss onset temperature (T_{onset}), mass loss endset temperature (T_{endset}), temperature of maximum rate of mass loss (T_{max}) and carbon yield at 1 000 °C were determined from the TG and DTG (Figures 3.1 and 3.2).

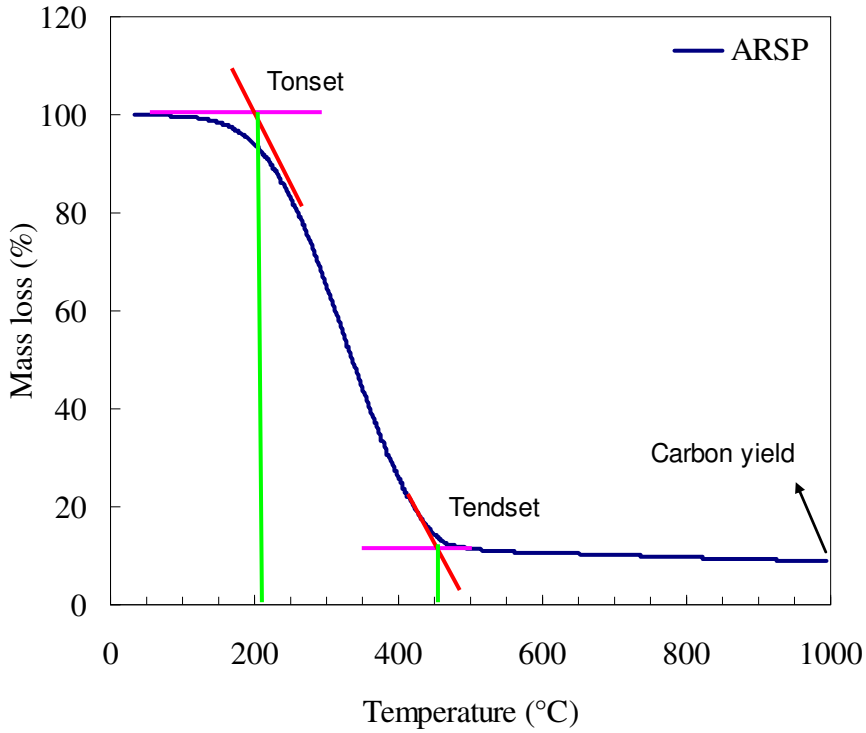

Figure 3.1: TGA curve showing an example of how the T_{onset}, T_{endset} and carbon yield were determined

The point of intersection to the curve segments before and after the inflection was taken as either T_{onset} or T_{endset}, T_{onset} being the first point and T_{endset} being the last point. The carbon yield is the residual mass obtained at 1 000 °C.

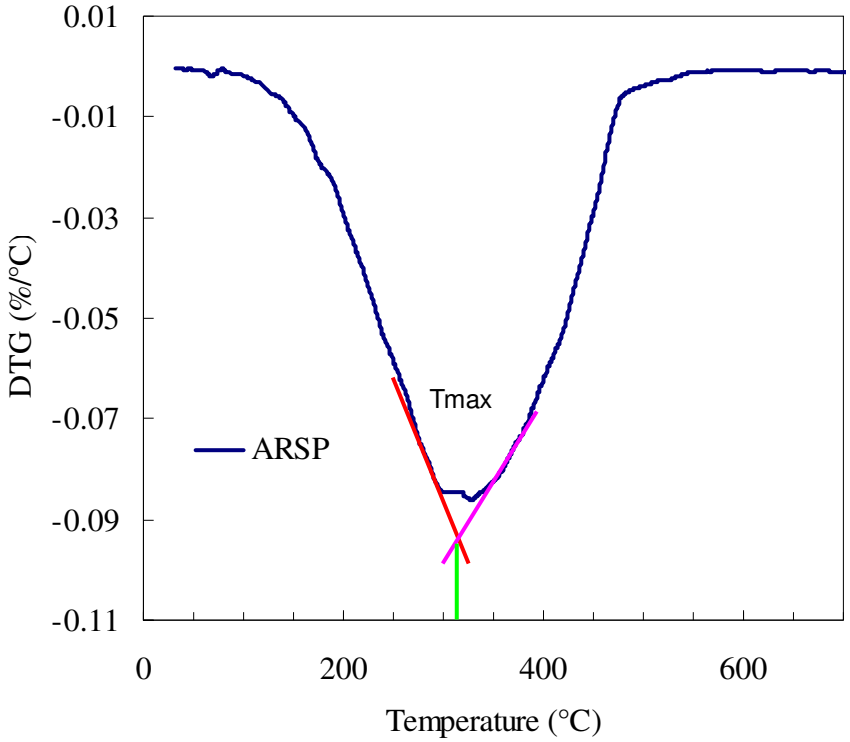

Figure 3.2: TGA curve showing an example of how the T_{max} was determined

3.4.1.3 Thermomechanical analysis (TMA)

TMA is a technique in which the dimensional changes in a sample are measured, while the temperature of the sample, in a specified atmosphere, is programmed (Haines, 1995). Quartz probes are fitted with thermocouples to measure the temperature and follow the movements of the samples, and a linear variable-density transducer is used to sense the probe movement and produce a related electrical signal (Fifield & Kealey, 1995). The sample is placed on a stage within the furnace. Then the probe rests upon it to sense changes in length. The probe and support are made from a material with a low and reproducible coefficient of thermal expansion, which also has low thermal conductivity. A number of different probes are available in order to optimise the test conditions. These include expansion, penetration, compression, flexure, extension and torsional measurements (Brown, 1988; Fifield & Kealey, 1995). Measurements can be made over the temperature range from –100 up to 1 000 ºC. The load or force applied to the sample can also be varied.

Preparation of pellets for TMA analysis

The pitch materials (about 0.4 g) in the form of a powder were pressed into a cylindrical pellet of 13 mm x ~3 mm in size using a steel mould and a hydraulic press. The samples were pressed with a mass (load) of 10 tons. Pressurising and depressurising was done at a very slow rate because a sudden pressure variation results in a cracked sample pellet. After pressing had been done, the pellets were ready for TMA analysis.

Measurement of the glass transition temperature (Tg)

A TMA Q400 instrument with a temperature reproducibility of ±2 °C was used to measure the glass transition temperature of the samples. Each sample pellet obtained as described above was placed on the stage supporting the sample during measurement. The instrument was operated in expansion mode with a 1 g (which is about 0.01 N) load on the expansion probe (flat probe), a nitrogen flow of 10 ml.min^{-1} and a heating rate of 10 °C.min^{-1}. The thermocouple probe was brought as close to the sample as possible. The quartz tube, along with the sample and probe, was surrounded by a cylindrical furnace for heating. Where necessary, liquid nitrogen was used to take measurements from subambient temperatures.

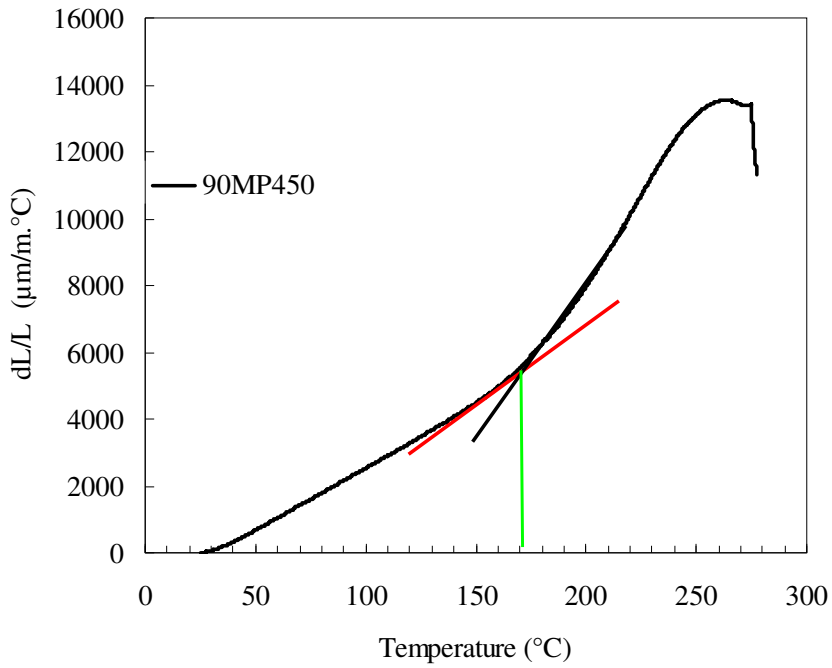

Figure 3.3: TMA curve showing an example of how the glass transition temperature was determined

Figure 3.3 above shows the linear expansion of a pitch sample with respect to temperature, determined by means of an expansion probe. (dL is the measured change of the sample length and L is the initial sample length). The change in the linear coefficient of expansion of the sample is an indication that the glass transition temperature, which spans a few degrees, has been reached. The glass transition temperatures were determined by drawing two tangents before and after the transition, as shown in Figure 3.3 above. The mid-point, or point of inflection of the transition, was taken as the glass transition temperature. However, in the pitches that are fully mesophase, the change in the slope is gradual, as opposed to a sudden change (see Figure 3.4 below). This makes the process of locating the glass transition temperature difficult. The values for such samples have been omitted from this dissertation. This method is also not immune to personal errors that can result from the drawing of tangents. However, it is reasonably reproducible with a difference of ±2 to 3 °C.

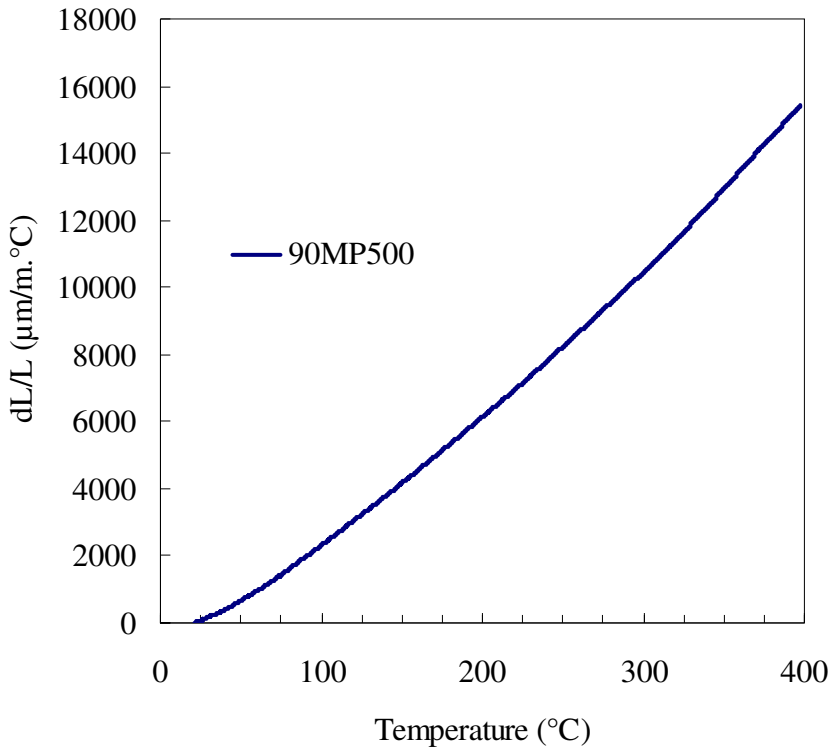

Figure 3.4: **TMA curve showing an example of how difficult it is to determine the glass transition temperature in a completely mesophase specimen**

Softening point temperature (Ts)

The measurements for the softening point temperature were obtained by placing a penetration probe (point end probe) of 100 g (at a force of 1 N) on the sample. The conditions used to obtain the softening point temperatures were the same as above, except for the force and probe used during the measurements.

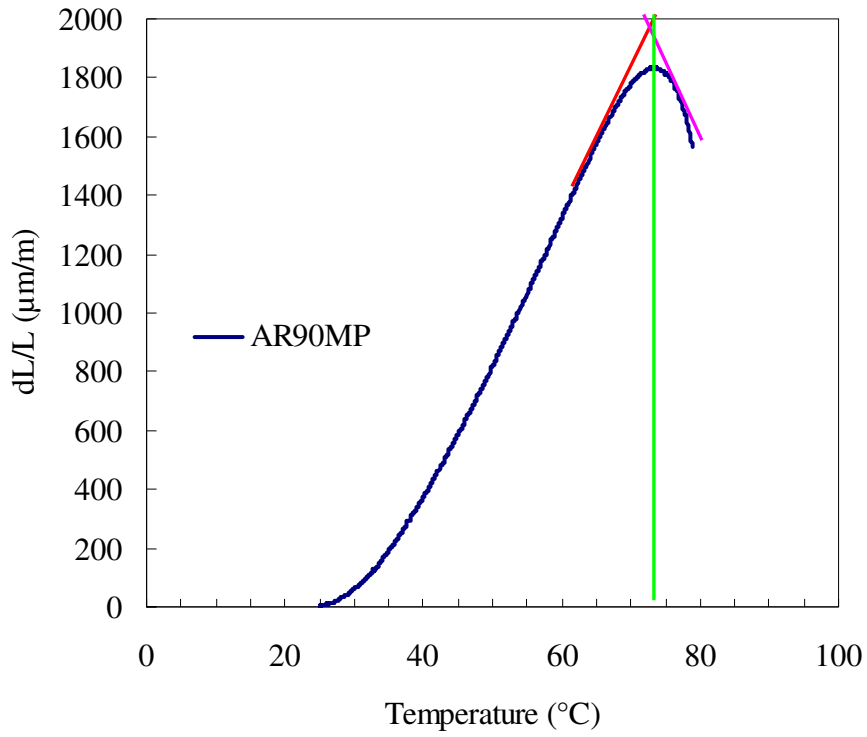

Figure 3.5: TMA curve showing an example of how the softening point temperature was determined

The TMA diagram in Figure 3.5 shows how the softening point was obtained by drawing tangents on the penetration curve before and after penetration. The procedures (expansion and penetration) were adopted from Benn (1989). The glass transition temperature and the softening point values are given in Appendix A, Table A9.

Obtaining the softening point temperature on mesophase samples is not as difficult as obtaining the glass transition temperature (see Figure 3.6 below).

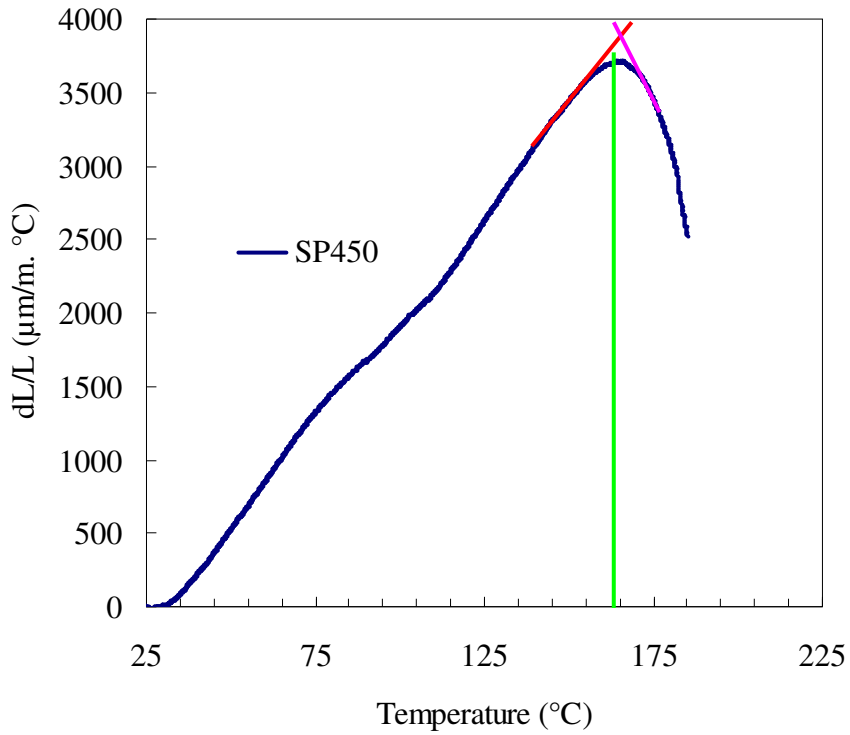

Figure 3.6: **TMA curve showing the measurement of the softening point temperature in a fully mesophase sample**

3.4.1.4 Elemental analysis (EA)

Elemental analysis is a process in which a sample is analysed for its elemental and sometimes isotopic composition. It is sometimes called 'ultimate analysis'. Elemental analysis can be qualitative (determining what elements are present) and quantitative (determining how much of each are present). It falls within the ambit of analytical chemistry, i.e. the set of instruments involved in interpreting the chemical nature of our world. The most common form of elemental analysis, CHN (carbon, hydrogen and nitrogen) analysis, is accomplished by combustion analysis. In this technique, a sample is burned in an excess of oxygen and various traps collect the combustion products, i.e. CO_2, H_2O and NO_2 (carbon dioxide, water and nitric oxide). The mass of these combustion products can be used to calculate the composition of the unknown sample. Trace elements can also be included as part of elemental analysis (wikipedia.org/wiki/Elementalanalysis).

3.4.1.5 The analysis of CHN

Elemental analysis of pitches for C, H, N and O was carried out using a Thermo Flash EA 1112 series at the University of Leeds, UK. Samples of 2 to 3 mg are weighed into a tin capsule. After the capsule has been folded, the sample is placed in the auto-sampler. The tin capsule enclosing the sample then falls into the reactor chamber where excess oxygen is introduced; the temperature rises instantly to approximately 1 800 °C, causing sample combustion. This produces CO_2, H_2O and NO_2, which pass through and separate in a chromatography column using high-purity helium as a carrier gas. The quantities are detected using a thermal conductivity detector and then compared with standards to determine the percentages of C, H and N. The results are presented as percentage by weight.

3.4.1.6 The analysis of oxygen

The same instrument used for the analysis of CHN was used to determine the percentages of oxygen. Samples of 2 to 3 mg are weighed into a silver capsule. After the capsule has been folded, the sample is placed in the auto-sampler. The silver capsule enclosing the sample falls into the reactor chamber at a temperature of 1 060 °C where it undergoes instant pyrolysis. This produces N_2, CO and H_2 which pass through and separate in a chromatography column using high-purity helium as carrier gas. The quantity of CO is detected using a thermal conductivity detector and then compared with standards to determine the percentage of oxygen. The results are also presented as percentage by weight.

3.4.2 Evolved gas analysis (EGA)

Evolved gas analysis (EGA) is a technique for determining the nature and amount of a volatile product(s) formed during the thermal degradation of materials (Xie & Pan, 2001). It involves the analysis of gaseous species evolved during combustion and/or pyrolysis. It also evaluates the chemical pathway of the degradation reaction by determining the decomposition products. Combining thermal analysis (TA) with gas-analytical techniques significantly enhances the possibilities for interpreting the mechanisms of thermally induced reactions. Several techniques can be used for evolved gas analysis (EGA), such as gas chromatography (GC), infrared (IR) or mass spectroscopy (MS), for gas detection

and analysis. This study focuses on the use of thermogravimetric mass spectrometric analysis (TG/MS).

3.4.2.1 Mass spectrometry (MS)

Mass spectrometry is an analytical technique that measures the ratio of mass to charge. Materials are ionised and fragmented by bombardment with a high-energy electron beam, by chemical ionisation, field ionisation, or fast atoms. The bombardment produces many fragments carrying a charge, facilitating their separation and detection by electrical and magnetic means. The fragment pattern is characteristic of the molecule studied. The mass spectrometer operates in a high vacuum, to prevent loss of charged fragments by collision with molecules of atmospheric gases or swamping of the sample spectrum (Fifield & Kealey, 1995). This results in a problem of interfacing the spectrometer with any thermoanalytical system. The evolved gas is extracted from the thermal analysis instrument through a heated capillary leak at suitable temperature. Jet or orifice separators are used to reduce the pressure before the MS. The sampling capillary is set as close as possible to the sample and may be heated up to around 250 ºC. A second stage reduction using a fine frit as a molecular leak may be added. This arrangement reduces the transfer time between the TG and the MS to less than one second (Haines, 1995).

A Thermostar^{TM} QMS 200 channeltron (detector) mass spectrometer linked to the TA SDTQ600 thermobalance was employed to record the gas evolution profiles. A heating rate of 10 °C.min^{-1} and a nitrogen flow rate of 50 ml/min^{-1} were used. The furnace has a gas inlet and an exit for the distilled material. To avoid secondary reactions, a probe was placed very close to the sample crucible of the thermobalance in the direction of the gas flow. The gas line between the TG and the MS was heated to 200 °C in order to avoid cold points and thus condensation of some of the gaseous products. Ionisation was carried out by an ion source of 2.84 mA at the filament, with an emission current of 1.92 mA.

3.4.3 Optical microscopy (OM)

Optical microscopy is technique used to determine the amount of mesophase in pitches. It is a statistically based technique (De Castro, 2006). Other uses of optical microscopy in the study of carbon materials are principally concerned with coal petrography, a discipline based on the measurement of reflectance from the coal surface and dealing with

coal materials in terms of macerals (Marsh, 1989). Its accuracy is questioned because spherules of under one micrometer cannot be seen by OM (De Castro, 2006). It must be stressed that this is only a comparative technique and that material characterised as isotropic may only be so depending on the level of resolution (Marsh, 1989).

Cokes produced on heat-treatment temperatures up to >700 K are termed 'anisotropic' because their polished surfaces exhibit optical activity when viewed under polarised light in an optical microscope. This activity results from the structures within the coke, which are macrocrystalline over a size range of 1 to 300 µm. The macrocrystallinity is based on the graphite lattice, i.e. the lattice of parallel layers of carbon atoms bonded into hexagons. The size and shape of the macrocrystallinity is best assessed by examination of polished surfaces of coke by optical microscopy using polarised light in conjunction with a half-wave retarder plate and parallel polars to create interference colours. The colours observed are yellow, blue and purple, but red is often noted as well. The colours created are not actual colours within the carbon surface. The origins of these colours are caused by the anisotropic nature of the macrocrystallinity based on the graphite lattice. Three modes of presentation of the lattice to the plane of polarised light were considered:

1. Basal plane presentation when basal planes are parallel to the polished surface
2. Prismatic edge presentation with the basal plane parallel to the plane of polarised light and at right angles to the polished surface
3. Prismatic edge presentation with the basal plane anti-parallel to the plane of polarised light but still at right angles to the polished surface (Markovic & Marsh, 1983).

The samples of the pitches and green cokes produced in this study were examined under polarised light in an optical microscope. Blocks with highly reflecting polished surfaces were prepared, using a Buehler alpha two-speed grinder-polisher equipped with a vector power head. To facilitate the polishing of brittle samples, a cross-section of each sample was mounted in Epo-kwick fast curing epoxy resin mixed with Epo-kwick hardener at a ratio of 5(resin):1(hardener). In order to expose the samples and prepare a flat surface, the initial grinding was carried out on a grinding disc fitted with 400, 600 and 1 200 grades of silicon carbide disc, over which water flowed continuously. Polishing was carried out with a soft synthetic porous pad, called ChemoMet I, followed by medium-hard woven silk cloth (VerduTex) over which the Masterprep polishing suspension of 0.05 µm was

sprayed. After being polished, the coke samples were mounted on glass slides with plasticine using a manual mounting press (Struers) to enhance evenness. The samples were protected by lens tissue during mounting to avoid scratching. They were then placed on the stage of a Leica DM2500M optical microscope fitted with a Leica DFC420 digital camera and examined by reflected polarised light under an oil-immersion Antiflex-epi Zeiss objective lens.

3.4.4 Infrared spectroscopy (IR)

IR is a technique based on the vibrational modes of molecules. The spectrum is obtained by passing infrared radiation through the sample and determining the fraction of incident radiation absorbed at a particular energy. IR can be used to study virtually any sample in virtually any state. Fourier transform infrared spectroscopy (FT-IR) provides information about functional groups in a substance (Stuart, 2004). It is one of the most versatile analysis techniques available for the study of complex mixtures such as coals and related materials. All carbonaceous solids essentially give the same bands in their IR spectra, differing in intensity (Guillén *et al*., 1995).

3.4.4.1 Diffuse reflectance infrared Fourier transform (DRIFT)

Diffuse reflectance is often used for powders and solids having a rough surface. The diffuse scattered radiation from the sample may be collected in a wide spatial angle. One can differentiate between two fractions of this radiation: one fraction is mirror reflected from uneven surfaces; the other fraction penetrates the sample, is partially absorbed and, via scattering processes in the interior, returns to the surface. In most cases, both reflection effects cannot be separated experimentally. The spectrum can be presented in two ways: as percentage transmittance (to be exact: the degree of pure spectral transmittance) vs. wavenumber, or as absorbance vs. wavenumber. While transmittance is often used in the interpretation of chemical groups present in the sample, absorbance, due to its linear dependence on concentration, provides the ability to make direct quantitative analytical measurements. Though FT-IR spectroscopy is capable of rapid non-destructive analysis with little sample preparation, it has its disadvantages with regard to carbonaceous materials. Carbonaceous materials disperse infrared radiation strongly, thus reducing the energy that reaches the detector (Alciaturi *et al*., 1996).

In this study, the IR spectra were recorded with a Collector diffuse reflectance accessory placed in a Perkin-Elmer Spectrum GX FT-IR spectrometer (Norwalk, CT, USA), using a mercury-cadmium telluride detector, operating at a room temperature. The samples in powder form were loaded into a DRIFT microcup and the surface was levelled. The spectra were recorded from 4000 to 600 cm^{-1} by averaging 16 scans at a resolution of 8 cm^{-1}. The spectra were rated against the background air spectrum.

3.4.4.2 Attenuated total reflectance (ATR)

Attenuated total reflectance is a versatile, non-destructive technique for obtaining the infrared spectrum of the surface of materials or the spectrum of materials either too thick or too strongly absorbing to be analysed by standard transmission spectroscopy. It is also known as internal reflection spectroscopy (IRS) or multiple internal reflectance (MIR). The sample is placed in contact with the internal reflection element (IRE), the light is totally reflected, generally several times, and the sample interacts with the evanescent wave resulting in the absorption of radiation by the sample at each point of reflection. The internal reflection element is made from a material with a high refractive index. The most commonly used internal reflection elements are zinc-selenide, silicon, germanium and diamond (Günzler & Gremlich, 2002).

ATR was used where the nature of the sample would not allow DRIFT to be used. A Perkin-Elmer Spectrum GX FT-IR spectrometer (Norwalk, CT, USA) fitted with a mercury–cadmium telluride detector, operating at room temperature, was used for analysis. A blank of zinc-selenium crystal was run prior to sample analysis. The sample was placed in contact with the zinc-selenium internal reflection element. It was then run as it was and the spectra were automatically subtracted to give the spectrum of the sample only. The spectra were recorded from 4000 to 600 cm^{-1} by averaging 16 scans at a resolution of 8 cm^{-1}.

CHAPTER 4: RESULTS AND DISCUSSION

4.1 Initial Characterisation of Pitches

Initial analysis was carried out to establish the differences between the four pitches used in this study. These pitches were selected according to their differences in origin or their preparation routes. The four pitches used in this study were: two pitches from different suppliers, named SP and 90MP, and two pitches (AOP9 and AOP10) obtained by air-blowing anthracene oil under different conditions. It was expected that the air blowing would result in cross-linked carbon, as well as condensed aromatic carbon as a result of oxidative dehydrogenation.

Table 4.1: Elemental analysis of the as-received materials

Sample ID	N (%wt)	C (%wt)	H (%wt)	O (%wt)	C/H	O/C
AR90MP	1.14	92.26	4.01	1.8[a]	1.93	0.02
ARAOP9	1.20	87.76	3.46	7.58[b]	2.13	0.07
ARAOP10	1.22	87.34	3.49	7.00[b]	2.10	0.06
ARSP	1.74	85.94	6.87	5.56[a]	1.05	0.05

[a] directly, [b] by difference (**Key:** AR: as-received; MP: Mittal pitch; SP: Sasol pitch, AOP: anthracene oil pitch; 9 and 10 are just numbers used to differentiate between the two AOPs. Note: oxygen on certain samples was determined by difference due to cost.)

The elemental analysis in Table 4.1 shows that the as-received pitches differ in many respects, i.e. nitrogen, carbon, hydrogen and oxygen contents, C/H ratio and O/C ratio. Its C/H ratio gives information about the aromaticity of a particular pitch – the higher the C/H ratio, the more aromatic is the pitch. Aromaticity therefore followed this order: ARAOP9> ARAOP10 >AR90MP >ARSP. It was expected that the ARSP would have the lowest aromaticity because it is a medium-temperature pitch and is more or less a tar.

Another interesting feature is that pitches differ in oxygen content. This has a profound effect on the pyrolysis behaviour of the pitches. According to Weinberg *et al*. (1988), the desirable range of oxygen content for the formation of mesophase is 2 to 6% by weight. Some details regarding the influence of oxygen on carbonisation have already been discussed in Section 2.5.3. The influence of oxygen and the initial level of aromaticity on the formation and development of mesophase in these pitches was expected to be of particular interest.

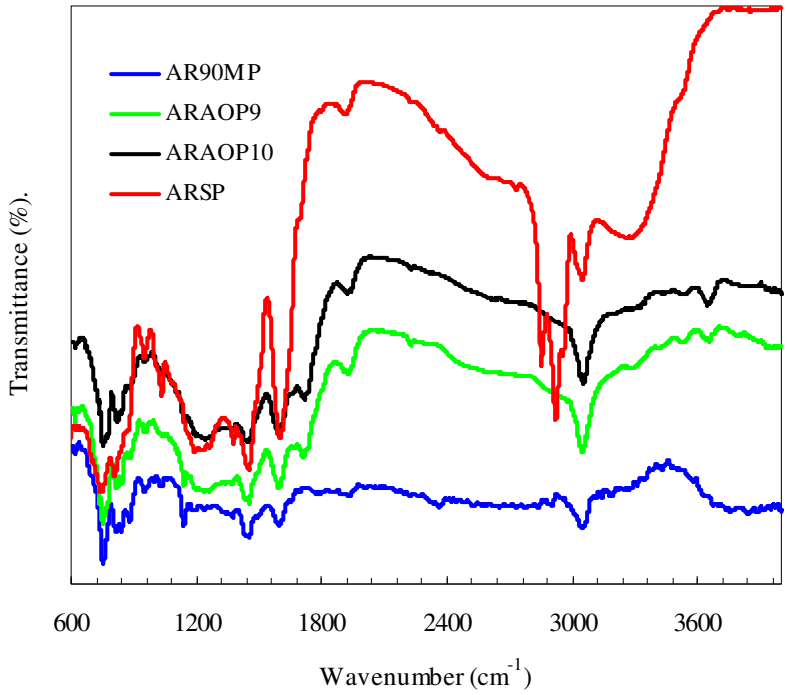

Figure 4.1: FT-IR curves for as-received pitches

Key: AR: as-received; MP: Mittal pitch; SP: Sasol pitch; AOP: anthracene oil pitch; 9 and 10 are just numbers used to differentiate between the two AOPs.

Table 4.2: Infrared spectral regions of interest

Band assignment	Wavenumber (cm^{-1})
Aryl-aryl/aryl-alkyl ether band	1 050 – 1 150 cm^{-1}
C–O	1 250 cm^{-1}
Methylene C–H in-plane bending	~1 440 cm^{-1}
Aromatic carbon-carbon ring breathing mode	~1 600 cm^{-1}
C=O stretching	1 700 cm^{-1}
Ester or anhydride	1 780 – 1 860 cm^{-1}
Triple bond stretching band	2 000 – 2 500 cm^{-1}
C-H aliphatic stretching mode (CH_3, CH_2, CH (tertiary)	2 800 – 3 000 cm^{-1}
C-H aromatic stretching mode	3 000 – 3 200 cm^{-1}
Hydroxyl (O-H)	3 000 –3 600 cm^{-1}

Figure 4.1 and Table 4.2 show the FT-IR curves and infrared spectral regions of interest respectively. Figure 4.1 illustrates that AR90MP, ARSP, ARAOP9 and ARAOP10 can be distinguished, but the curves do not provide significant differences between materials of similar origin (ARAOP9 and AROP10). The main differences between ARSP, AR90MP and ARAOP9 and ARAOP10 are observed on the characteristic bands of C-H structures. From the analysis of the band at 3000 – 3100 cm^{-1} (related to aromatic hydrogen, H_{ar}) and those between 2800 and 2980 cm^{-1} (aliphatic hydrogen, H_{al}), it can be observed that AR90MP, ARAOP9 and ARAOP10 have a much higher content of H_{ar} than H_{al} and the opposite is true of ARSP. In fact these former pitches have no bands attributable to H_{al} (2800 –2980 cm^{-1}). All pitches have bands around 1440 cm^{-1} (methylene C–H in-plane bending) and 1600 cm^{-1}(C=C stretching).

Once again, another important feature is the presence of oxygen in the samples since it has a huge impact on the thermal behaviour of the pitch. ARSP shows bands corresponding to oxygen groupings in the 3000 – 3600 cm^{-1} region for OH and another at ~1860 cm^{-1} for the ester or anhydride band.

Oxygen in the AR90MP pitch is represented by the overtone peak at 3000 – 3600 cm^{-1} for OH and by the ether band at 1133 cm^{-1}. ARAOPs do not show the absorption that can be attributed to OH-containing functional groups (the 3000 – 3600 cm^{-1} region). However, their oxygen bands appear as the ester or anhydride at ~1860 cm^{-1}, as the C=O at 1700 cm^{-1} and as the ether at 1133 cm^{-1}.

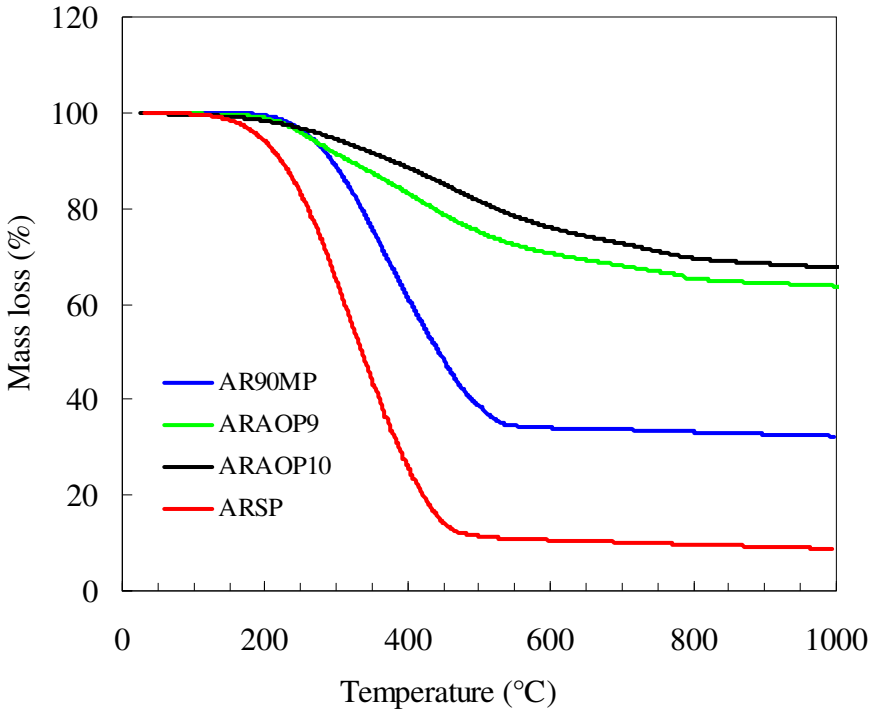

Figure 4.2: Thermogravimetric mass loss curves for as-received pitches obtained under nitrogen, at 10 °C.min^{-1}

Key: AR: as-received; MP: Mittal pitch; SP: Sasol pitch; AOP: anthracene oil pitch; 9 and 10 are just numbers used to differentiate between the two AOPs.

Figure 4.2 shows that the as-received materials differ in terms of carbon yield at 1 000 °C. ARSP has the lowest carbon yield, followed by AR90MP, ARAOP9 and ARAOP10. The mass loss onset temperature and mass loss endset temperature also differ from pitch to pitch. The mass loss onset temperatures (T_{onset}) increase in the following order: ARSP < ARAOP9 < AR90MP < ARAOP10.

Figure 4.2 also gives a measure of the thermal stability of the precursor. This is related to the parameters that reflect the composition and temperature dependence of physical properties of the precursors. It is clear from the above observations that the materials differ in species of low molecular mass and behave differently during pyrolysis.

Table 4.3: Summary of some of the properties that differentiate the as-received materials

Sample ID	T_{onset}[a] (°C)	T_{max}[b] (°C)	T_{endset}[c] (°C)	Tg[d] (°C)	Ts[e] (°C)	Carbon yield (%)
AR90MP	260	387	520	32	74	32
ARAOP9	225	272	649	89	185	48
ARAOP10	230	476	630	95	218	68
ARSP	210	330	475	4	7	9

[a] mass loss onset temperature; [b] temperature of maximum rate of mass loss; [c] mass loss endset temperature; [d] glass transition temperature; [e] softening point temperature (**Key:** AR: as-received; MP: Mittal pitch; SP: Sasol pitch; AOP: anthracene oil pitch; 9 and 10 are just numbers used to differentiate between the two AOPs. Note: the number in front of the AOP is used to differentiate between the two pitches.)

Table 4.3 shows that the values of the softening point temperature (Ts), carbon yield (CY), glass transition temperature, mass loss onset temperature, temperature of maximum rate of mass loss and mass loss endset temperature show interesting differences between the pitches. The details of each property are discussed in the succeeding sections.

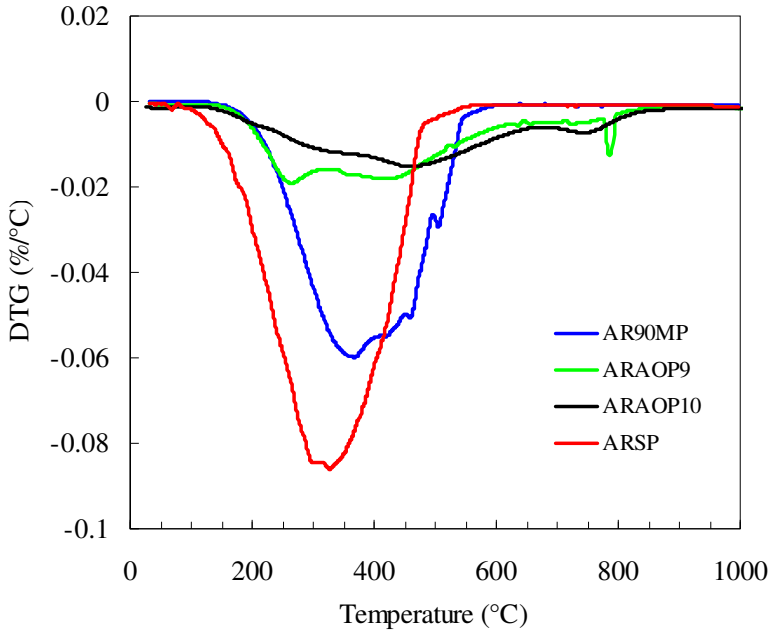

Figure 4.3: Derivative mass loss curves for as-received materials obtained under nitrogen, at 10 °C.min^{-1}

Key: AR: as-received; MP: Mittal pitch; SP: Sasol pitch; AOP: anthracene oil pitch; 9 and 10 are just numbers used to differentiate between the two AOPs.

The DTG traces in Figure 4.3 show that the as-received materials lose mass either as a single event (ARSP), in two steps (ARAOP10), as three events (AR90MP) or in three stages (ARAOP9). As discussed in the literature survey, mass loss results from the volatilisation of the species of lower molecular mass initially present or formed by pyrolysis reactions. The different profiles are probably the result of the different chemical reactions that are taking place due to different chemical compositions. With ARSP, the release of species of low molecular mass occurs mainly concurrently with some other reaction, hence a single step. The different chemical reactions taking place will be deduced from the TG/MS data.

4.2 Summary of Initial Characterisation

The parameters given above show that as-received pitch materials differ in many aspects. The most important aspects from the perspective of elemental analysis and FT-IR are the aromaticity and oxygen content. The aromaticity of the pitches studied follows the order ARAOP9 > ARAOP10 > AR90MP > ARSP. The AOPs and SP have high oxygen contents. However, the oxygen content of SP is within the desired range for mesophase development. The pitches also respond differently to heat treatment and have different mass loss onset temperatures, temperatures of maximum rate of mass loss, mass loss endset temperatures and carbon yields. SP has the lowest carbon yield consistent with a high aliphatic content as determined by FT-IR and elemental analysis. The more aromatic the pitch, the higher the carbon yield. From this observation it was expected that the pitches would give products with different mesophase characters.

Another interesting feature is the presence of QI in 90MP. This feature is clearly shown by the optical microscopy discussed in the succeeding sections. All the other pitches did not show the presence of QI on optical microscopy.

4.3 Elemental Analysis of Heat-treated Materials

Table 4.4: Elemental analysis of ARSP and its heat-treatment residues

Sample ID	N (%wt)	C(%wt)	H(%wt)	O(%wt)[a]	C/H	O/C
ARSP	1.74	85.94	6.87	5.56	1.05	0.05
SP380	2.07	87.58	4.69	4.39	1.57	0.04
SP400	2.23	87.59	4.75	4.50	1.55	0.04
SP420	2.26	88.31	4.46	4.00	1.66	0.03
SP450	2.33	88.46	3.45	4.12	2.15	0.04
SP500	2.25	89.08	3.39	3.58	2.21	0.03

[a] directly. (**Key:** AR: as-received; SP: Sasol pitch; the number in front of the codes is the heat-treatment temperature)

Table 4.4 presents the change in chemical composition of the ARSP pitch during its transformation to green coke. Nitrogen increases up to 420 °C and decreases thereafter. This behaviour indicates that the nitrogen-containing compounds present are stable up to 420 °C and start to evolve thereafter. Grzyb *et al*. (2004) produced green cokes from blends of coal tar pitch and poly(4vinylpyridine) or oxidised poly(4vinylpyridine) polymers or these polymers alone. The idea was to produce carbonaceous materials enriched with nitrogen. They found that poly(4vinylpyridine) depolymerises on heat treatment, leading to the rupture of the pyridinic ring. This resulted in the evolution of light nitrogen-bearing compounds as HCN and NH_3, leading to a reduced content of nitrogen in the green cokes produced from the blend or polymers alone. They also found that oxidising this polymer prior to blending resulted in thermally more stable backbone retention of nitrogen in the structure. This information could be used as a model to explain the behaviour of the pitches used in this study. It highlights the fact that the evolution of nitrogen depends on the kind of nitrogen present in the system.

The oxygen content decreases a little, but a significant amount remains in the structure at 500 °C. Its decrease might be due to oxygenated compounds of low molecular mass that evaporate during the heat treatments, or that are removed as decomposition products of thermal reaction. On the other hand, the remaining oxygen indicates that the oxygenated compounds present are less reactive and/or less volatile (Sima *et al.,* 2003).

Another significant factor that is evident is the high hydrogen content which results in a correspondingly low C/H ratio. This feature shows that this pitch is highly aliphatic. However, its aliphatic character decreases on heat treatment (increase in carbon and decrease in hydrogen) in favour of aromaticity (increasing C/H ratio) due to condensation reactions. At 500 °C the C/H ratio is only about the same as that of the other starting materials.

Table 4.5: Elemental analysis of AR90MP and its heat-treatment residues

Sample ID	N (%wt)	C (%wt)	H (%wt)	O (%wt)[a]	C/H	O/C
AR90MP	1.14	92.26	4.01	1.8	1.93	0.02
90MP380	1.12	92.43	3.56	1.2	2.18	0.01
90MP400	1.11	93.25	3.55	1.2	2.20	0.01
90MP420	1.03	93.20	3.63	1.1	2.15	0.01
90MP450	0.99	93.76	3.34	0.85	2.36	0.01
90MP500	1.09	94.31	2.75	1.15	2.88	0.01

[a] directly. (**Key:** AR: as-received; MP: Mittal pitch; the number in front of the codes is the heat-treatment temperature.)

Table 4.5 illustrates that AR90MP is highly aromatic, consistent with the FT-IR results. The aromaticity also increases with heat treatment as seen from the increase and decrease in carbon and hydrogen respectively, culminating in an increase in the C/H ratio. Oxygen decreases up to 380 °C and remains fairly constant thereafter. The 450 °C result is probably due to some uncertainty or error in the measurement.

The nitrogen content stays more or less the same throughout heat treatment. There is a significant difference between ARSP and AR90MP in terms of the oxygen and C/H ratio (aromaticity). Interestingly, ARSP still has a high oxygen content after heat treatment. This was expected to have a profound effect on mesophase formation and development.

Table 4.6: Elemental analysis of ARAOP10 and its heat-treatment residues

Sample ID	N (%wt)	C (%wt)	H (%wt)	O (%wt)[b]	C/H	O/C
ARAOP10	1.22	87.34	3.49	7.00	2.10	0.06
AOP10380	1.38	88.00	3.19	7.43	2.31	0.06
AOP10400	1.33	87.72	3.15	7.8	2.34	0.07
AOP10420	1.38	88.04	3.07	7.51	2.41	0.06
AOP10450	1.36	88.43	3.02	5.72	2.44	0.06
AOP10500	1.36	89.57	2.78	6.29	2.70	0.05

[b] by difference. (**Key:** AR: as-received; MP: Mittal pitch; AOP: anthracene oil pitch; 10 is the number used to identify the AOP and the number in front of the codes is the heat-treatment temperature. Note: oxygen was determined by difference due to cost.)

Table 4.7: Elemental analysis of ARAOP9and its heat-treatment residues

Sample ID	N (%wt)	C (%wt)	H (%wt)	O (%wt)[b]	C/H	O/C
ARAOP9	1.20	87.76	3.46	7.58	2.13	0.07
AOP9380	1.36	87.87	3.28	7.49	2.25	0.06
AOP9400	1.31	88.02	3.33	7.34	2.22	0.06
AOP420	1.37	88.66	3.14	6.83	2.23	0.06
AOP9450	1.41	88.69	3.15	6.75	2.36	0.06
AOP9500	1.32	88.40	3.33	6.95	2.37	0.06

[b] by difference. (**Key:** AR: as-received; AOP: anthracene oil pitch; 9 is the number used to identify the AOP and the number in front of the codes is the heat-treatment temperature. Note: oxygen was determined by difference due to cost.)

The elemental analysis of ARAOP10 in Table 4.6 and ARAOP9 in Table 4.7 shows that nitrogen, carbon and aromaticity (C/H ratio) increase with heat treatment. Hydrogen and oxygen decrease. The reasons for this have already been suggested in the preceding sections. The most interesting feature is that both pitches have a high percentage of oxygen content coupled with high aromaticity, i.e. different from SP which has a high oxygen content but low aromaticity. The aromaticity does not increase much during heat treatment as compared with 90MP and SP. The oxygen content also remains high.

4.4 Summary of the Elemental Analysis of Heat-treated Materials

Generally, the aromaticity of all systems increases with heat treatment as reflected by the increase in their C/H ratios. ARSP has a high oxygen content and high aliphatic content as opposed to the AOPs which show high oxygen and high aromaticity. AR90MP has low oxygen and high aromaticity. The oxygen and hydrogen contents decrease in all the pitches. The nitrogen content of 90MP remains more or less the same throughout heat treatment, whereas that of SP and the AOPs increases.

4.5 FT-IR Analysis

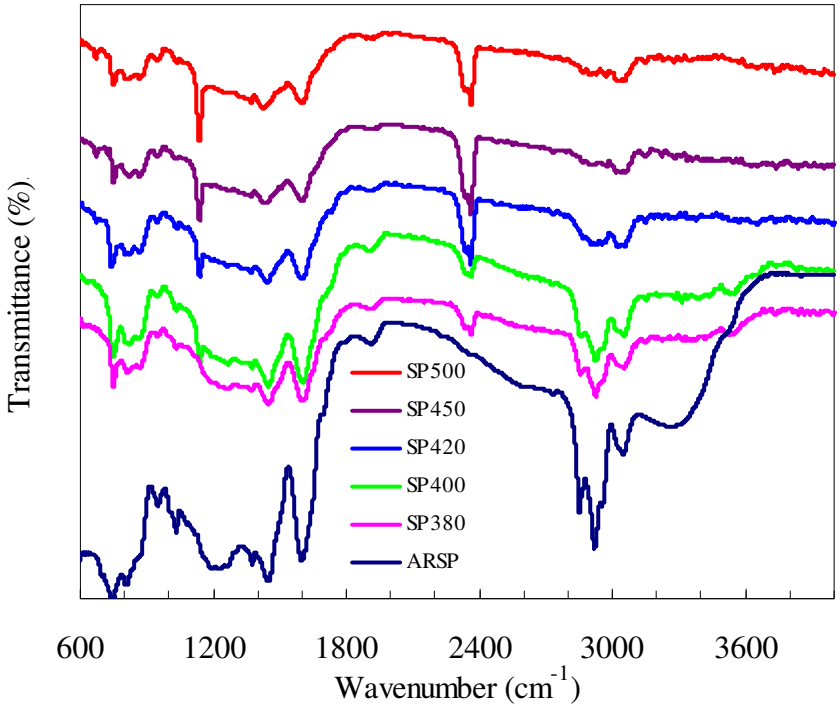

Figure 4.4: DRIFT spectra of ARSP and heat treated SP under nitrogen, at 10 °C.min^{-1}

Key: AR: as-received; SP: Sasol pitch; the number in front of the codes is the heat-treatment temperature.

Infrared spectroscopy was performed on the samples in order to obtain information about the functional groups present in the samples and how they change with heat treatment. In Figure 4.4, the FT-IR spectrum of ARSP shows a low intensity of the peak related to aromatic hydrogen (3000 – 3100 cm^{-1}) and high intensity for the aliphatic hydrogen (2800 – 2980 cm^{-1}), which is consistent with the elemental analysis. There is a significant band

corresponding to oxygen bonds (O-H in the 3000 – 3600 cm^{-1} interval). This band disappears with heat treatment and, interestingly, the aryl-aryl/aryl-alkyl ether band develops at 1050 – 1150 cm^{-1}. The formation of the ether band is probably due to the formation of the oxygen cross-links during heat treatment. This feature is corroborated by the elemental analysis in Table 4.4 which shows that oxygen is not entirely lost with heat treatment.

Another interesting feature is that a triple bond stretching band (2000 – 2500 cm^{-1}) also develops with heat treatment. It is not clear whether it is due to carbon-carbon or carbon-nitrogen triple bond stretching. All the spectra of SP have a band at around 1440 cm^{-1} (methylene C–H in-plane bending) and at 1600 cm^{-1} (an aromatic carbon-carbon ring breathing mode). Even though the aliphatic hydrogen band vanishes with heat treatment, the methylene hydrogen bending suggests that aliphatic carbon is not entirely consumed by heat treatment.

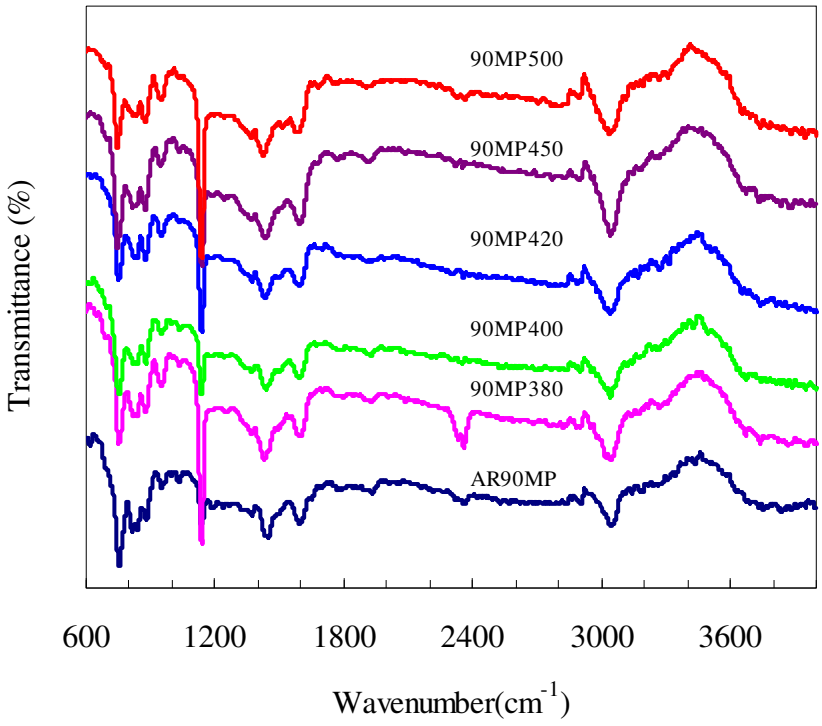

Figure 4.5: DRIFT spectra of AR90MP and heat-treated 90MP under nitrogen, at 10 °C.min^{-1}

Key: AR: as-received; MP: Mittal pitch; the number in front of the codes is the heat-treatment temperature.

Figure 4.5 shows that AR90MP has more aromatic than aliphatic hydrogen. The aliphatic peak at around 2915 cm^{-1} is not present. It is, however, presented by the methylene C–H in-plane bending band (at around 1440 cm^{-1}). AR90MP and the heat-treated samples show overtone peaks at wavenumbers that are characteristic of the OH band (at 3000 – 3600 cm^{-1}). The overturning is caused by the different particle size distributions. This band does not disappear as expected, but the elemental analysis (Table 4.5) shows that the oxygen in the system is reduced with heat treatment. With heat treatment, a peak denoting aryl-aryl or aryl-alkyl ethers develops at around 1050 –1150 cm^{-1}. This shows that part of the oxygen forms cross-links. A triple bond stretching band (at 2000 – 2500 cm^{-1}) only appears in AOP450. Once again, it is not clear whether this is due to carbon-carbon or carbon-nitrogen triple bond stretching.

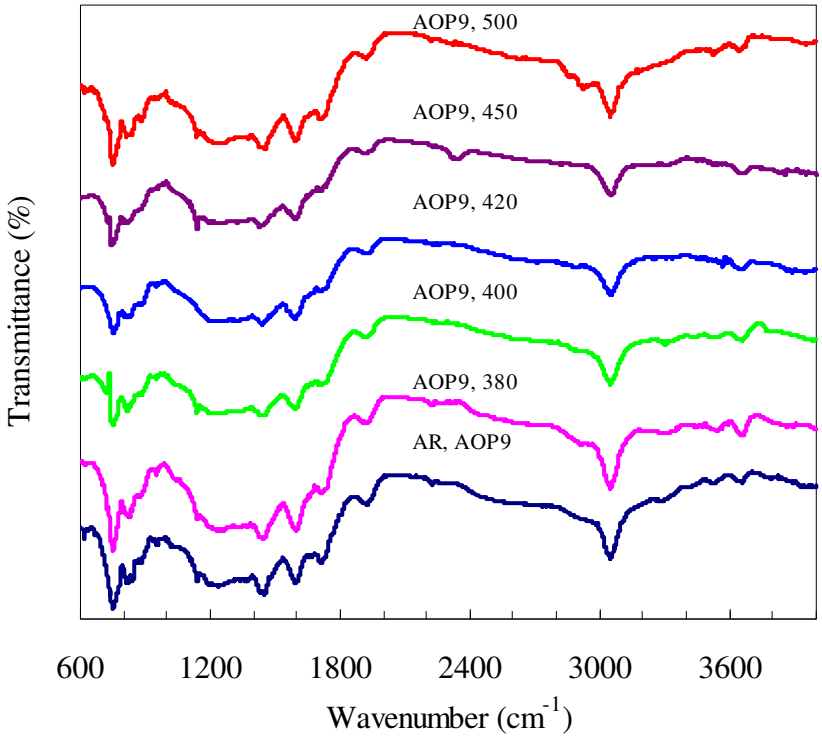

Figure 4.6: DRIFT spectra of ARAOP9 and heat-treated AOP9 obtained under nitrogen, at 10 °C.min^{-1}

Key: AR: as-received; AOP: anthracene oil pitch; 9 is the number used to identify the AOP; the number in front of the codes is the heat-treatment temperature.

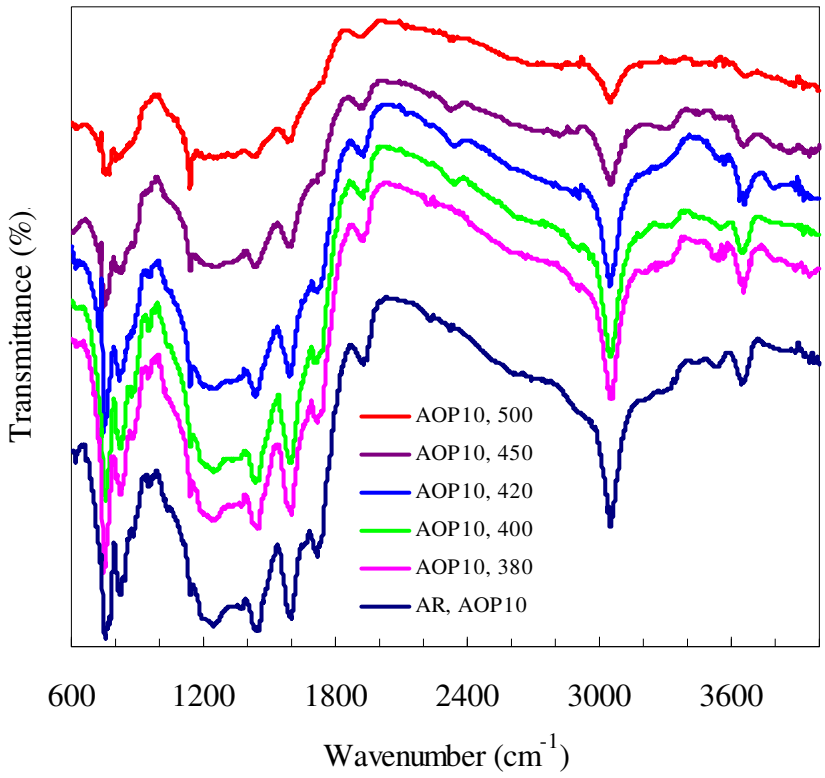

Figure 4.7: DRIFT spectra of ARAOP10 and heat-treated AOP10 obtained under nitrogen, at 10 °C.min^{-1}

Key: AR: as-received; AOP: anthracene oil pitch; 10 is the number used to identify the AOP; the number in front of the codes is the heat-treatment temperature.

Figures 4.6 and 4.7 show that ARAOP10 and ARAOP9 and their heat-treatment products are highly aromatic. There is no band for aliphatic hydrogen (at 2800 – 2980 cm^{-1}); its aliphatic carbons are represented by the band at 1440 cm^{-1} (methylene C–H in-plane bending). There are not many structural changes with heat treatment. All pitches have no OH band (3000 – 3600 cm^{-1}). Their high oxygen content can be attributed to the ester or anhydride (at ~1860 cm^{-1}), the C=O band at 1700 cm^{-1} and the C-O-C band at 1050 – 1150 cm^{-1}. The C-O-C band increases in its intensity with heat treatment, the ester or anhydride band remains almost the same, whereas the C=O band disappears at 450 °C.

4.6 Summary of FT-IR Analysis

There are significant structural changes in ARSP and AR90MP. The major points of interest are the changes in the aliphatic, aromatic and oxygen-related functional groups. There is a significant change in these functional groups in SP. The aliphatic and oxygen bands decrease as the system becomes more aromatic. The pitch also forms aryl-aryl or

aryl-alkyl ethers and triple bond stretching bands. However, the behaviour of SP is different from that of 90MP and the AOPs. The AOPs do not show much of a structural difference. All the bands remain almost the same as those of the parent pitch. On the other hand, 90MP shows the formation of a very intense peak due to aryl-aryl or aryl-alkyl ethers. FT-IR analysis also shows that the pitches differ in the nature of the oxygen present, which will result in different reactions taking place during pyrolysis. The oxygen in SP and 90MP is mainly due to the OH groups present, whereas in the AOPs it is due to the ester or anhydride (at ~1860 cm^{-1}) and the C=O band at 1700 cm^{-1}.

4.7 Thermal Analysis (TGA/DTG)

Thermal analysis, and specifically TG/DTG, can provide important information on the decomposition kinetics and phase transitions of pitches. The most important parameter from a coking perspective is the carbon yield as a function of heat-treatment temperature. The carbonisation of pitches proceeds in stages. This can be characterised by parameters such as mass loss onset temperature (T_{onset}), mass loss endset temperature (T_{endset}), mass loss temperature range (T_{onset}–T_{endset}), temperature of maximum rate of mass loss (T_{max}) and carbon yield (CY) at 1 000 °C.

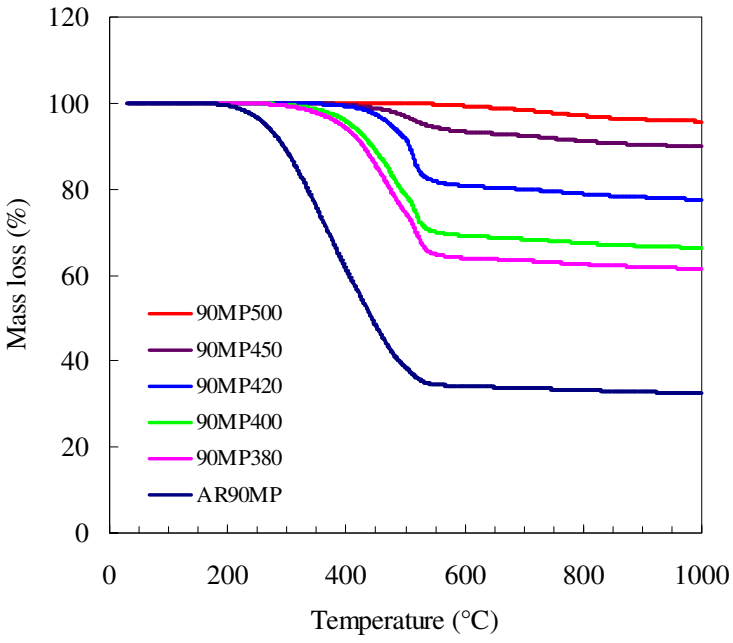

Figure 4.8(a): Thermogravimetric mass loss curves for AR90MP and heat-treated 90MP under nitrogen, at 10 °C.min^{-1}

Key: AR: as-received; MP: Mittal pitch; the number in front of the codes is the heat-treatment temperature.

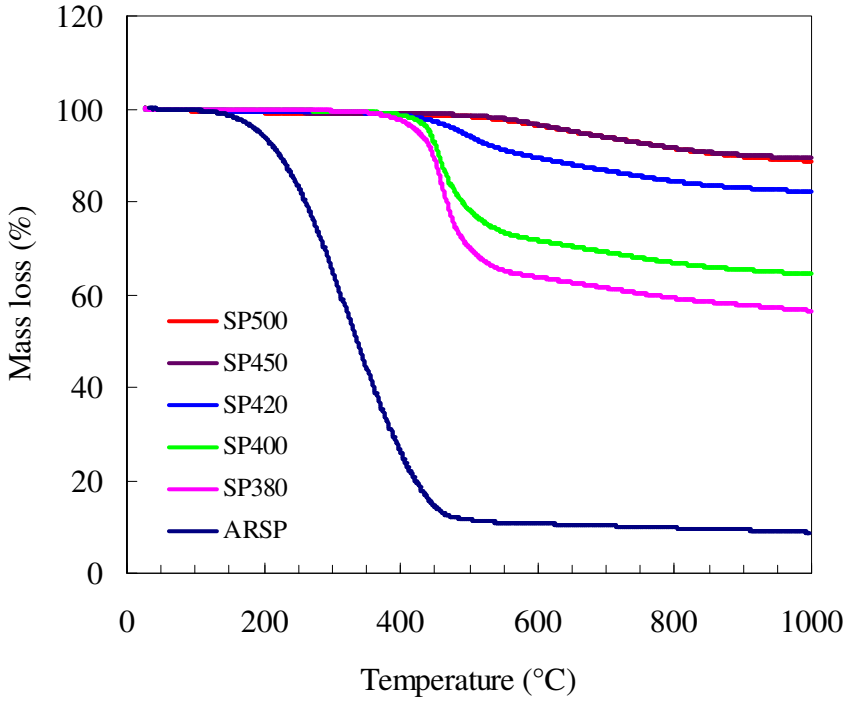

Figure 4.8(b): Thermogravimetric mass loss curves for ARSP and heat-treated SP under nitrogen, at 10 °C.min^{-1}

Key: AR: as-received; SP: Sasol pitch; the number in front of the codes is the heat-treatment temperature.

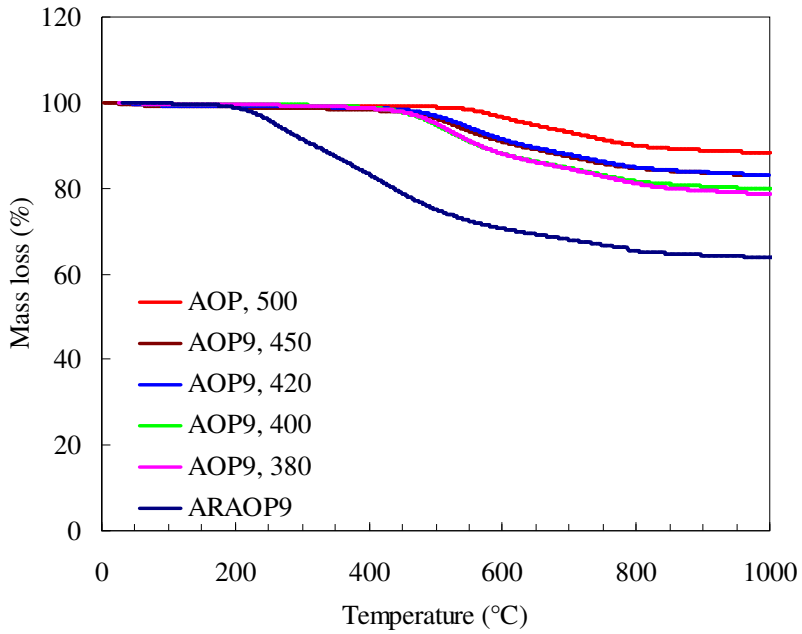

Figure 4.8 (c): Thermogravimetric mass loss curves for ARAOP9 and heat-treated AOP9 under nitrogen, at 10°C.min^{-1}

Key: AR: as-received; AOP: anthracene oil pitch; 9 is the number used to identify the AOP; the number in front of the codes is the heat-treatment temperature.

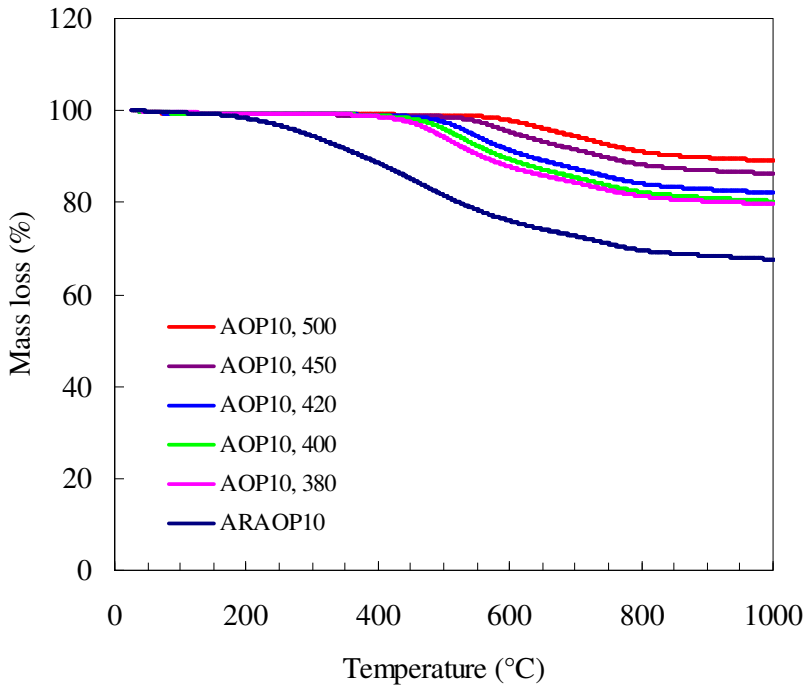

Figure 4.8 (d): Thermogravimetric mass loss curves for ARAOP10 and heat-treated AOP10 under nitrogen, at 10 °C.min^{-1}

Key: AR: as-received; AOP: anthracene oil pitch; 10 is the number used to identify the AOP; the number in front of the codes is the heat-treatment temperature.

The TG curves in Figures 4.8(a-d) of pitches heat treated up to 1 000 °C show low carbon yields for the as-received pitch materials (differing percentages). As expected, their respective heat-treatment residues show increased carbon yields (decreased content of volatiles). In all heat-treated samples, the mass loss onset temperatures occur at higher temperatures than in their respective as-received materials. Mass loss is a result of the volatiles already present, or results from pyrolytic degradation reactions or from simultaneous processes.

TGA shows that the T_{onset} shifts with heat treatment. This is probably because the species with low molecular mass (aliphatic content) have already evolved during the previous treatment. The FT-IR and elemental analyses demonstrate that the aromaticity is increasing, strengthening the suggestion that the initial mass loss is due to aliphatics.

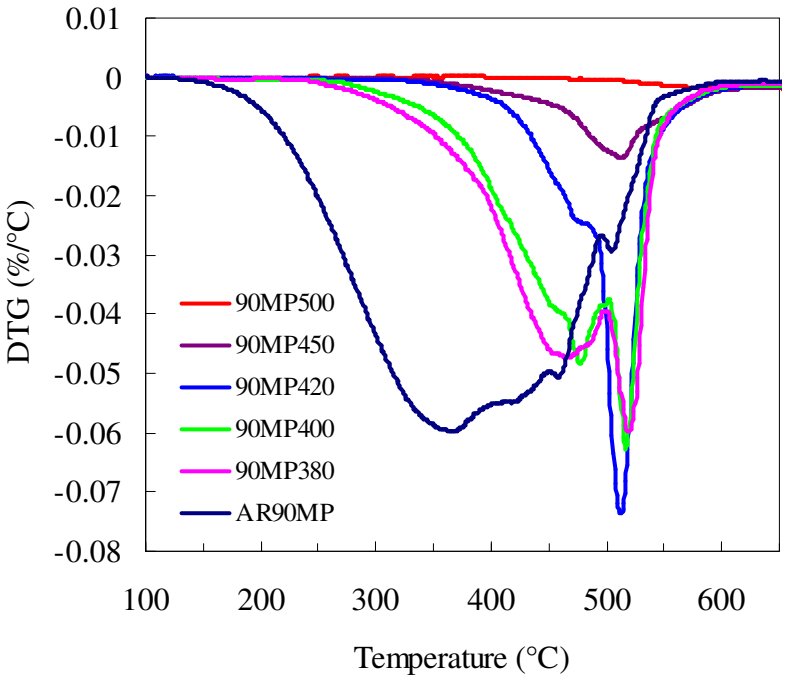

Figure 4.9(a): Derivative mass loss curves for AR90MP and heat-treated 90MP under nitrogen, at 10 °C.min^{-1}

Key: AR: as-received; MP: Mittal pitch; the number in front of the codes is the heat-treatment temperature.

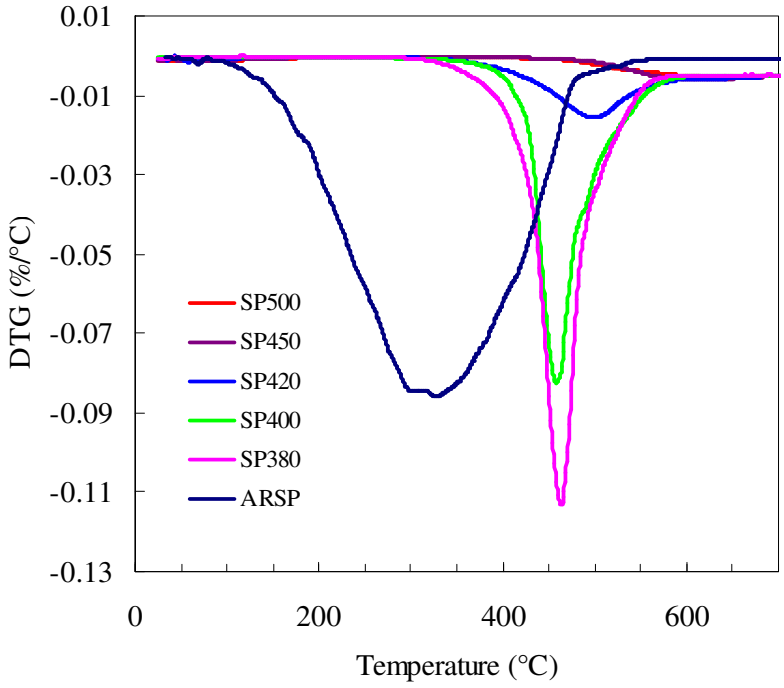

Figure 4.9(b): Derivative mass loss curves for ARSP and heat-treated SP under nitrogen, at 10 °C.min^{-1}

Key: AR: as-received; SP: Sasol pitch; the number in front of the codes is the heat-treatment temperature

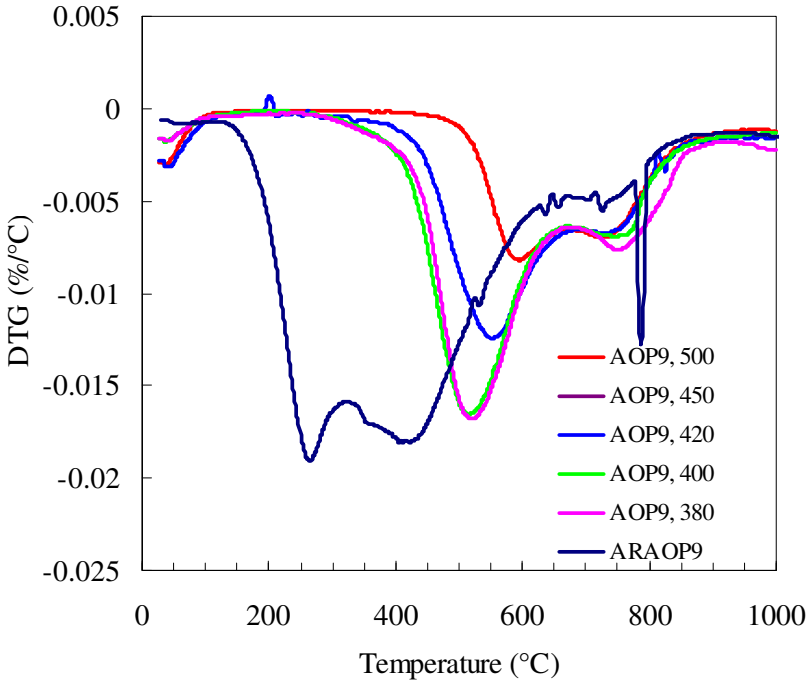

Figure 4.9(c): Derivative mass loss curves for ARAOP9 and heat-treated AOP9 under nitrogen, at 10 °C.min^{-1}

Key: AR: as-received; AOP: anthracene oil pitch; 9 is the number used to identify the AOP; the number in front of the codes is the heat-treatment temperature.

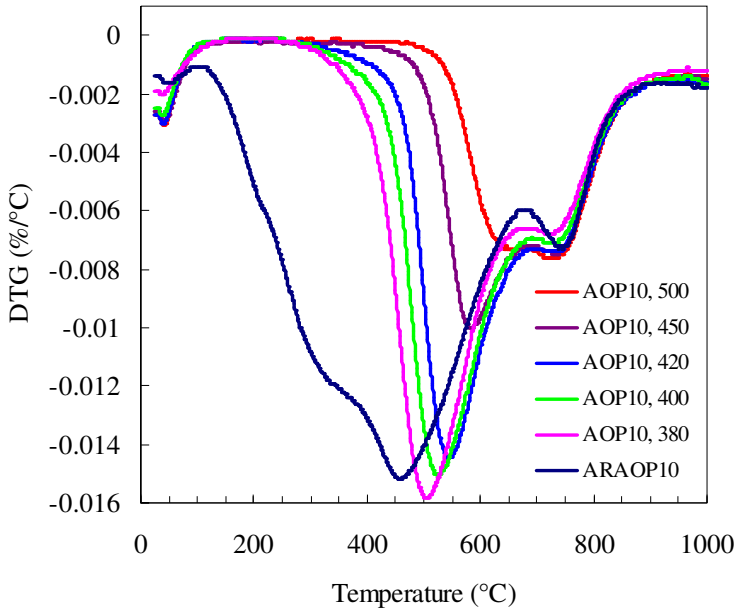

Figure 4.9(d): Derivative mass loss curves for ARAOP10 and heat-treated ARAOP10 under nitrogen, at 10 °C.min^{-1}

Key: AR: as-received; AOP: anthracene oil pitch; 10 is the number used to identify the AOP; the number in front of the codes is the heat-treatment temperature.

Figures 4.9(a-d) are the DTG curves of the pitches. They show that, relative to those of their as-received materials, the temperatures of maximum rate of mass loss (T_{max}) shift with heat-treatment temperature to higher temperatures in all pitches, except for ARAOP9. The temperature of maximum rate of mass loss occurs at higher temperatures for ARAOP9. It regresses with initial heat treatment and then shifts to a higher temperature as the heat treatment progresses. ARAOP10, AR90MP and ARSP and their heat-treated samples complete mass loss at approximately the same temperatures as their respective as-received materials. ARAOP9 does not finish mass loss at the same temperature as the heat-treated samples. Its first and fourth (final mass loss) peaks disappear with heat treatment. The second peak shifts to higher temperatures with heat treatment and the third one loses its intensity. The reaction that occurred in the previous heat treatment may have affected the behaviour of the residue, especially on the final mass loss (ARAOP9). High temperature bands are ascribed to the mass loss derived from the thermal condensation reactions.

4.7.1 The effect of the heating rate on thermal events

The effect of the heating rate on the thermal behaviour of pitches was also evaluated.

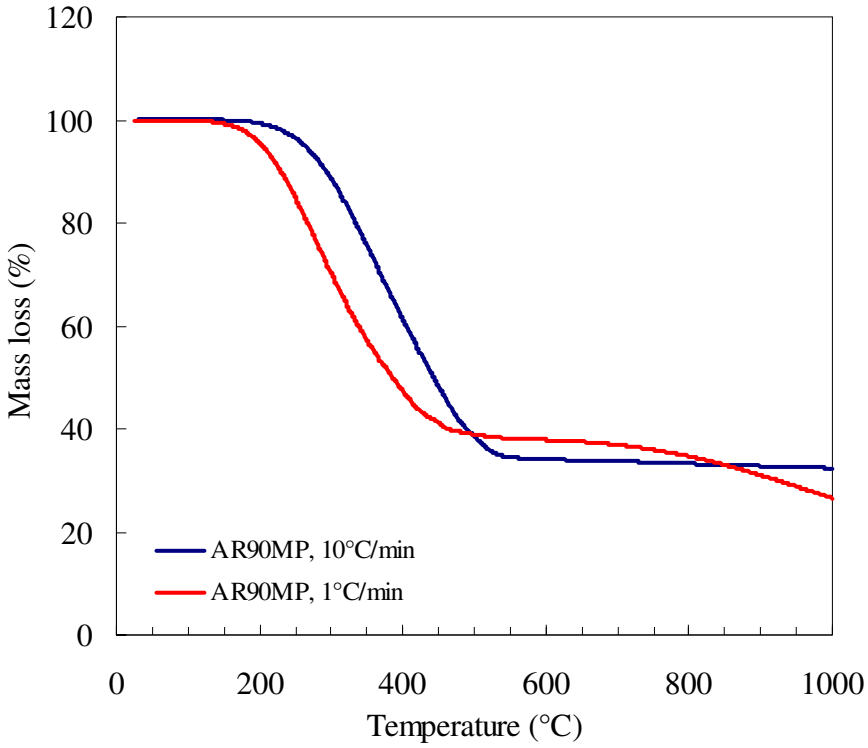

Figure 4.10: Thermogravimetric mass loss for AR90MP under nitrogen, at different heating rates, 10 °C.min^{-1} and 1 °C.min^{-1}

Key: AR: as-received; MP: Mittal pitch.

The TG curves in Figure 4.10 show that the carbon yield is greater at 10 °C.min^{-1} than at 1 °C.min^{-1}. The reason might be that, at lower heating rates, the exposure time at a given temperature is longer than at higher heating rates. A heating rate of 10 °C.min^{-1} as compared with 1 °C.min^{-1} displaces the mass loss onset temperature (T_{onset}) towards higher values. Bermejo *et al.* (1994) attributed this to thermal inertia. Heating at 1°C.min^{-1} also results in a lower mass loss endset temperature.

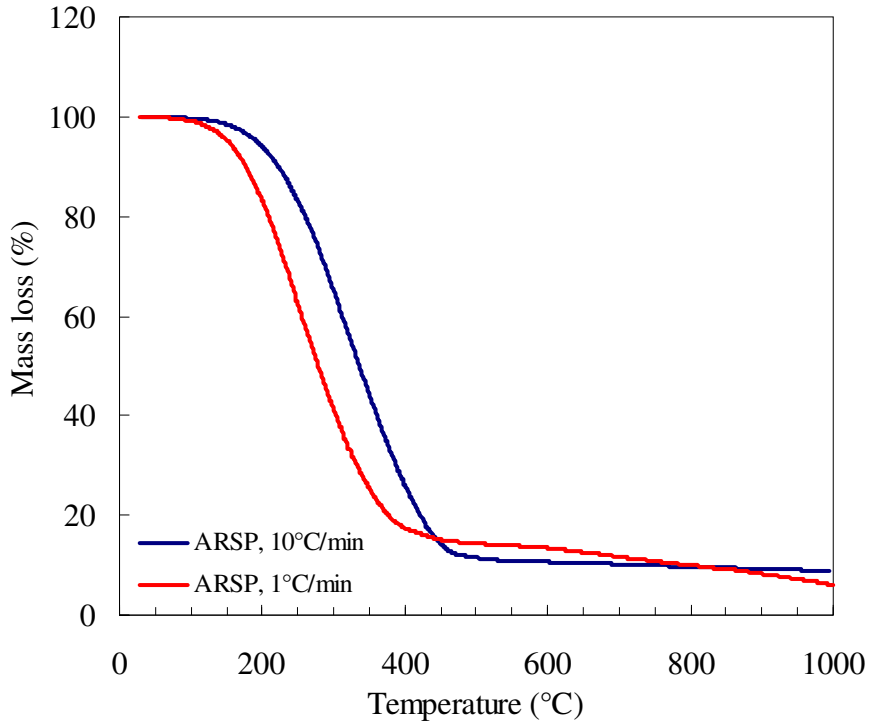

Figure 4.11: Thermogravimetric mass loss for ARSP under nitrogen, at different heating rates, 10 °C.min^{-1} and 1 °C.min^{-1}

Key: AR: as-received; SP: Sasol pitch.

Figure 4.11 illustrates that a heating rate of 1 °C.min^{-1} lowers the carbon yield. The mass loss onset and mass loss endset temperatures start and finish at lower temperatures (1 °C.min^{-1}).

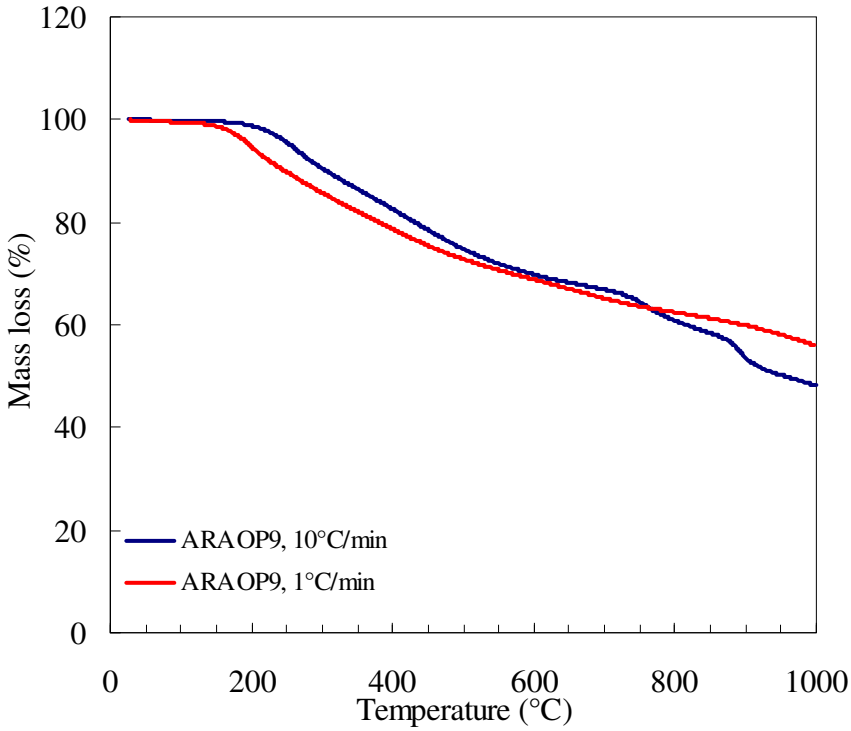

Figure 4.12: Thermogravimetric mass loss for ARAOP9 under nitrogen, at different heating rates, 10 °C.min^{-1} and 1 °C.min^{-1}

Key: AR: as-received; AOP: anthracene oil pitch; 9 is the number used to identify the AOP.

The TGA curves in Figure 4.12 show that at 1 °C.min^{-1}, the mass loss onset temperature start at lower temperatures but the carbon yield is higher at lower heating rate.

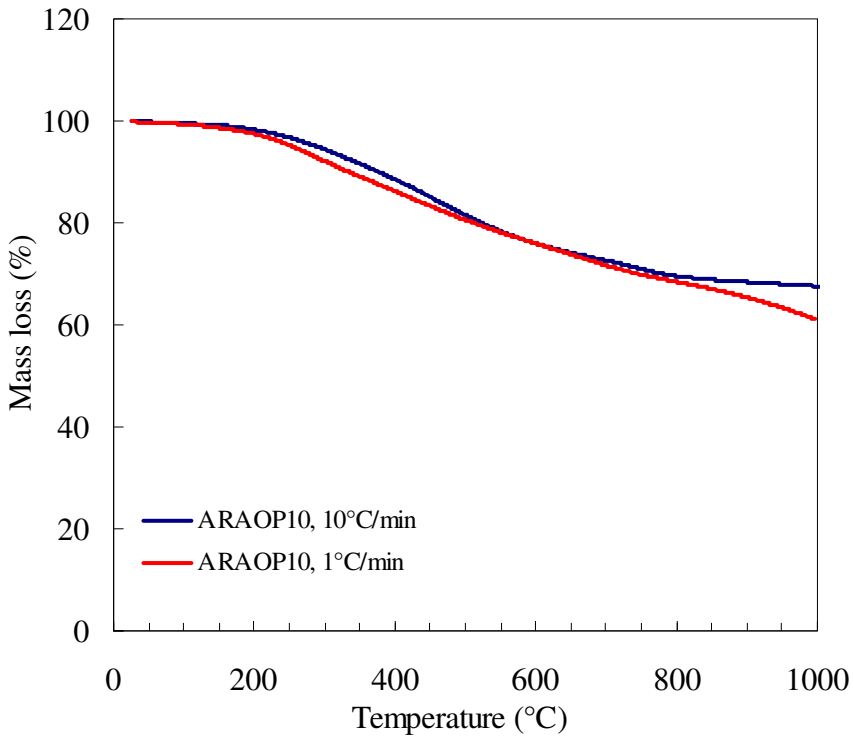

Figure 4.13: Thermogravimetric mass loss for ARAOP10 under nitrogen, at different heating rate, 10 °C.min^{-1} and 1 °C.min^{-1}

Key: AR: as-received; AOP: anthracene oil pitch; 10 is the number used to identify the AOP.

The TGA results in Figure 4.13 show that at a heating rate of 1 °C.min^{-1}, the mass loss onset temperature is lower. The heating rate of 1 °C.min^{-1} does not clearly show the mass loss endset temperature. The carbon yield is low at the lower heating rate.

4.8 Summary of Thermogravimetric Analysis

The thermal behaviour of pitches is dependent on the composition of a particular pitch. The more species of low molecular weight a pitch contains, the lower the carbon yield becomes. The thermal treatment history and the heating rate employed also have a profound effect on subsequent behaviour. They increase the carbon yield and shift the mass loss endset temperature and the temperature of maximum rate of mass loss to higher temperatures. Generally, a lower heating rate results in a low mass loss onset temperature, a low mass loss endset temperature and a low carbon yield. Therefore, from the perspective of carbon yield it is worthwhile to use a higher heating rate.

4.9 Thermogravimetric Mass Spectrometric Analysis (TG/MS)

TG/MS was used to get qualitative information about the evolution of the different volatiles produced during pyrolysis. Possible chemical reactions occurring during heat treatment are deduced from this and in this way information about the processes involved in mesophase formation is gathered. According to García *et al.* (2002), the most important products evolved during the pyrolysis process are H_2, CO, CO_2, H_2O and CH_4. They arrived at this conclusion from a literature on coal pyrolysis. Therefore the above species will also be considered in this study. García *et al.* (2002) noted that each compound (ion) detected in the mass spectrometer has its own response factor. Therefore the intensities of the same compound, released from different samples, can be compared. However, in the case of the intensities of different *m/z* signals, it is only possible to compare the shape and the characteristic temperatures of the peaks. The same interpretation is used in this study. It should also be noted that for each compound to be compared quantitatively or semi-quantitatively the signals must be normalized to the mass of the sample and the maximum of the total intensity of the experiment.

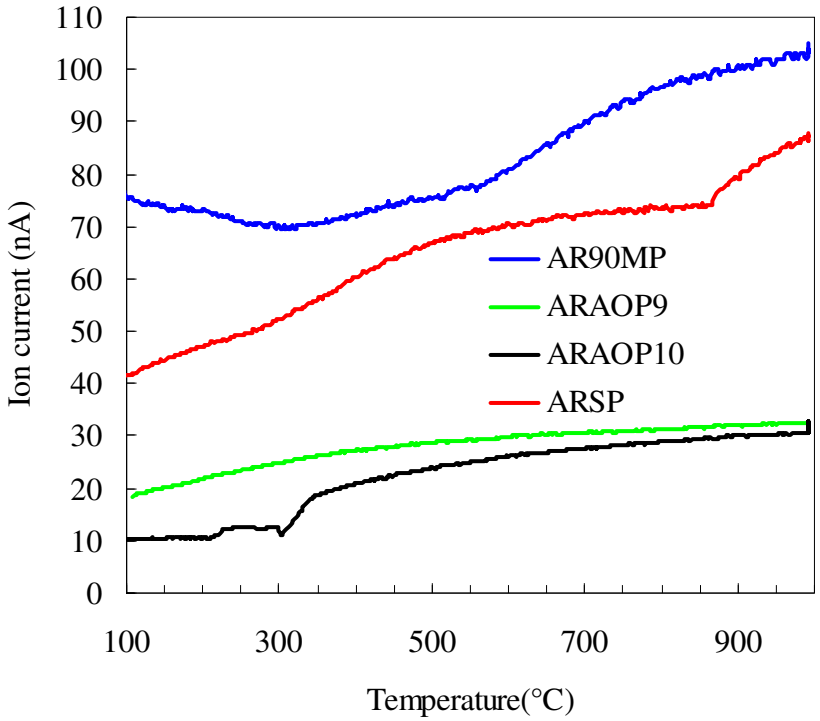

Figure 4.14: H_2 evolution profiles obtained under nitrogen, at 10 ^{o}C.min^{-1}

Key: AR: as-received; MP: Mittal pitch; SP: Sasol pitch; AOP: anthracene oil pitch; 9 and 10 are just numbers used to differentiate between the two AOPs.

In Figure 4.14 above, all the samples evolve hydrogen to differing extents, starting at different temperatures. They all evolve H_2 to up to 1 000 °C. The evolution of H_2 at high temperatures is due to the polyaromatic condensation reactions that occur in several superimposed stages (García *et al.,* 2002). The oxygen content is believed to play an important role in the release of H_2 at high temperatures. It is believed that the higher the oxygen content, the lower the H_2 emission due to the formation of H_2O (Arenillas *et al.*, 1999). The mechanism is thought to involve the formation of new cross-linkages between molecules by hydrogen abstraction to form H_2O and new C-C bonds (Mokoena *et al.,* 2008).

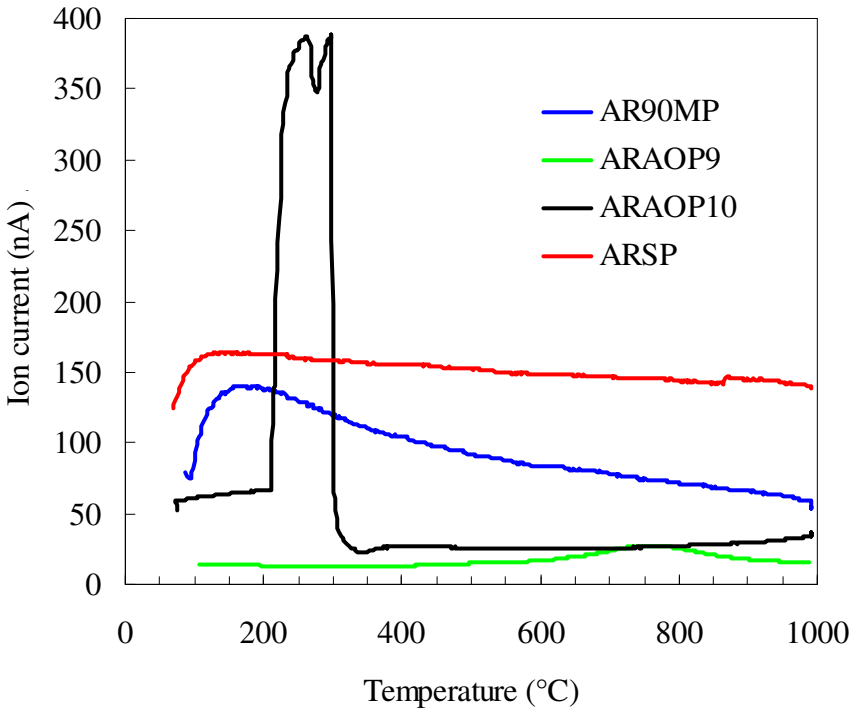

Figure 4.15: H_2O evolution profiles obtained under nitrogen, at 10 °C.min^{-1}

Key: AR: as-received; MP: Mittal pitch; SP: Sasol pitch; AOP: anthracene oil pitch; 9 and 10 are just numbers used to differentiate between the two AOPs.

Figure 4.15 presents the evolution of H_2O. AR90MP and ARSP evolve H_2O mainly at the temperatures that are characteristic of moisture present in the sample. Elemental analysis (Table 4.1) showed that ARSP and AR90MP contain both oxygen and hydrogen. The

mechanism suggested by Mokoena *et al*. (2008), i.e. the formation of H_2O by hydrogen abstraction, occurs to a lesser extent. It is mentioned in Section 4.3 that the decrease in oxygen is either due to oxygenated compounds of low molecular mass that evaporate during heat treatment or it is removed as decomposition products of thermal reactions. In this case it appears that the oxygen is lost mainly in compounds of low molecular mass and not as the products of thermal reactions. ARAOP9 and ARAOP10 support the idea of the formation of H_2O by hydrogen abstraction.

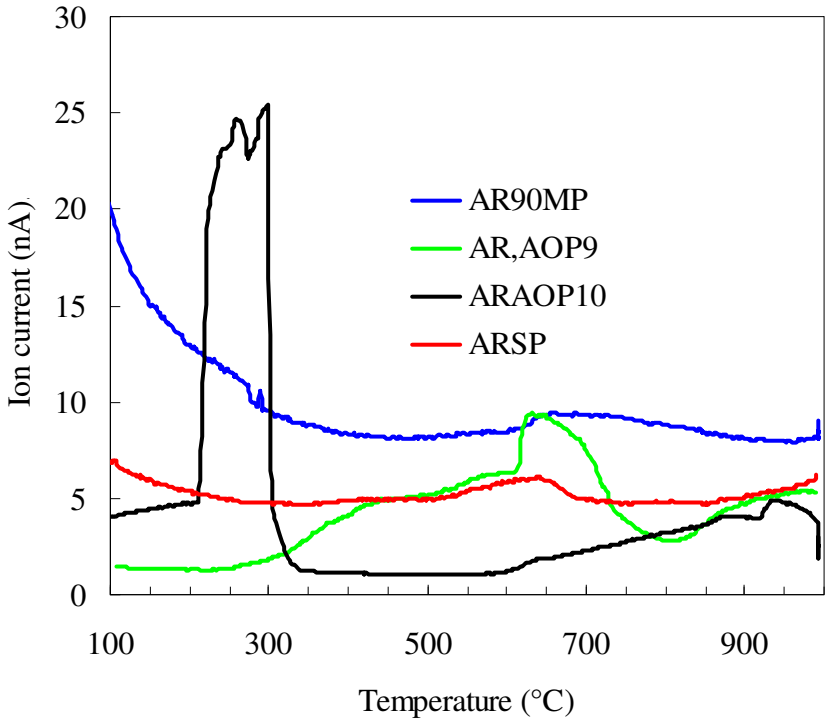

Figure 4.16: CO_2 evolution profiles obtained under nitrogen, at 10 °C.min^{-1}

Key: AR: as-received; MP: Mittal pitch; SP: Sasol pitch, AOP: anthracene oil pitch; 9 and 10 are just numbers used to differentiate between the two AOPs.

Figure 4.16 shows that CO_2 evolves at different temperatures, depending on the pitch. From the profile presented above, ARAOP10 evolved CO_2 at approximately the same temperature that it evolved H_2O. This means that several processes are taking place in this temperature range. Also, its second evolution peak starts at approximately 650 °C. At low temperatures (first evolution temperature), CO_2 is derived from aliphatic and aromatic carboxyl and carboxylate groups and at high temperatures (second evolution temperature), it is formed from thermally more stable ether structures, quinones and oxygen-bearing heterocycles (Arenillas *et al*., 1999). ARAOP9 reveals the

superimposition of evolution due to both carboxyl and carboxylate groups, whereas AR90MP and ARSP show evolution due to the ether structures, as seen previously from the FT-IR studies.

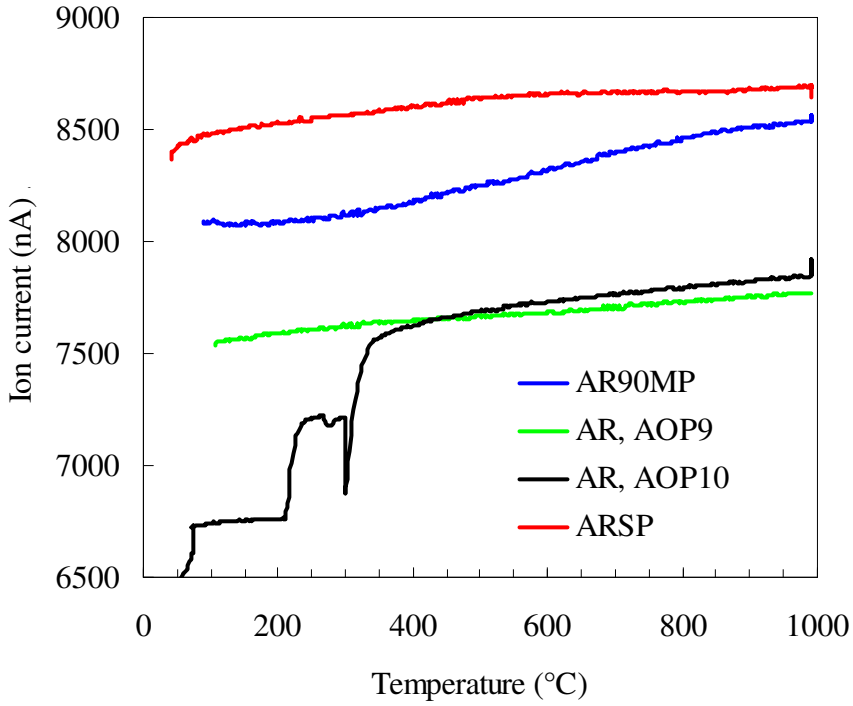

Figure 4.17: CO evolution profiles obtained under nitrogen, at 10 °C.min^{-1}

Key: AR: as-received; MP: Mittal pitch; SP: Sasol pitch; AOP: anthracene oil pitch; 9 and 10 are just numbers used to differentiate between the two AOPs.

Figure 4.17 shows the CO evolution profile. All samples evolve CO up to 1 000 °C. The evolution of CO at high temperatures (>600 °C) indicates the occurrence of important aromatic condensation reactions (García *et al.,* 2002). Figure 4.14 also showed that H_2 evolves up to 1 000 °C and that the evolution of H_2 at high temperatures is due to condensation reactions, supporting the possibility of such reactions. These reactions occur until the end of the run.

The acid anhydrides and phenols are believed to account for CO formation. The mechanism is thought to evolve phenoxy radicals derived from phenol which react with methane and rearrange to release CO (García *et al.,* 2002).

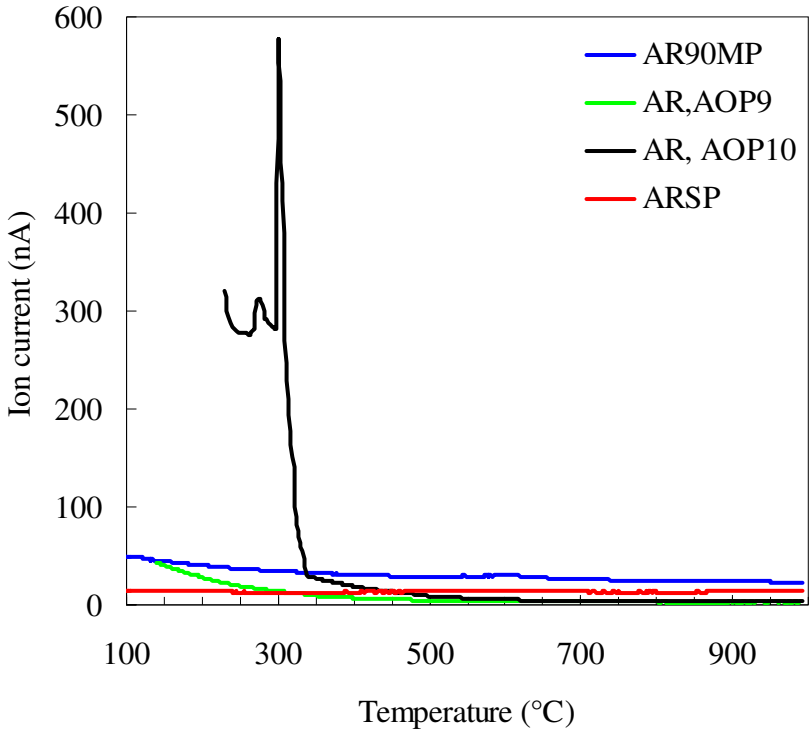

Figure 4.18: CH_4 evolution profiles obtained under nitrogen, at 10 °C.min^{-1}

Key: AR: as-received; MP: Mittal pitch; SP: Sasol pitch; AOP: anthracene oil pitch; 9 and 10 are just numbers used to differentiate between the two AOPs.

Figure 4.18 shows the CH_4 evolution profiles. The thermal decomposition of aliphatic groups is responsible for the evolution of CH_4 (García *et al.,* 2002) or it may be due to the cross-linking of hydroaromatic and aryl methyl groups (Arenillas *et al.*, 1999). Surprisingly, ARSP releases virtually no methane, although the FT-IR analysis (Figure 4.1) shows that it contains some aliphatic groups.

The mechanism of CO evolution during pyrolysis discussed above might be responsible for the lack of methane release. The evolution of CH_4 is considerably higher in as-received AOP10, but its release ends at approximately 340 °C. Most of its species evolve significantly in this temperature range, probably because it is very reactive in this range. This behaviour does not favour mesophase formation.

4.10 Summary of Thermogravimetric Mass Spectrometric Analysis

The temperature of evolution of the same species differs from pitch to pitch, indicating that the pitches studied react differently. These differences probably emanate from their

different chemical compositions and from the different chemical reactions occurring during transformation. In all the pitches H_2O, CO_2 and CH_4 do not evolve at the same temperatures. H_2 and CO also evolve to different extents. The dominant reaction among all the pitches is the condensation reaction, which is accompanied by the evolution of H_2 and CO.

4.11 Optical Microscopy

The structure of resultant green cokes was studied by means of the optical texture of polished surfaces of the samples using optical microscopy. The formation of mesophase in different pitches, which received identical treatments (same pyrolysis series), was examined to compare the development of mesophase, growth and coalescence.

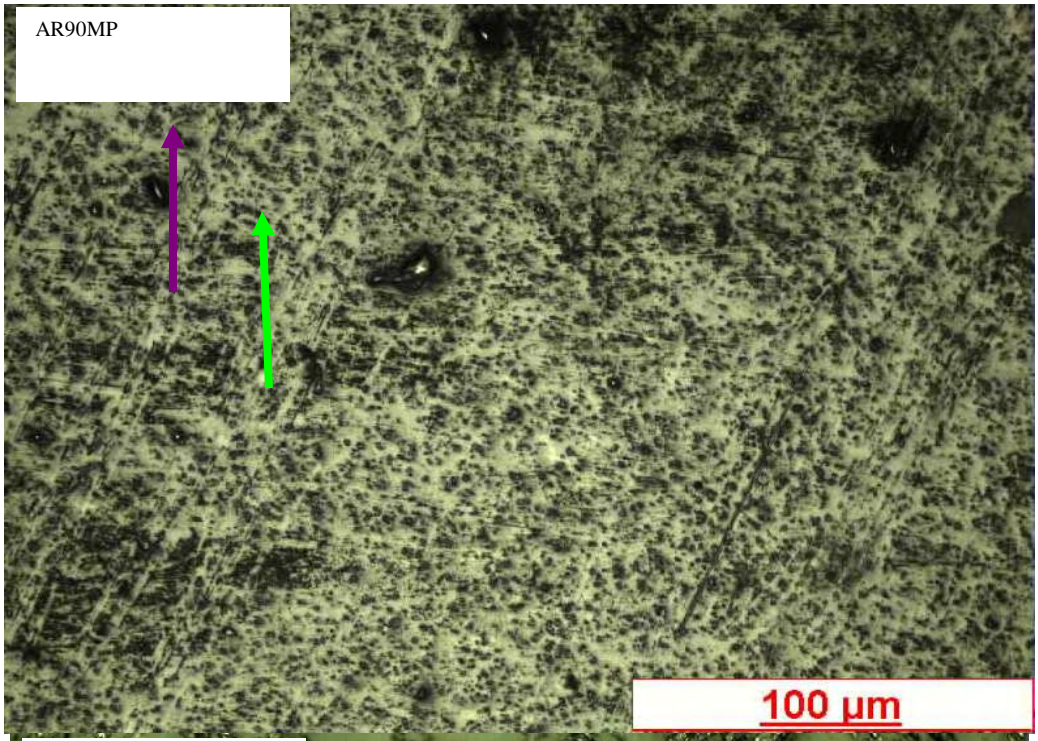
AR90MP
100 µm


90MP380
50 µm

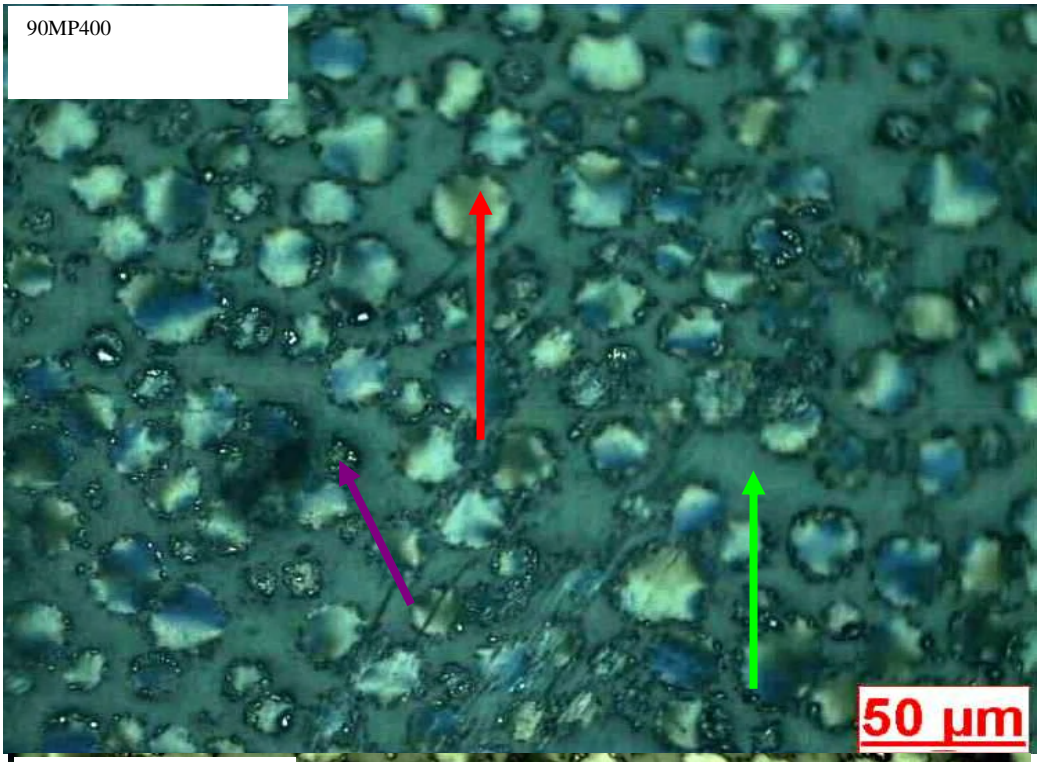
90MP400
50 µm

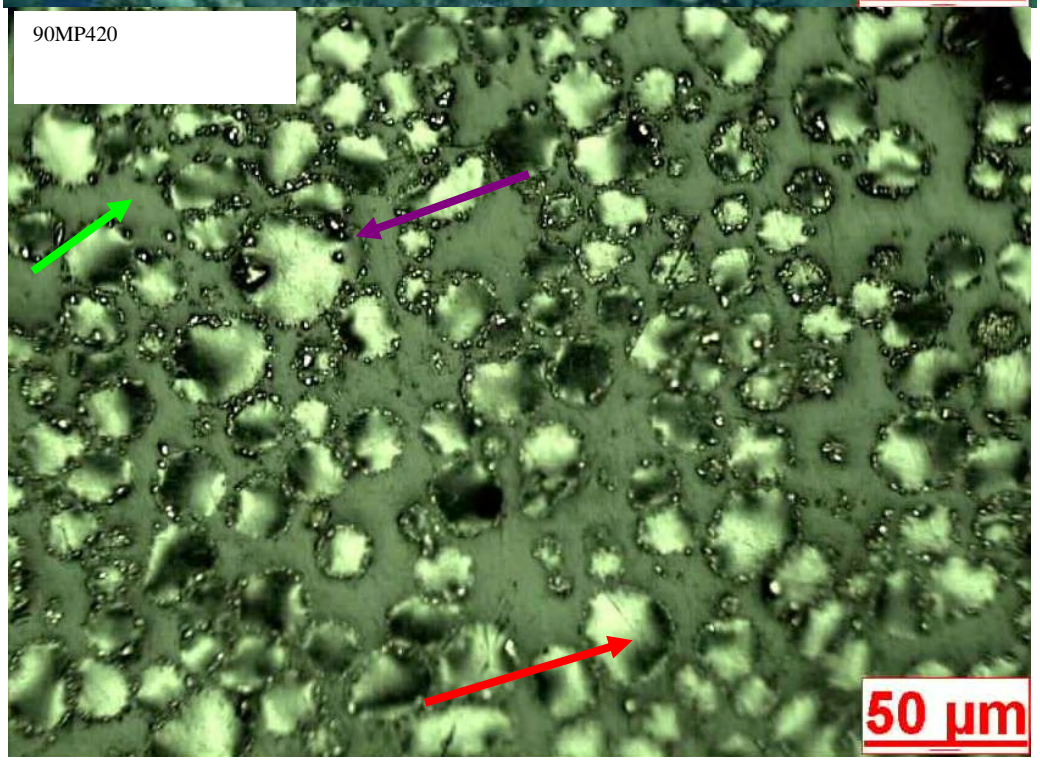
90MP420
50 µm

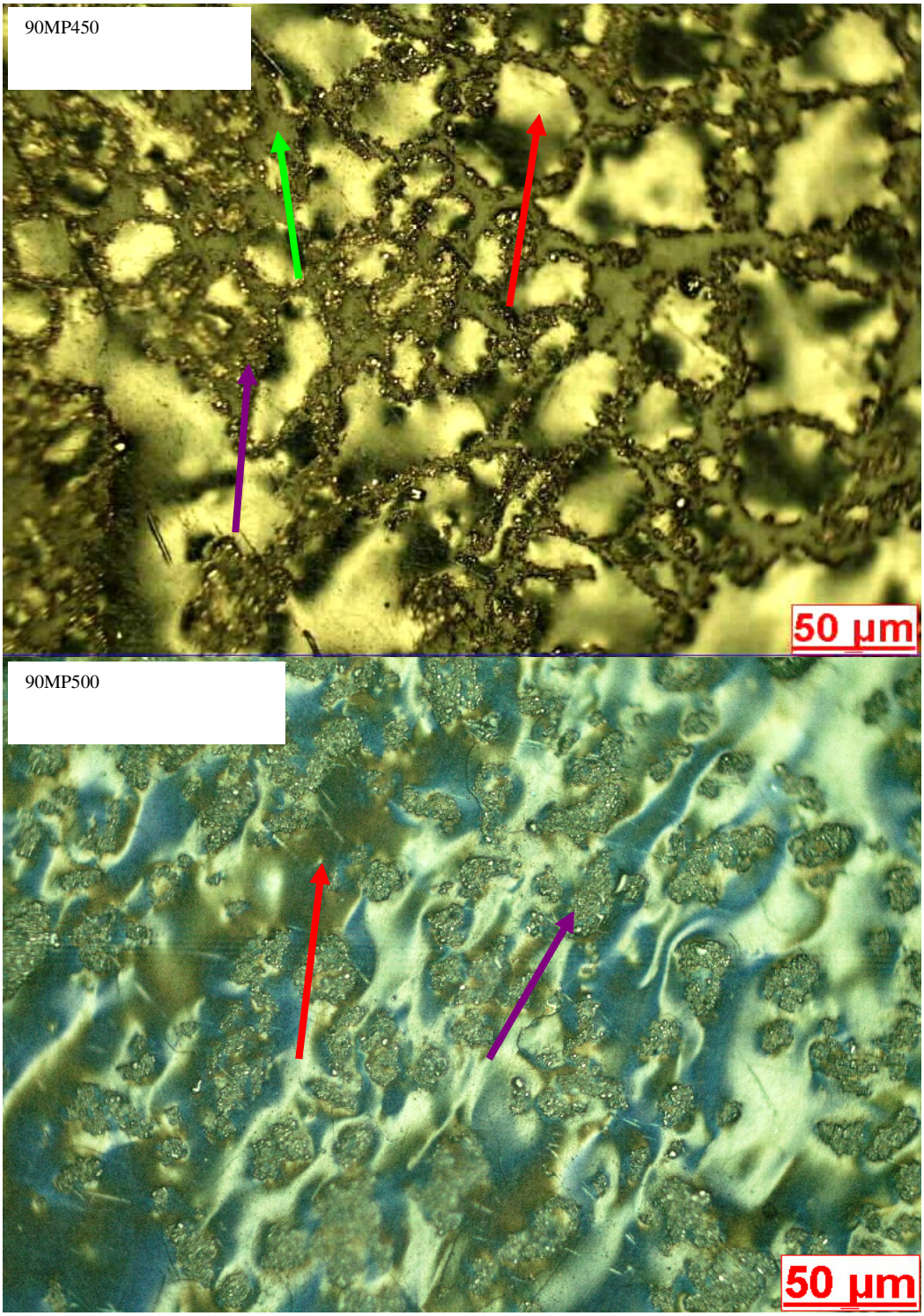

Figure 4.19: Optical micrographs of as-received material and green cokes obtained by pyrolysis of 90MP to different temperatures

Key: AR: as-received; MP: Mittal pitch; the number in front of the codes is the heat-treatment temperature; isotropic phase (green arrow); quinoline insolubles (purple arrow); and mesophase (red arrow). Note: Microscopic analysis was conducted on each sample using a microscope under polarized light and retarder plate

The micrographs in Figure 4.19 show that all the samples contain quinoline insolubles (QI). The micrographs of the heat-treated pitch samples show that 90MP380 is still isotropic, although it has a high C/H ratio. This means that the polyaromatic hydrocarbons (PAHs) present in the pitch do not reach adequate size and molecular structure to allow mesophase formation at this temperature. 90MP400 contains mesophase, with the QI at the periphery of the mesophase spherules. However, in spite of the presence of QI in the system, the spheres coalesce (90MP450); parts of them flow at 500 °C but the flow of the other parts is disrupted by the QI that formed agglomerates and were excluded from the mesophase.

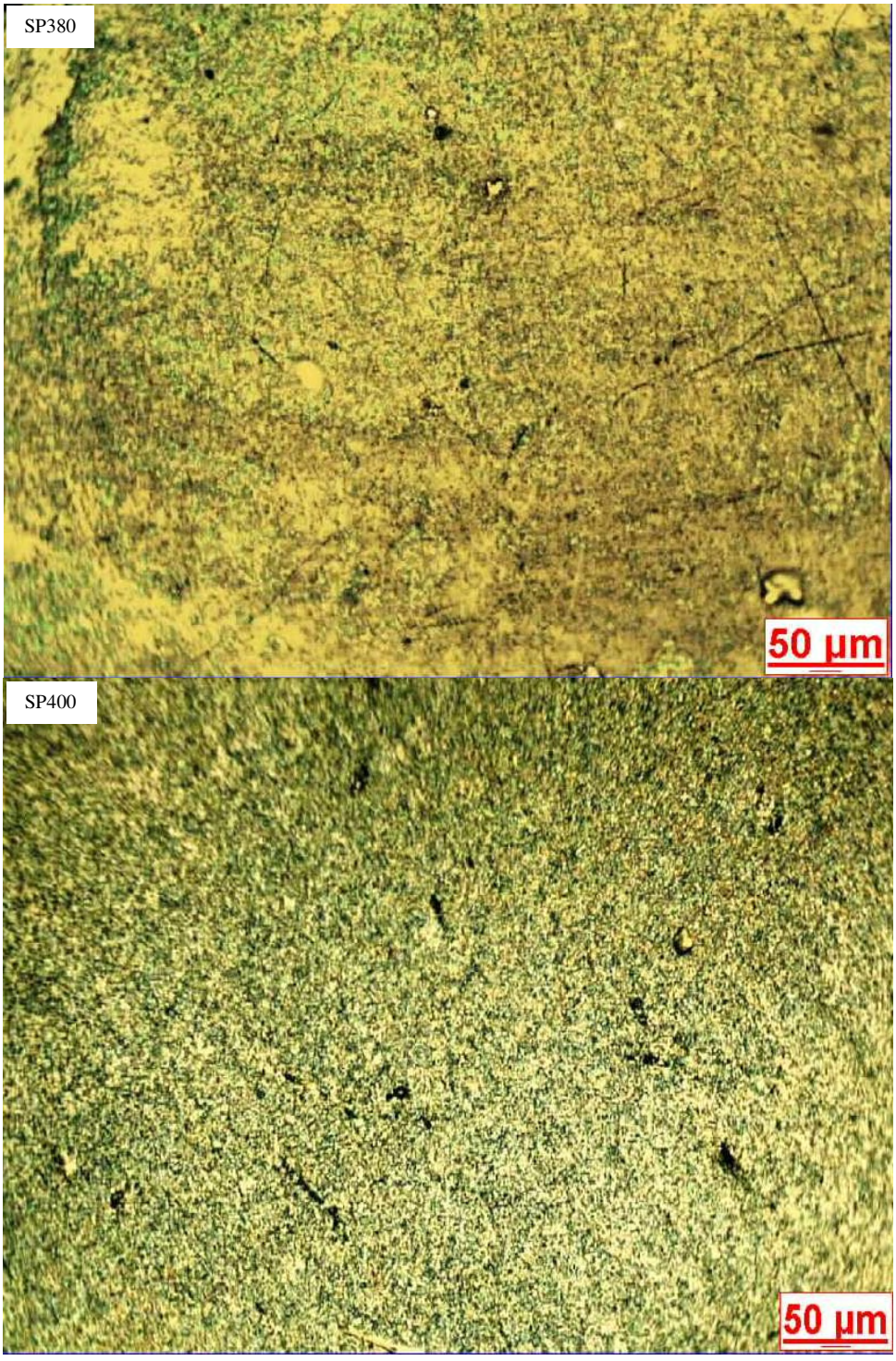
SP380
50 µm
SP400
50 µm


SP420
50 µm

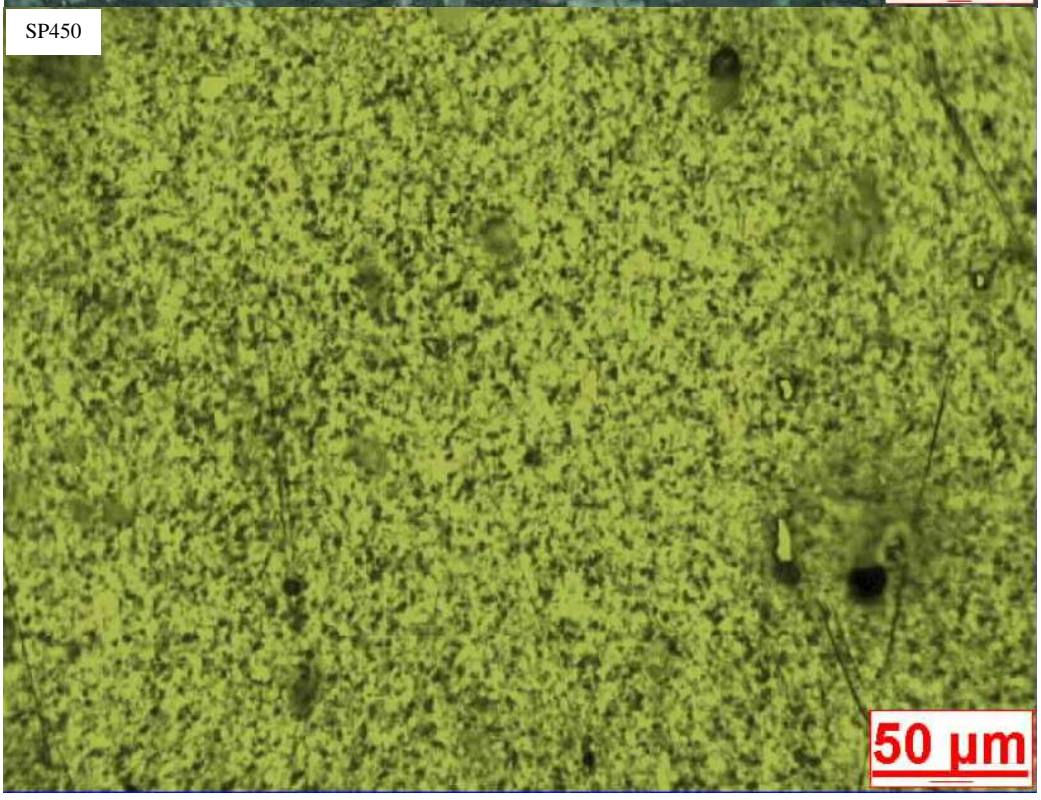
SP450
50 µm

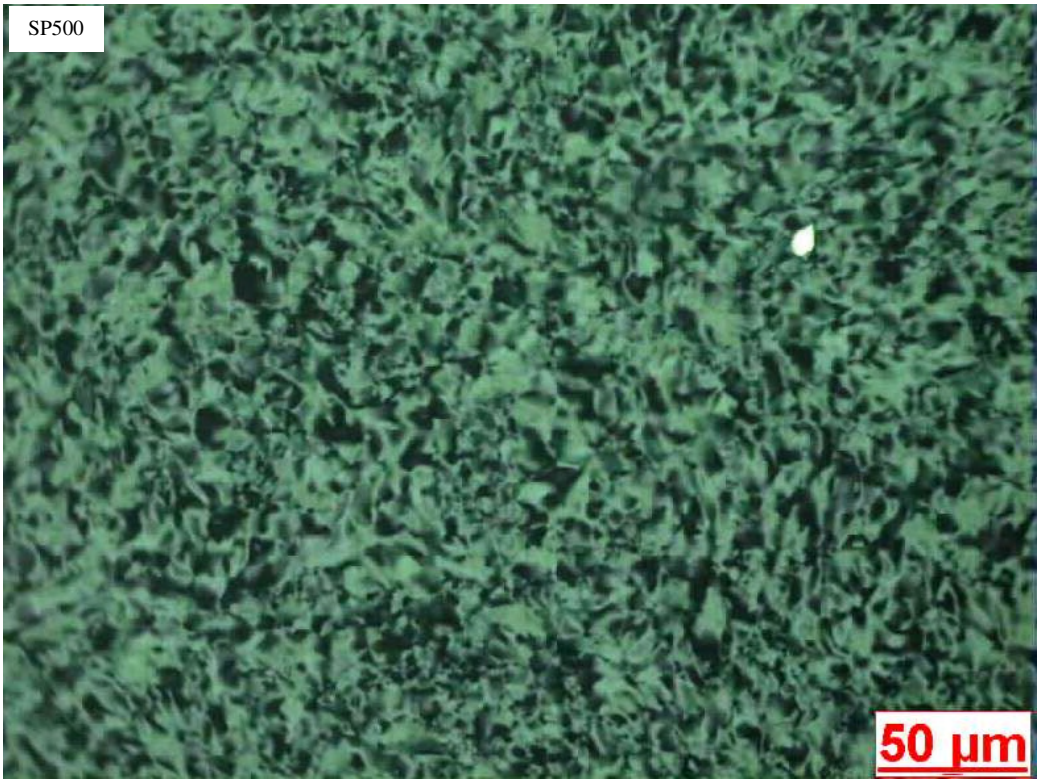

Figure 4.20: Optical micrographs of green cokes obtained by pyrolysis of SP to different temperatures

Key: SP: Sasol pitch; the number in front of the codes is the heat-treatment temperature; isotropic phase (green arrow) and mesophase spheres (red arrow). Note: ARSP is not included because the nature of the sample does not allow polishing. Note: Microscopic analysis was conducted on each sample using a microscope under polarized light and retarder plate.

The micrographs in Figure 4.20 indicate that SP380 has fine mosaic anisotropy, apart from its low C/H ratio of 1.57, which is the reflection of the aromaticity of the system. The optical texture improves with increasing heat-treatment temperature (SP400 shows fine-grained mosaic and SP420 shows mesophase spheres). The micrograph of SP450 shows that the domains and the texture improve further on heat treatment, forming coarser domains (SP500).

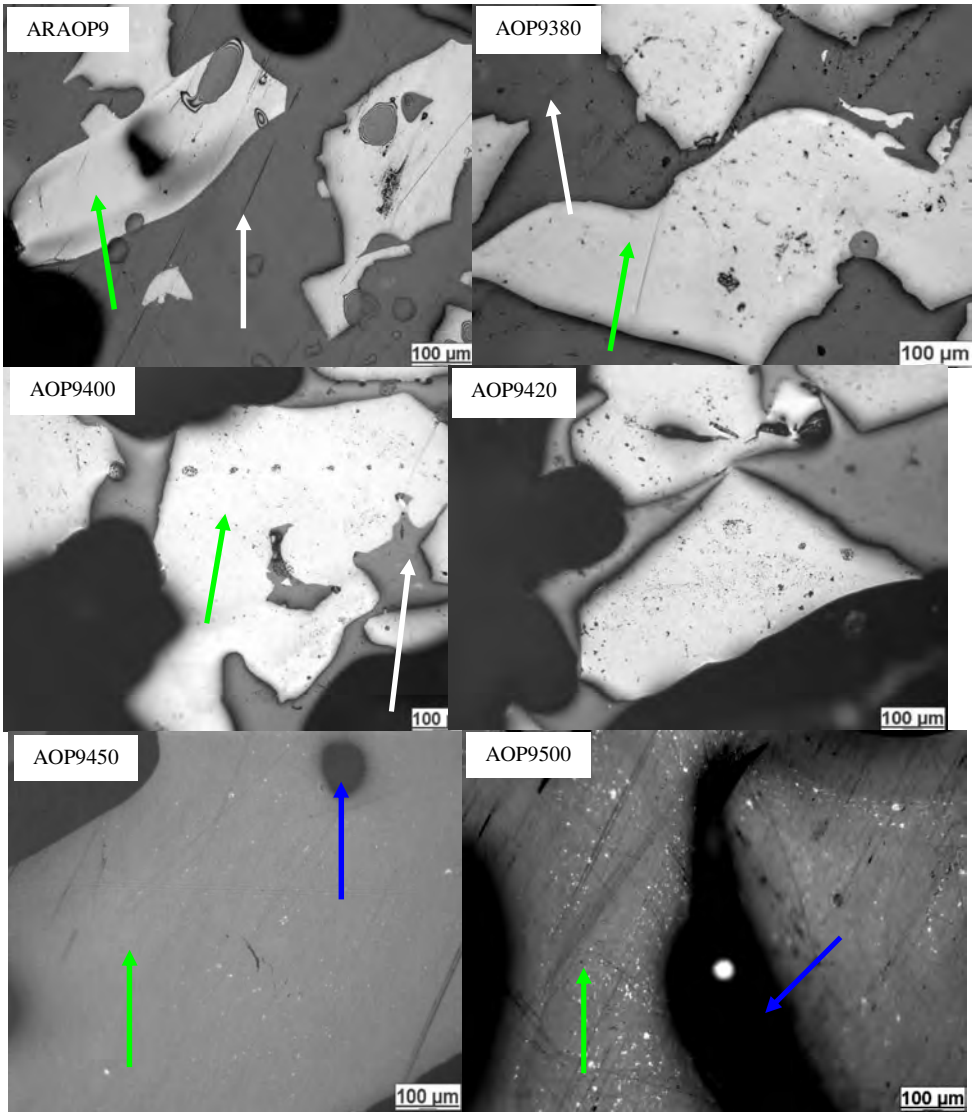

Figure 4.21: Optical micrographs of as-received material green cokes obtained by pyrolysis of AOP9 to different temperatures

Key: AR: as-received; AOP: anthracene oil pitch; the number in front of the codes is the heat-treatment temperature; isotropic phase (green arrow); resin (white arrow); and pore (blue arrow). Note: Microscopic analysis was conducted on each sample using a microscope under normal light (no polarizer).

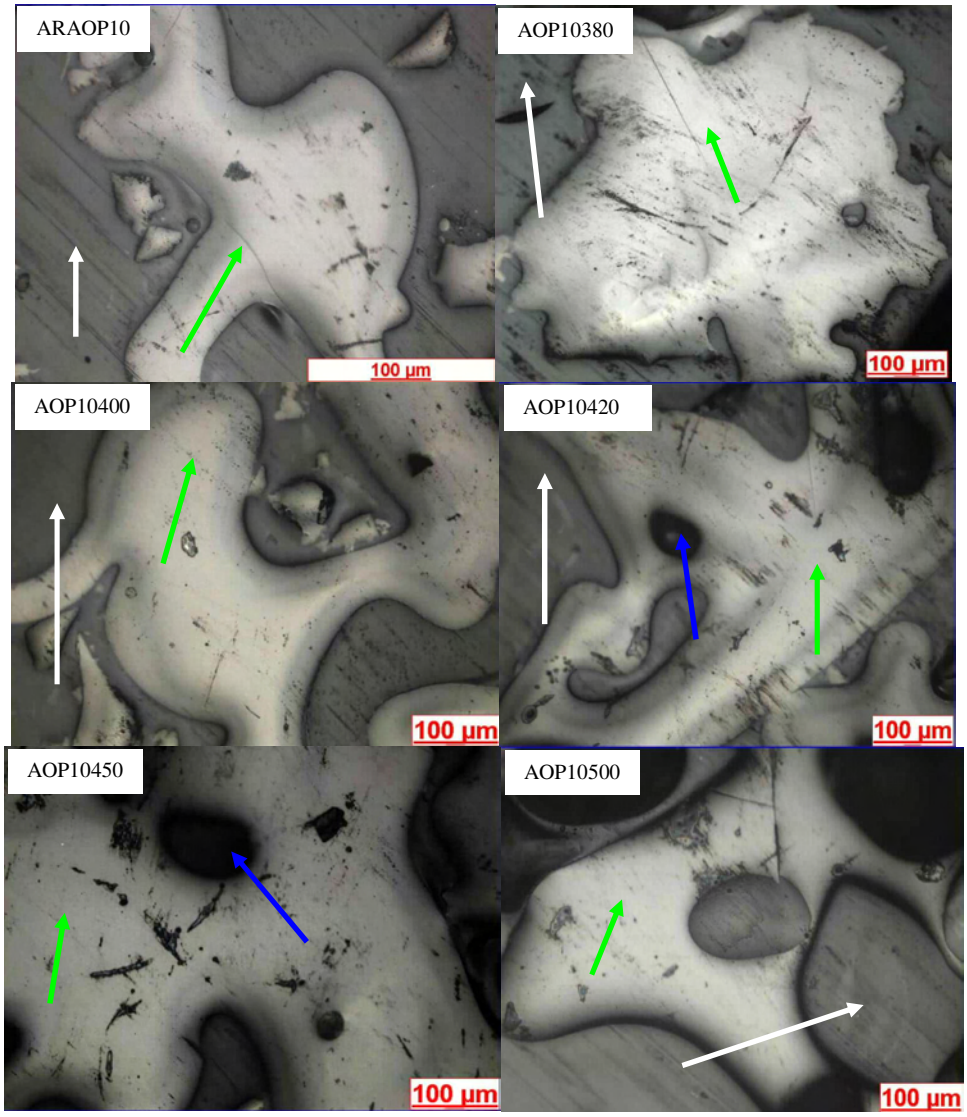

Figure 4.22: Optical micrographs of as-received material and green cokes obtained by pyrolysis of AOP10 to different temperatures

Key: AR: as-received; AOP: anthracene oil pitch; the number in front of the codes is the heat-treatment temperature; isotropic phase (green arrow); resin (white arrow); and pore (blue arrow). Note: Microscopic analysis was conducted on each sample using a microscope under normal light (no polarizer).

The micrographs of the all the AOPs (AOP9 and AOP10) do not show any anisotropy (no mesophase development). It is mainly oxygen that is responsible for this behaviour. AOP9 and AOP10 have oxygen contents of 7.58 and 7.00 respectively. The lack of mesophase is consistent with Weinberg *et al.*'s (1998) finding that a precursor needs to have 2 to 6% by weight of oxygen for it to develop mesophase. A high oxygen content is thought to result from harsh treatment during the preparation of the pitch. It is believed to form cross-links that will not allow the planar molecules to form (Ruland, 1965).

4.12 Summary of Optical Microscopy Findings

The results show that although SP and 90MP do form mesophase, the nature of their mesophases and how they improve differ dramatically. SP improves from fine-grained mosaic anisotropy at 380 °C to coarse domains at 500 °C. On the other hand, 90MP is still isotropic at 380 °C and starts to show mesophase spheres at 400 °C; the spheres coalesce at 450 °C and flow at 500 °C. Another major difference between these two pitches is that SP is fully mesophase at between 450 and 500 °C (no QI), whereas 90MP (with QI) only becomes completely mesophase at 500 °C. There is also a dramatic change in the optical texture of SP from 420 to 450 °C, as opposed to the gradual change observed in 90MP. The AOPs do not form mesophase, probably because of their high oxygen contents resulting from harsh treatment during their preparation.

4.13 Transformation Diagrams

Transformation diagrams are used to give details of the transition from pitch to green coke. They offer the opportunity to relate certain parameters to the extent of pyrolysis.

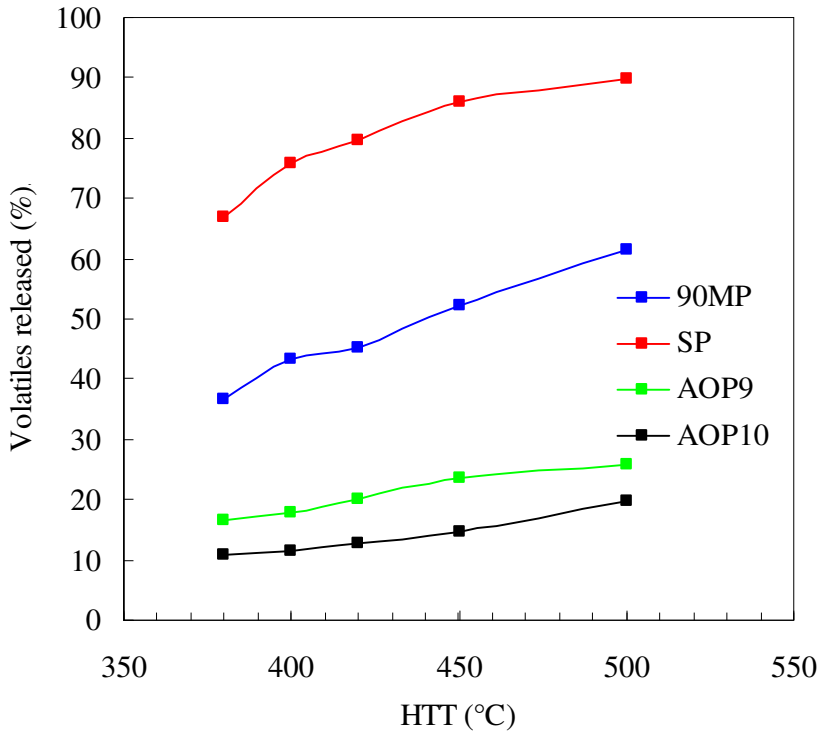

Figure 4.23: Curves of green-coke yield vs heat-treatment temperature (HTT)

Key: MP: Mittal pitch; SP: Sasol pitch; AOP: anthracene oil pitch; 9 and 10 are just numbers used to differentiate between the two AOPs. Note: For each final temperature, holding time was one hour.

Figure 4.23 show the percentages of volatiles released vs. heat-treatment temperature (HTT). This property is used to measure of the degree of pyrolysis that has occurred. The figure also shows that these pitches have different compositions of low-molecular-mass species. The volatiles released are simply: 100% minus the green-coke yield. (The green-coke yield is the residual mass obtained at a particular heat-treatment temperature divided by the initial mass of the pitch multiplied by 100%). Their values are presented in Appendix A, Tables A5 to A8. The percentages of volatiles released are low at low heat-treatment temperature and high at high heat-treatment temperature. Figure 4.23 also depicts that at a given heat-treatment temperature, the pitches do not show the same percentages of volatiles released. These are released in the following order: SP > 90MP > AOP9 > AOP10.

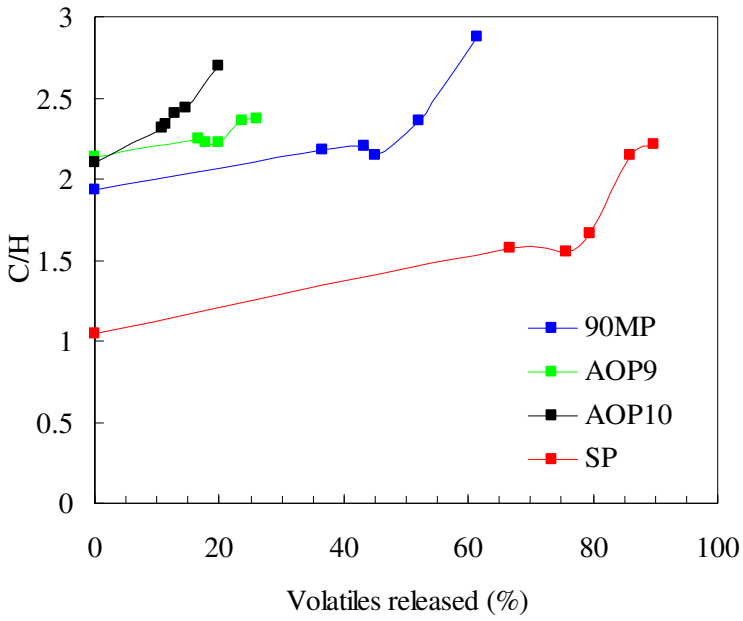

Figure 4.24: Relationship between C/H ratio and volatiles released

Key: MP: Mittal pitch; SP: Sasol pitch; AOP: anthracene oil pitch; 9 and 10 are just numbers used to differentiate between the two AOPs. Note: the C/H points where x equals zero are for the as-received materials, each line represents members of the pyrolysis series for each pitch studied.

Figure 4.24 illustrates that the C/H ratio and the volatiles released have a positive correlation, so that the more volatile matter is removed, the more aromatic the residue becomes. In spite of the lower aromaticity of 90MP as compared with the AOPs, 90MP becomes more aromatic than the rest of the pitches at 500 °C. The graphs also emphasise the observations made regarding Figure 4.23.

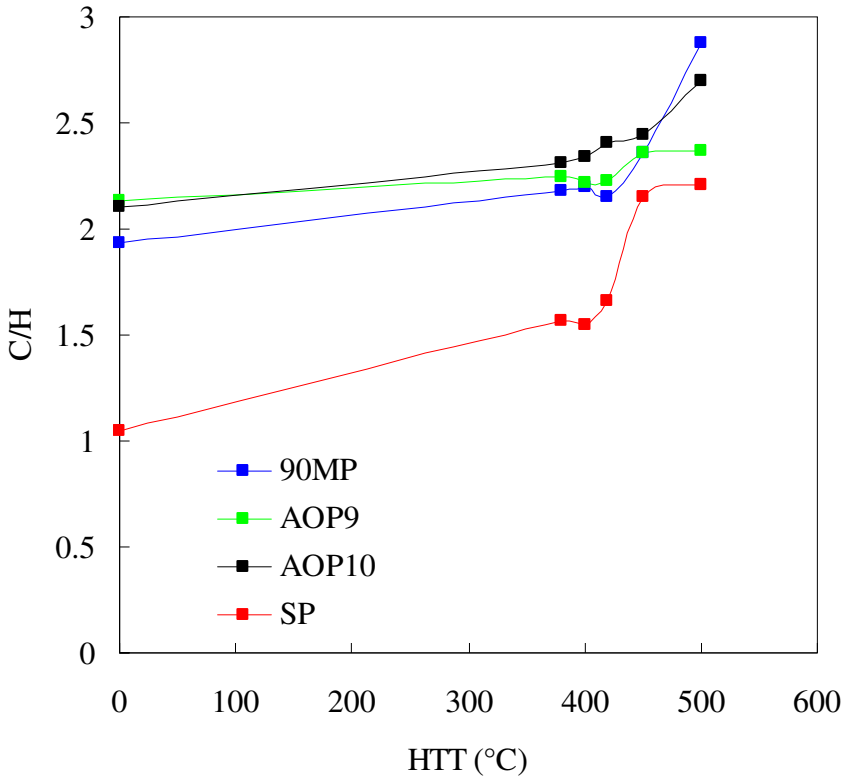

Figure 4.25: Relationship between C/H ratio and heat-treatment temperature (HTT)

Key: MP: Mittal pitch; SP: Sasol pitch; AOP: anthracene oil pitch; 9 and 10 are just numbers used to differentiate between the two AOPs; HTT: heat-treatment temperature. Note: the C/H ratio points where x equals zero are for the as-received materials; each line represents members of the pyrolysis series for each pitch studied.

Figure 4.25 shows that in all the pitches studied the C/H ratio increases as pyrolysis progresses. Evaporation and the thermal condensation reactions that take place during thermal treatment are thought to be responsible for the change in the C/H ratio. The curves are more or less the same, but differ in terms of the aromaticity of the pitches and of their heat-treatment products. The C/H ratio of 90MP increases steadily and surpasses that of the AOPs, which start off at higher C/H ratios. This ratio changes significantly from 450 to 500 °C. Although the aromaticity of SP also changes significantly, it has the lowest C/H ratio. The region of significant change is >400 °C.

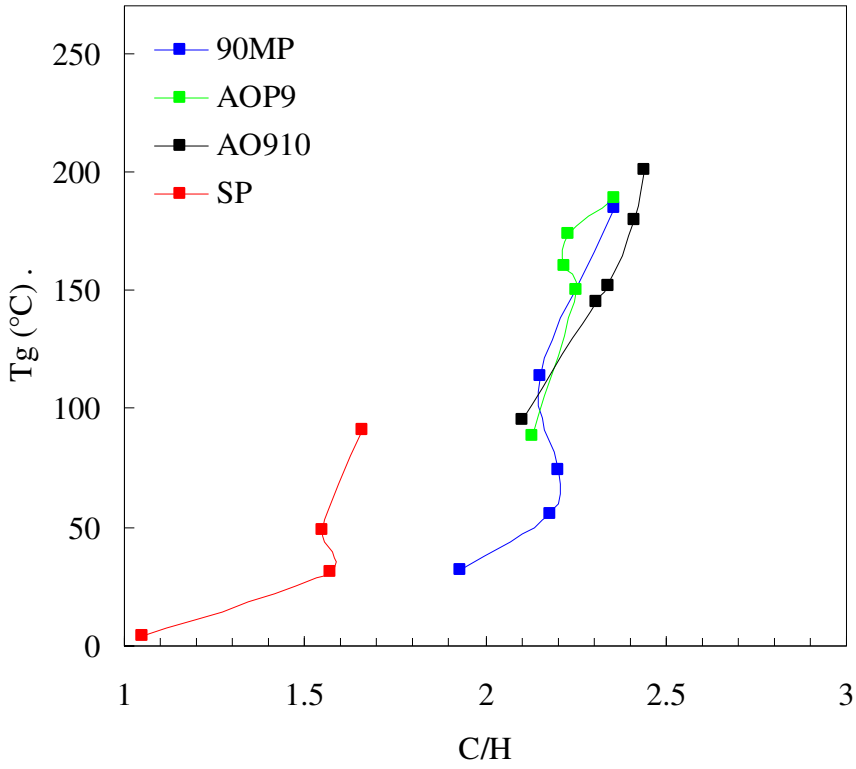

Figure 4.26: Relationship between glass transition temperature (Tg) and C/H ratio

Key: MP: Mittal pitch; SP: Sasol pitch; AOP: anthracene oil pitch; 9 and 10 are just numbers used to differentiate between the two AOPs. Note: Some Tg points are omitted due to difficulty in locating them; the C/H ratio points where x equals zero are for the as-received materials; each line represents members of the pyrolysis series for each pitch studied.

Figure 4.26 shows that the glass transition temperature (Tg) of each pitch increases as its C/H ratio increases. These curves in turn also give information about the relationship between the aromaticity and the glass transition temperature. The more aromatic the pitch becomes, the higher the glass transition temperature. The three pitches (90MP and the two AOPs) show more or less similar dependence of Tg on the C/H ratio. However, the relationship for SP is significantly different. It shows a considerably stronger dependence of Tg on the C/H ratio. The significant change is observed from the first point to the second, when there is a noteworthy change in composition.

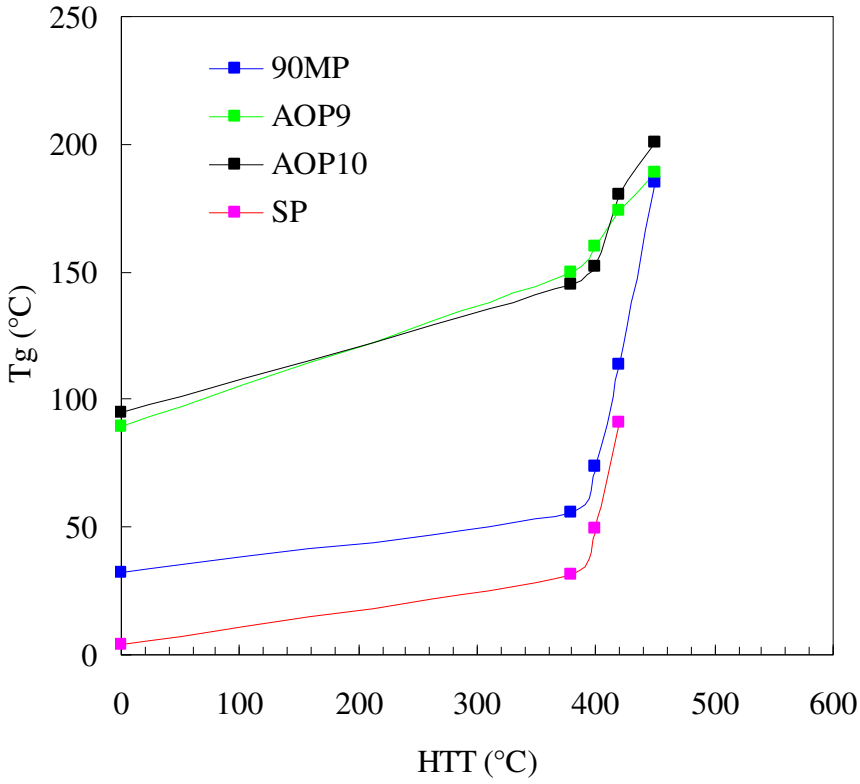

Figure 4.27: Change in glass transition temperature (Tg) and heat-treatment temperature (HTT)

Key: MP: Mittal pitch; SP: Sasol pitch; AOP: anthracene oil pitch; 9 and 10 are just the numbers used to differentiate between the two AOPs; HTT: heat-treatment temperature; Tg: glass transition temperature. Note: Some Tg points are omitted due to difficulty in locating them; the Tg points where x equals zero are for the as-received materials; each line represents members of the pyrolysis series for each pitch studied.

Figure 4.27 illustrates the change in glass transition temperature (Tg) as a function of heat-treatment temperature. At the reaction temperatures used, all systems are well above their respective glass transition temperatures. The AOPs have glass transition temperatures much higher than those of SP and 90MP. They are expected to have much higher viscosities at the reaction temperatures. High viscosities at reaction temperatures result in lack of mesophase development. This could be the reason why both the AOPs have isotropic textures.

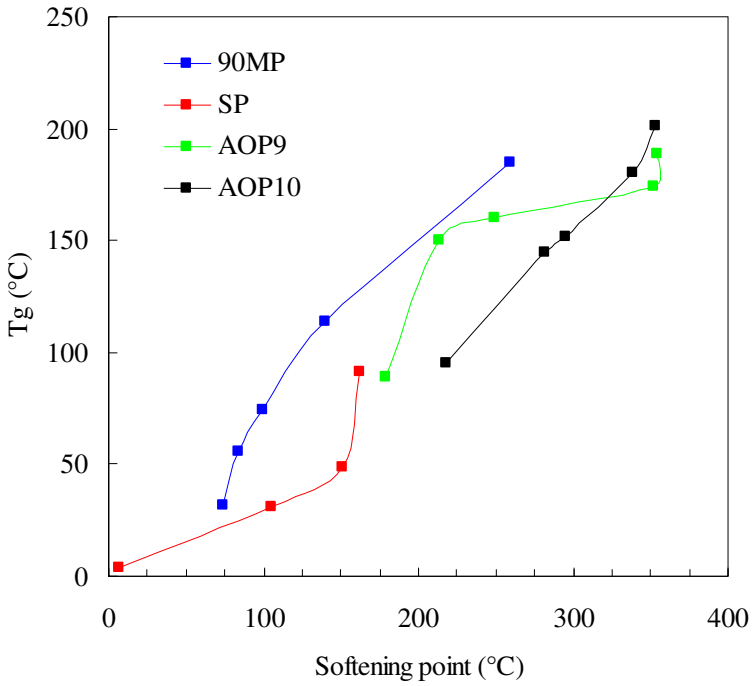

Figure 4.28: Relationship between glass transition temperature (Tg) and softening point temperature (Ts)

Key: MP: Mittal pitch; SP: Sasol pitch; AOP: anthracene oil pitch; 9 and 10 are just the numbers used to differentiate between the two AOPs; each line represents members of the pyrolysis series for each pitch studied.

Figure 4.28 presents the glass transition temperature (Tg) and the softening point temperature (Ts). It shows that they have a positive correlation. Barr & Lewis (1982) found that the glass transition temperature value has a fixed relation to the softening point temperature. They found that Tg is 80% of Ts and came up with an equation to explain this relation (Tg/Ts = 0.80). Khandare *et al.* (1996), on other hand, found that such correlations depend on the approach, i.e. they depend on the position (on the curve) at which the points are taken. They reported that Tg is 89% of Ts. None of the results presented here are in agreement with either of these claims. The correlation coefficient for each pitch is given in Appendix A, Table A10. Barr & Lewis (1982) used TMA (penetration mode) and DSC to determine the Tg, whereas Khandare *et al.* (1996) used the dilatometery approach. The TMA results were only 3 to 5 °C lower than those of DSC. This suggests that the correlation depends on the technique used or on the probe if the same technique is used. In this study the same technique and the same probe were used for Tg determination. However, the correlation amongst the pitches studied still differed. This suggests that the correlation also depends on the pitch studied.

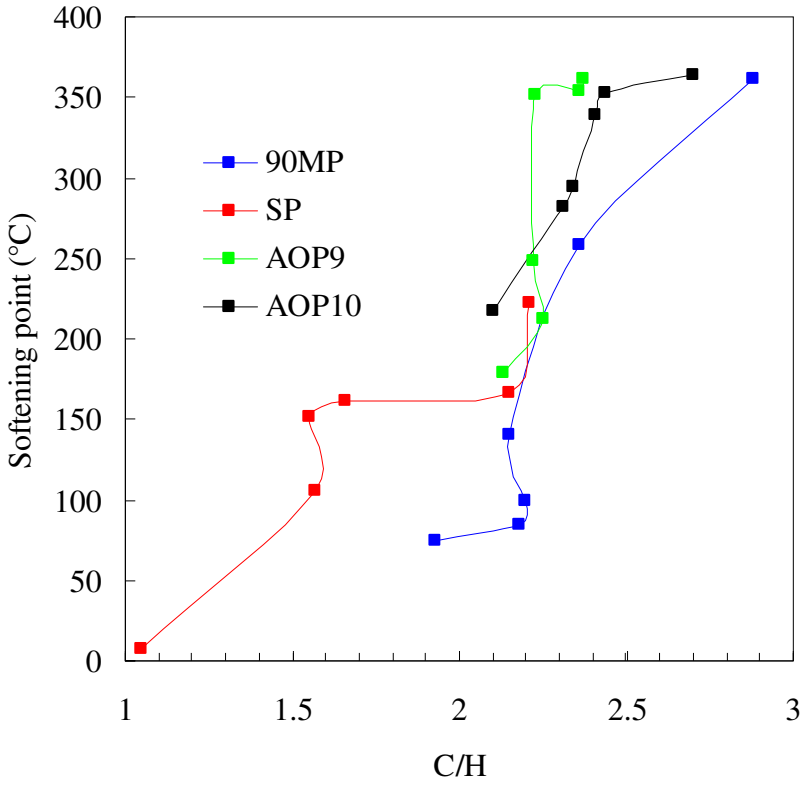

Figure 4.29: Relationship between C/H ratio and softening point temperature (Ts)

Key: MP: Mittal pitch; SP: Sasol pitch; AOP: anthracene oil pitch; 9 and 10 are just numbers used to differentiate between the two AOPs; each line represents members of the pyrolysis series for each pitch studied.

Figure 4.29 illustrates that the softening point temperature (Ts) of all the pitches studied increase as the C/H ratio increases. The above relationship shows the dependence of softening point temperature on the aromaticity of the system.

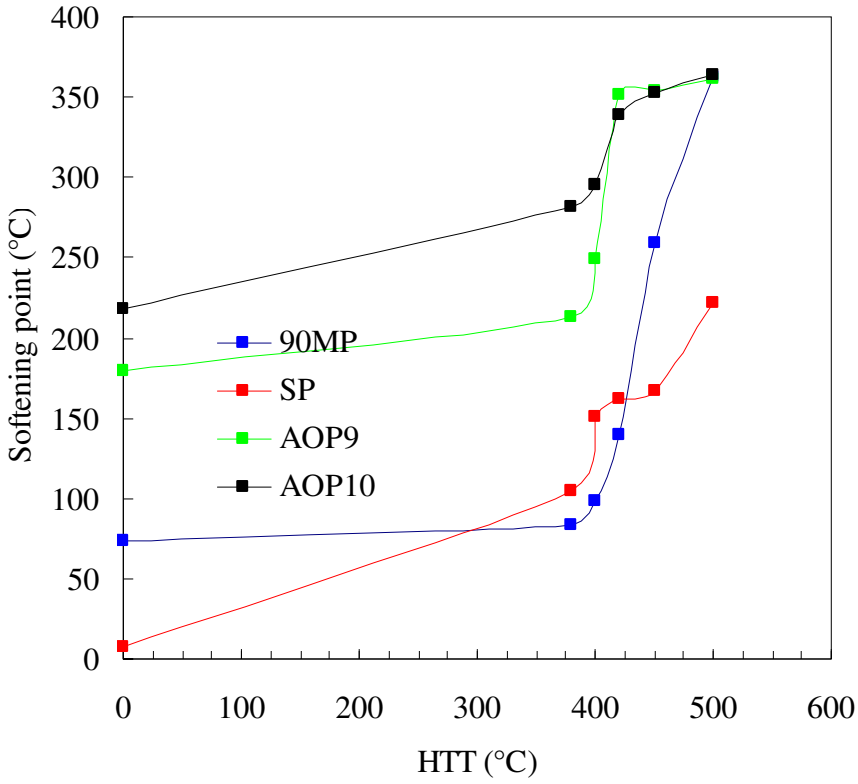

Figure 4.30: Change in softening point temperature with heat-treatment temperature (HTT)

Key: MP: Mittal pitch; SP: Sasol pitch; AOP: anthracene oil pitch; 9 and 10 are just numbers used to differentiate between the two AOPs; HTT: heat-treatment temperature. Note: the softening point temperatures where x equals zero are for the as-received materials; each line represents members of the pyrolysis series for each pitch studied.

Figure 4.30 shows the relation between the softening point temperature (Ts) and the heat-treatment temperature (HTT). It indicates that the dependence of Tg on HTT is more or less similar to that of the glass transition temperature, the C/H ratio and the release of volatiles. At the reaction temperatures used, the softening point temperatures of the AOPs are higher than those of SP and 90MP. The AOPs are expected to be more viscous at these reaction temperatures. These observations corroborate those made regarding the glass transition temperature. The softening point temperature of 90MP rises rapidly from 450 to 500°C, probably because the mesophase reaches the solidification stage where viscosity approaches the maximum.

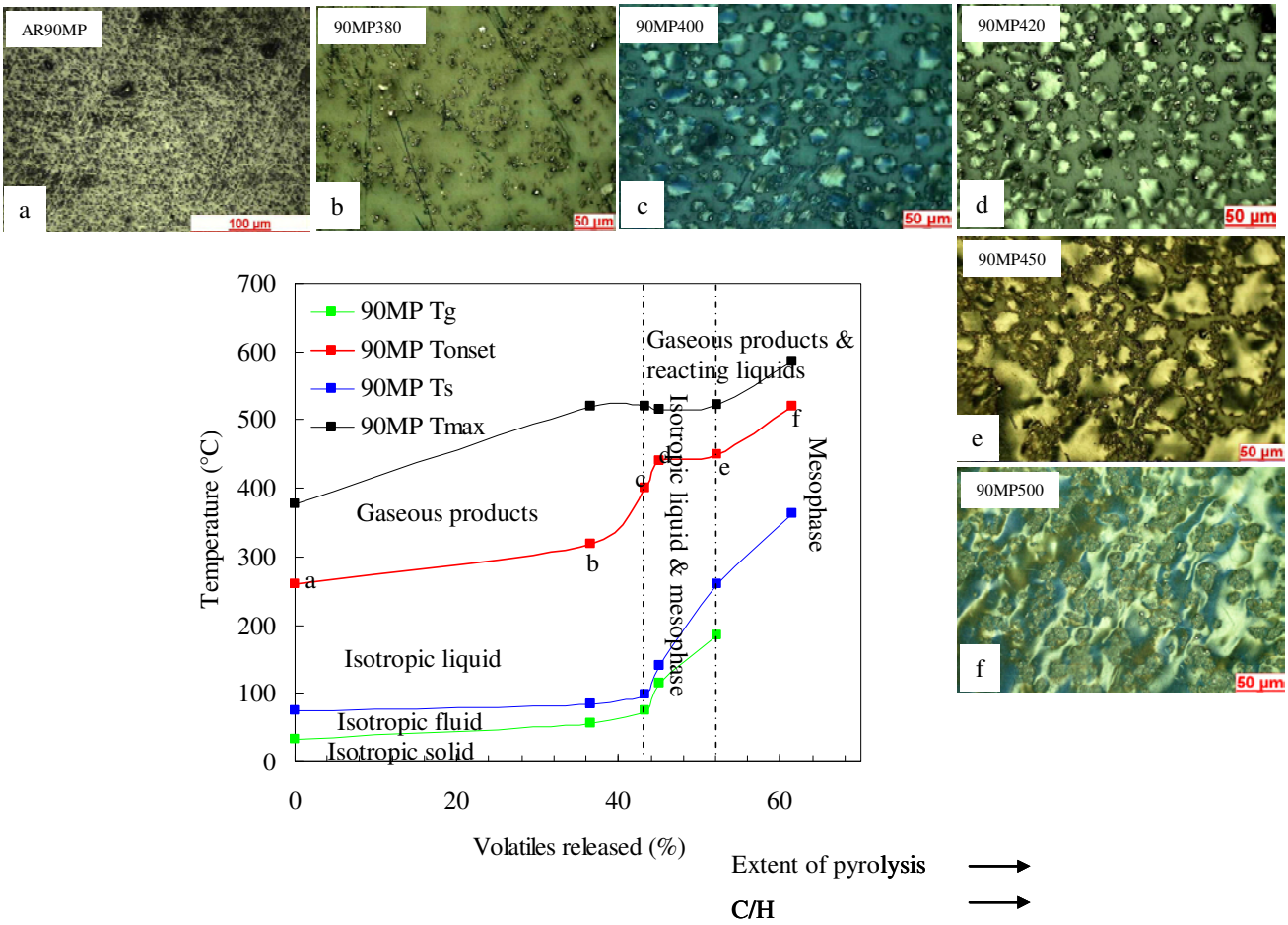

Figure 4.31: Schematic transformation diagram for 90MP undergoing thermal pyrolysis to green coke

Key: MP: Mittal pitch; Tg: glass transition temperature; T_{onset}: mass loss onset temperature; Ts: softening point temperature; T_{max}: temperature of maximum rate of mass loss. Note: the temperature points where x equals zero are for the as-received materials.

Figure 4.31 presents a diagram of volatiles released against different characteristic temperatures. The volatiles released have a positive correlation with the C/H ratio. Therefore the characteristic temperatures are also related to the C/H ratio and the extent of pyrolysis. This figure summarises the transformation diagrams discussed above. It provides more information than just the relationship between two particular parameters presented earlier. It offers an advantage in that it shows the region where the system is isotropic, isotropic plus mesophase, and fully mesophase, and shows what happens to the characteristic temperatures. It also shows the region of gaseous products released and the region where the system is a reacting liquid(s). The region between the T_{onset} and the Tg lines defines the region of stable fluid. The region above the T_{onset} can represent either the gaseous products or the gaseous products plus the reacting liquid. The pictures around the graph give an idea of the region of isotropy and mesophase.

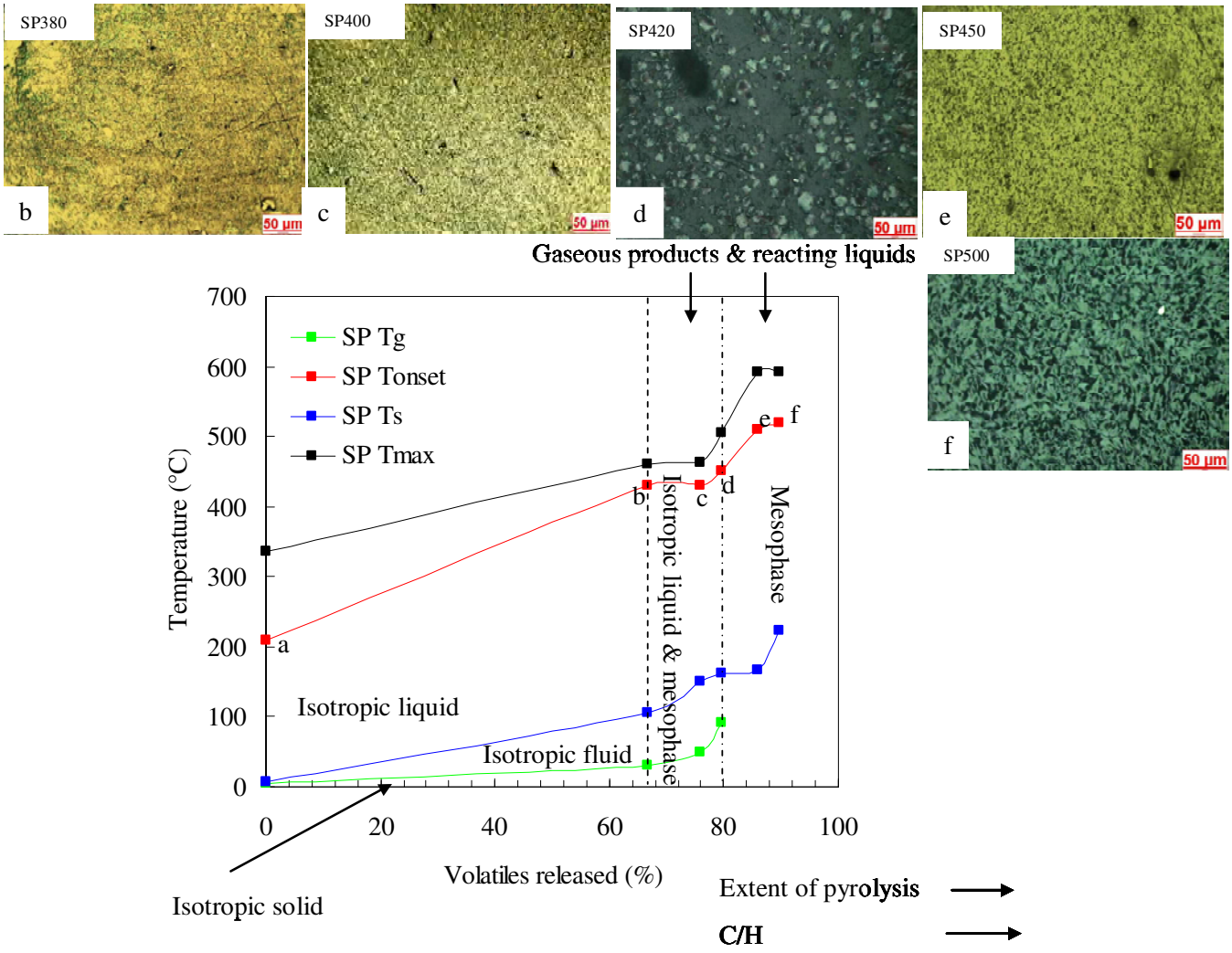

Figure 4.32: Schematic transformation diagram for SP undergoing thermal pyrolysis to green coke

Key: SP: Sasol pitch; Tg: glass transition temperature; T_{onset}: mass loss onset temperature; Ts: softening point temperature; T_{max}: temperature of maximum rate of mass loss. Note: the temperature points where x equals zero are for the as-received materials.

Figure 4.32 gives more or less the same information as the previous figure. They differ with regard to the extent of volatiles released and the corresponding characteristic temperatures. The region of isotropic plus mesophase is also narrow, whereas the complete mesophase occurs over a wider range.

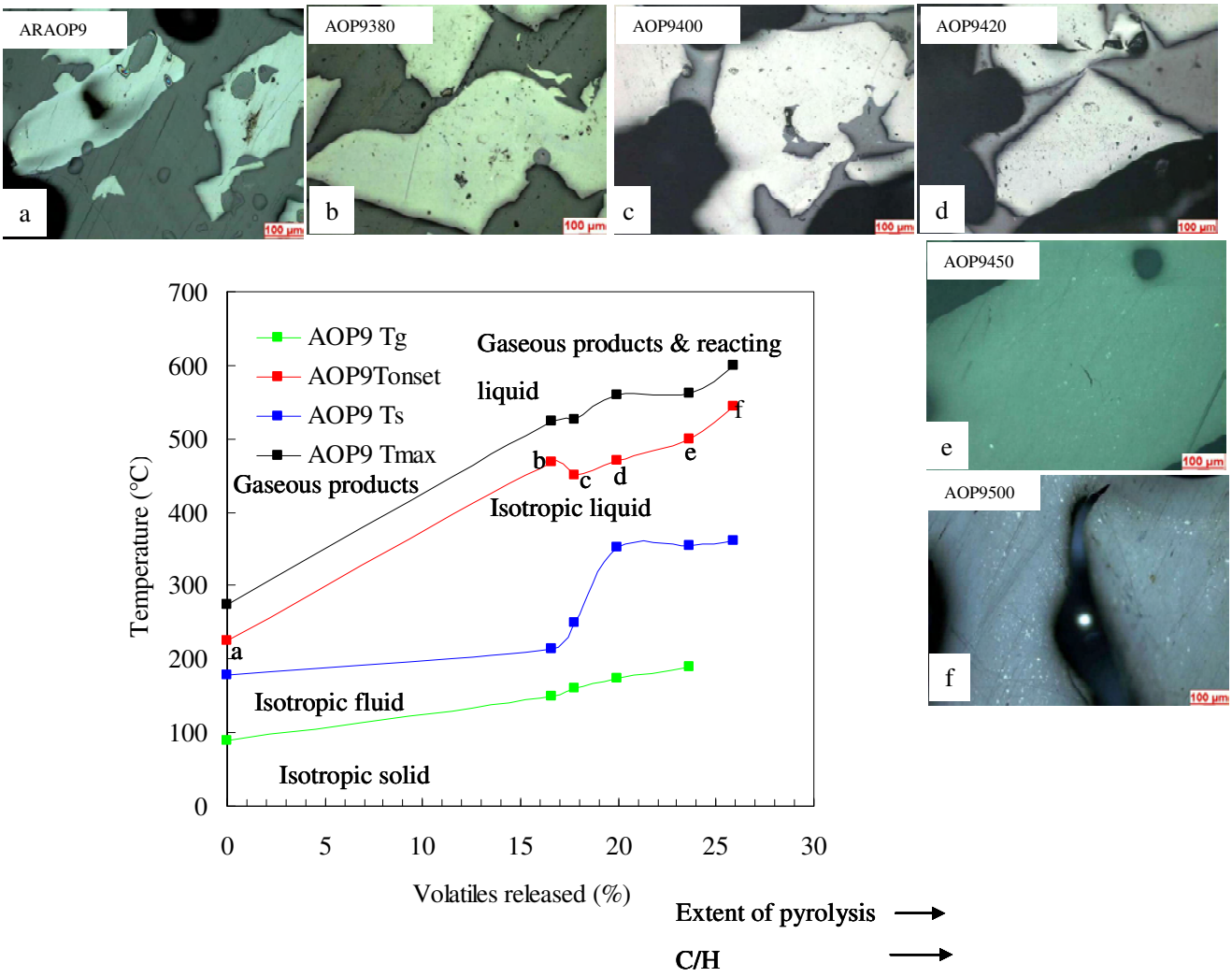

Figure 4.33: Schematic transformation diagram for AOP9 undergoing thermal pyrolysis to green coke

Key: AOP: anthracene oil pitch; 9 is the number used to identify the AOP; Tg: glass transition temperature; T_{onset}: mass loss onset temperature; Ts: softening point temperature; T_{max}: temperature of maximum rate of mass loss. Note: the temperature points where x equals zero are for the as-received materials.

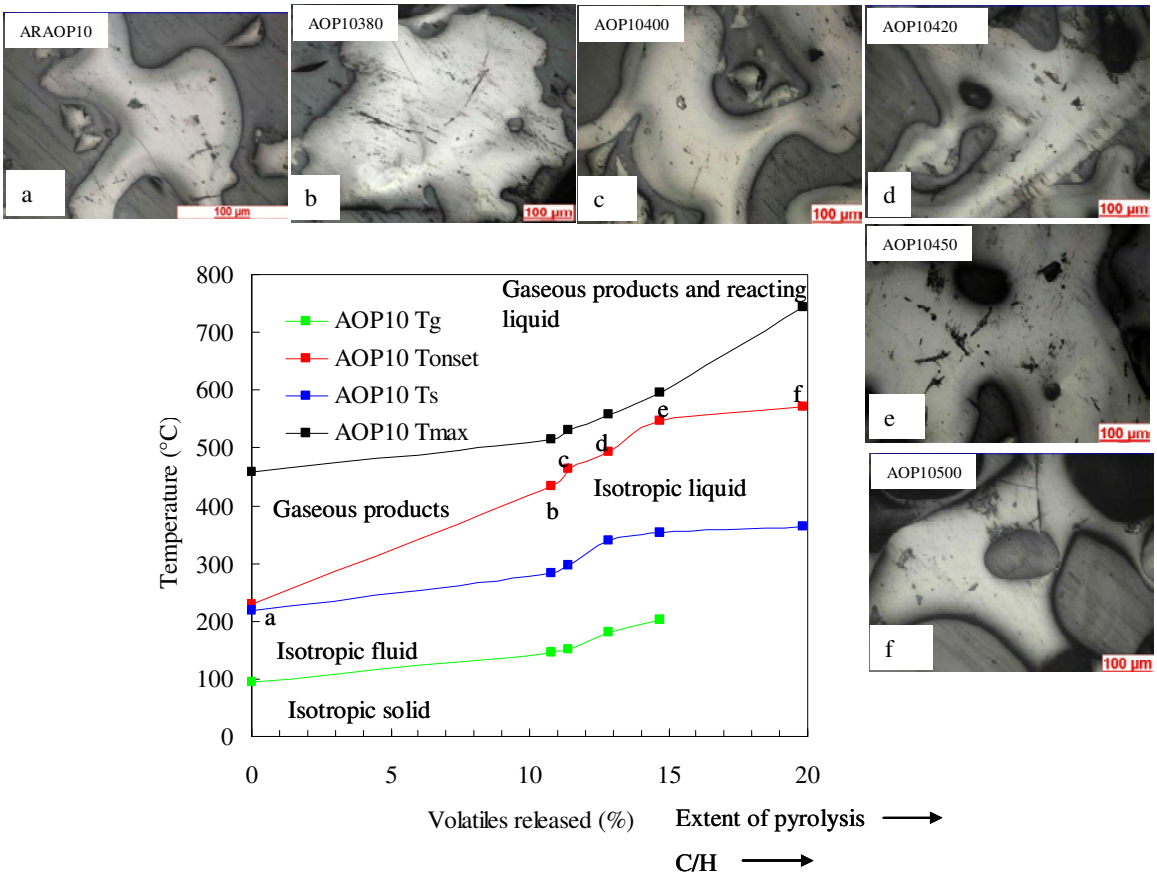

Figure 4.34: Schematic transformation diagram for AOP10 undergoing thermal pyrolysis to green coke

Key: AOP: anthracene oil pitch; 10 is the number used to identify the AOP; Tg: glass transition temperature; T_{onset}: mass loss onset temperature; Ts: softening point temperature; T_{max}: temperature of maximum rate of mass loss. Note: the temperature points where x equals zero are for the as-received materials.

Figures 4.33 and 4.34 illustrate that the AOPs do not have a region of liquid crystal (mesophase), but do have a region of gaseous products and reacting liquid. The isotropic liquid persists up until the end of both the diagrams.

4.14 Summary of Findings from Transformation Diagrams

SP and 90MP differ in their percentages of volatiles released and the corresponding characteristic temperatures. They differ in the region of isotopic, isotropic plus mesophase and fully mesophase. SP is fully mesophase at SP450, whereas 90MP becomes fully mesophase at 90MP500. The AOPs have the isotropic region, gaseous products and gaseous plus reacting liquid, but no mesophase.

CHAPTER 5: CONCLUSIONS

Pitches that develop mesophase have the potential to be future sources of coke and graphitisable carbon. They can be used to manufacture high-performance carbons.

The thermal treatment of pitches results in either isotropic or anisotropic optical texture, depending on the composition of the pitches. The kind of mesophase formed is also dependent on the pitch composition. In this study optical microscopy revealed that only medium-temperature pitch (Sasol pitch – SP) and high-temperature pitch (Mittal pitch – 90MP) develop mesophase. 90MP contains quinoline insolubles (QI) which had a negative impact on coalescence. However, the mesophase did coalesce and eventually formed coarse and needle-coke-like flow domains at 500 °C. SP showed an improvement in texture from the mosaic to the coarse domain at 500 °C, but no flow domains like 90MP. Another major difference between these two pitches is that SP is fully mesophase at between 450 and 500 °C, whereas 90MP only become completely mesophase at 500 °C. There is also a dramatic change in the optical texture of SP from 420 to 450 °C, as opposed to the gradual change observed in 90MP. These results are attributed to the different chemical compositions of the as-received pitches as determined by elemental analysis. SP and 90 MP are both promising starting materials from which high-performance carbon materials can be produced. The most striking feature is the ability of SP to be fully mesophase with a C/H ratio that is nearly equivalent to that of its isotropic 90MP counterpart.

The anthracene oil pitches (AOPs) do not form mesophase and they are therefore are not good carbonisation precursors. They have a high oxygen content which is thought to form cross-links and increase the reactivity of the pitch constituents, resulting in an isotropic product. Their inability to develop mesophase is consistent with the findings reported in the literature. Weinberg *et al*. (1988) found that the pitch should have 2 to 6%wt of oxygen for it to develop mesophase.

The main conclusion is that mesophase formation and development depend on the chemical nature of the as-received material. SP has a high oxygen content and low aromaticity, 90MP has a low oxygen content and high aromaticity, and both the AOPs have high oxygen contents and high aromaticity.

The parameters related to pitch processing, such as carbon yield, initial mass loss temperature, final mass loss temperature and temperature of maximum rate of mass loss, can be determined by thermogravimetric analysis (TGA). The thermal behaviour of the pitch is then related to the pitch composition. TGA showed that the starting materials have various carbon yields as a result of their different percentages of low-molecular-mass species. The carbon yield increased in this order: SP < 90MP < AOP9 < AOP10. SP has the lowest carbon yield. This observation is consistent with its high aliphatic content (low C/H ratio) as determined by Fourier transform infrared (FT-IR) and elemental analysis. As expected, the pitches' respective heat-treatment residues show increased carbon yield (decreased volatile content). In all the heat-treated samples, mass loss onset temperatures occur at higher temperatures than in their respective as-received materials. The shift in mass loss onset temperature, accompanied by the increased carbon yield, shows that the low-molecular-mass species had already evolved during the preceding heat treatment.

The results further indicate that the process of preparing mesophase, i.e. the heat-treatment process, affects the elemental composition and changes the structure of the pitch. This was confirmed by elemental analysis, the most important features being the carbon hydrogen (C/H) ratio (aromaticity) and oxygen content. The system has to be more aromatic with less oxygen to form mesophase. The aromaticity of the system increases with heat treatment, which justifies the formation of mesophase as observed in the optical micrographs. The information given by the micrographs complements that given by infrared spectroscopy about the functional groups and the chemical nature (aromaticity) of the samples and how they change with heat treatment. Structural evolution during heat treatment was followed by FT-IR analysis which also helps to differentiate between the pitches. However, it fails to differentiate between pitches from similar origins (the AOPs). The structure was found to change remarkably in SP, followed by 90MP. This is evidenced by the loss of certain functional groups (mainly aliphatic) and the formation of others (aryl-aryl/aryl-alkyl ether band). The FT-IR analysis of SP shows a more pronounced loss of aliphatic content as the heat treatment progresses.

Additional data about the evolution of different volatile products was obtained by thermogravimetric mass spectroscopic analysis (TG/MS). This shows that the pitches undergo different chemical reactions during thermal decomposition, as seen by the timing and extent of the evolution of certain species. For example, H_2O, CO_2 and CH_4 do not evolve at the same temperature for all the pitches. H_2 and CO also evolve to different extents. The dominant reaction among all the pitches is the condensation reaction, which is accompanied by the evolution of H_2 and CO.

The as-received materials and heat-treated materials were also investigated using thermogravimetric analysis (TMA). This technique was used to determine the glass transition temperatures and softening point temperatures, which were found to increase with heat treatment and hence to be related to the changes in the compositional and structural characteristics of the materials through the carbonisation process. They were found to have direct proportionality with the aromaticity of the system.

All the techniques used in this study gave complementary insights into the processes occurring during mesophase formation. Possible processes in the pyrolysis of pitch have been given in the transformation diagrams in this dissertation. They indicate the interrelationships between different parameters and thus give a more detailed picture of the processes taking place during mesophase formation and development.

REFERENCES

Alciaturi, C. E., Escobar, M. E. and Vallejo, R. (1996). Prediction of coal properties by derivative DRIFT spectroscopy. *Fuel*, *75*(4): 491-499.

Arenillas, A. and Rubiera F., Pis, J.J. (1999). Simultaneous thermogravimetric–mass spectrometric study on the pyrolysis behaviour of different rank coals. *J. Anal. Appl. Pyrolysis, 50*: 31–46.

Barr, J. B and Lewis, I. C. (1982). Characterisation of pitches by differential scanning calorimetry and thermomechanical analysis. *Thermochimica Acta, 52*: 297-304.

Bartle, K. D., and Özel, Z. M. (2002). Production of mesophase pitch from coal tar and petroleum pitches using Supercritical Fluid Extraction. *Turk. J. Chem., 26*: 417-424.

Benn, M. (1989). *Pitch-mesophase-carbon Transformation Diagrams and the Fabrication of Carbon Materials.* PhD thesis, University of Sheffield, England.

Bermejo, J., Granda, M., Menéndez, R and Tascón, J. M. D. (1994). Comparative analysis of pitches by extrography and thermal analysis technique. *Carbon*, *32*(5): 1001-1010.

Bonnamy, S. (1999). Carbonization of various precursors. Effect of heating rate Part I: Optical microscopy studies *Carbon 37*: 1691–1705.

Brooks, J. D. and Taylor, G. H. (1965). The formation of graphitising carbons from the liquid phase. *Carbon, 3*(2): 185-186.

Brown, M. E. (1988). *Introduction to Thermal Analysis: Techniques and Applications*. London: Chapman and Hall.

Brzozowska T., Zieliński J, and Machnikowski, J. (1998). Effect of polymeric additives to coal tar pitch on carbonisation behaviour and optical texture of resultant cokes. *J. Anal. Appl. Pyrolysis, 48*: 45–58

Chang, C. F. and Lewis, L. C. (1998). *Proceedings of the International Carbon Conference,* Strasbourg, France, pp 39-40.

de Castro, L. D. (2006). Anisotropy and mesophase formation towards carbon fibre production from coal tar and petroleum pitches - a review. *J. Braz. Chem. Soc, 17*(6).

Dumont, M., Dourges M. A., Bourrat X., Pailler R., Naslain R., Babot O., Birot, M., and Pillot J.P. (2005). Carbonisation behaviour of modified synthetic mesophase pitches. *Carbon 43*: 2277–2284

Fanjul, F., Granda, M., Santamaría, R., Bermejo, J. and Menéndez, R. (2001). Assessment of the oxidative stabilisation of carbonaceous mesophase by thermal analysis techniques. *J. Anal. Appl. Pyrolysis, 58–59*: 911–926.

Fifield, F. W and Kealey, D. (1995). *Principles and Practice of Analytical Chemistry*, 4th edition. Glasgow: Blackie Academic and Professional.

Fitzer, E., Kochling, K. H., Boehm, H. P. and Marsh, H. (1995). *IUPAC Recommendations. Recommended Terminology for the Description of Carbon as a Solid.*

García, R., Arenillas, A., Crespo J. L., Pis, J. J and. Moinelo, S. R. (2002). A comparative Tg-Ms study of the carbonisation behavior of different pitches. *Energy & Fuels, 16*: 935-943.

Grzyb, B., Machnikowski, J., and Weber, J. V. (2004). Mechanism of co-pyrolysis of coal tar pitch with polyvinylpyridine. *J. Anal. Appl. Pyrolysis*, *72*: 121-130.

Guillén, M. D., Iglesias, M. J., Domínguez, A. and Blanco, C. G. (1995). Fourier transform infrared study of coal tar pitches. *Fuel*, *74*(11): 1595-1598.

Günzler, H. and Gremlich, H. (2002). *IR Spectroscopy: An Introduction*, Weinheim, Germany: Wiley-VCH Verlag GmbH.

Haines, P. J. (1995). *Thermal Methods of Analysis; Principles, Applications and Problems*. Glasgow: Blackie Academic and Professional.

Hurt, R. H. and Hu, Y. (1999). Thermodynamics of carbonaceous mesophase *Carbon*, *37*(2): 281-292.

Imamura, T., Nakamiso, M., and Honda, H. (1978). Formation of carbonaceous mesophase at lower temperature. *Carbon 16*: 487-490

Khandare, P. M, Zondlo, J. W and Pavlovic, A. S. (1996). The measurement of the glass transition temperature of mesophase pitches using a thermomechanical device. *Carbon, 34*(5): 663-669.

Lewis, I. C. and Kovac, C .A. (1977). The role of free radicals and molecular size in mesophase pitch. *Carbon, 16*(6): 425-429.

Lim, Y and Lee, B.I. (1993). Enhanced mesophase formation of petroleum pitch by polyaromatic hydrocarbon addition. *Journal of materials science, 28*: 3741-3748.

Machnikoski, J., Machnikoska, H., Brzozowska, T. and Zieliński, J. (2002a). Mesophase development in coal tar pitch modified with various polymers. *J. Anal. Appl. Pyrolysis, 65*: 147-160.

Machnikowski, J., Kaczmarska, H., Gerus-Piaseckaa, I., Díezb, M. A., Alvarezb, R. and García, R. (2002b). Structural modification of coal-tar pitch fractions during mild oxidation – Relevance to carbonisation behavior. *Carbon, 40*: 1937–1947.

Markovic, V and Marsh, H. (1983). Microscopic techniques to examine structure in anisotropic cokes. *J. Microscopy*, *132*(3): 345-352.

Marsh, H., Lantham, C.S. and Gray, E.M. (1985). The structure and behaviour of QI material in pitch. *Carbon 23*(5): 555-570.

Marsh, H. and Menéndez, R. (1988). Carbons from pyrolysis of pitches, coals and their blends. *Fuel Process. Technol., 20*: 269-296.

Marsh, H. (1989). *Introduction to Carbon Science.* London: Butterworth.

Marsh, H. and Rodriques-Reinoso, F. (2000). *Sciences of Carbon Materials*, Publicaciones de la Universidad de Alicante.

Marsh, H. and Walker, P. L. (1979). In: Walker, P. L. Jr and Thrower, P. A. (Eds). *Chemistry and Physics of Carbon*, 15, New York: Marcel Dekker.

Marsh, H., Martínez-Escandell, M. and Rodríguez-Reinoso, F. (1999). Semicokes from pitch pyrolysis: Mechanisms and kinetics. *Carbon*, *37*(3): 363-390.

Martínez-Alonso, A., Bermejo, J. and Tascón, J. M. D., (1992). Thermoanalytical studies of pitch pyrolysis: Comparison with polycyclic aromatic hydrocarbons. *J. Therm. Anal., 38*: 811-820.

Martínez-Escandell, M., Torregsa, P., Marsh, H., Rodríguez-Reinoso, F., Santamaría-Ramírez, R., Gómez-De-Salazar, C. and Romero-Palazón, E. (1999). Pyrolysis of petroleum residues. I. Yields and product analyses. *Carbon*, *37*(10): 1567-1582.

Menéndez, R., Granda, M., and Bermejo, J., (1997). Relationships between pitch composition and optical texture of cokes. *Carbon 35*(4): 555-562.

Metzinger, Th. and Hüttinger K. J. (1997). Investigations on the cross-linking of binder pitch matrix of carbon bodies with molecular oxygen. Part I. Chemistry of reactions between pitch and oxygen. *Carbon*, *35*(7): 885-892.

Mianowski, A., Blazewicz, S. and Robak, Z. (2003). Analysis of the carbonization and formation of coal tar pitch mesophase under dynamic conditions. *Carbon, 41*(12): 2413-2424.

Mochida, I., Yoon, S and Qiao, W. (2006). Catalysts in Syntheses of Carbon and Carbon Precursors. *J. Braz. Chem. Soc.,17*(6): 1059-1073.

Mochida, I., Korai, Y., Ku, C., Watanabe, F. and Sakai, Y. (2000). Chemistry of synthesis, structure, preparation and application of aromatic-derived mesophase pitch. *Carbon*, *38*(2): 305-328.

Mochida, I., Sone, Y., and Korai, Y. (1985). Preparation and properties of carbonaceous mesophase-II highly soluble mesophase from ethylene tar modified using aluminum chloride as a catalyst. *Carbon, 23*(2): 175-178.

Mochida, I., Maeda, K. and Takeshita, K. (1977). Structure of anisotropic spheres obtained in the course of needle coke formation. *Carbon, 15*(1): 17-23.

Mochida, I., Shimizu, K., Korai, Y., Otsuka H. and Fujiyama, S. (1988). Structure and carbonization properties of pitches produced catalytically from aromatic hydrocarbons with HF/BF_3. *Carbon, 26(*6): 843-852.

Mokoena, K., Van der Walt, T. J., Morgan, T. J., Herod, A. A. and Kandiyoti, R. (2008). Heat treatment of medium-temperature Sasol–Lurgi gasifier coal-tar pitch for polymerizing to higher value products. *Fuel, 87*(6): 751-760.

Mrozowski, S. (1954). Mechanical strength, thermal expansion and structure of cokes and carbons. *Proceedings of the Conference on Carbon,* University of Buffalo, Buffalo, New York.

Oberlin, A. (1984). Carbonization and graphitisation. *Carbon, 22*(6): 521-541.

Pérez, M., Granda, M. García, R., Santamaría, R., Romero, E. and Menéndez, R. (2002). Pyrolysis behaviour of petroleum pitches prepared at different conditions. *J. Anal. Appl. Pyrolysis*, *63*(2): 223-239.

Pierson, H. O. (1993). Handbook of Carbon, Graphite, Diamond, and Fullerenes: Properties, Processing, and Applications, Published by William Andrew Inc.

Rand, B., Appleyard, S. P. and Yardim, M. F. (1998). *Design and Control of Structure of Advanced Carbon Materials for Enhanced Performance. Series E: Applied Sciences*. Dordrecht/Boston/London: Kluwer Academic Publishers, p. 374.

Riggs, D. and Diefendorf, R. D. (1980). Forming optically anisotropic pitches. *US Patent 4 208 267*.

Romovacek, G. R., McCullough, J.P. and Perrotta, A. J. (1983). Formation of mesophase in coal tar pitches. Influence of pyrolytic carbon particles. *Fuel, 62*(10): 1236-1238.

Ruland, W. (1965). X-ray studies on the carbonisation and graphitisation of acenaphthylene and bifluorenyl, *Carbon, 2*: 365 – 378.

Sima, L., Blanco, C., Santamaría, R., Granda, M., Slaghuis, H. and Menéndez R. (2003). Relationship between chemical composition and pyrolysis behaviour of a medium temperature pitch (or Lurgi-gasifier pitch). *Fuel Process. Technol., 84*(1-3): 63-77.

Singer, L S. (1985). The mesophase in carbonaceous pitches. *Faraday Discuss. Chem. Soc., 79*: 265-272

Stuart, B. (2004). *Infrared Spectroscopy: Fundamentals and Application*. Chichester, UK: Wiley.

Tillmans, H., Pietzka, G. and Panals, H. (1978). Influence of the quinoline-insoluble matter in pitch on carbonization behaviour and structure of pitch coke. *Fuel, 57*(3): 171-173

Wang, Y., Korai, Y., Mochida, I., Nagayama, K., Hatano, H. and Fukuda, N. (2001). Modification of synthetic mesophase pitch with iron oxide Fe_2O_3. *Carbon 39*: 1627-1634.

Weinberg, V. L., Sadeghi., M. and Yen, T. F. (1998). Treatment of carbonaceous materials. *US patent: 4 773 985.*

Wendlandt, W. W. (1986). *Thermal Analysis,* 3rd edition. New York: Wiley.

Whitehouse, S. and Rand, B. (1982). Pitch-coke Interactions. *Proc. 16th Biennial Conference on Carbon (Carbon '82)*, Elsevier.

wikipedia.org/wiki/Elementalanalysis

wikipedia.org/wiki/Mesogen

Xie, W. and Pan, W. P. (2001). Thermal characterization of materials using evolved gas analysis. *J. Therm. Anal. Cal., 65*: 669-685.

Yang, J. P., Stansberry, G., Zondlo, J. W., and Stiller, A. H. (2002). Characteristics and carbonisation behaviors of coal extracts. *Fuel Process. Technol., 79*(3): 207-215.

Zimmer, J. E. and White, J. L. (1982). "Disclination Structures in Carbonaceous Mesophase", in: *Advances in Liquid Crystals*, Vol. 5, Ed. G. H. Brown (Academic Press, New York) 157.

APPENDIX A

Table A1: Carbon yield of pitches at 1 000 °C under nitrogen, at 10 °C.min^{-1}

Sample ID	Carbon yield (%)
ARAOP10	67.5
AOP10, 380	79.7
AOP10. 400	80.26
AOP10, 420	82.07
AOP10, 450	86.2
AOP10, 500	89.0

Table A2: Carbon yield of ARAOP9 and heat-treated samples at 1 000 °C under nitrogen at 10 °C.min^{-1}

Sample ID	Carbon yield (%)
ARAOP9	48
AOP9, 380	78
AOP9, 400	80
AOP9, 420	83
AOP9, 450	84
AOP9, 500	88

Table A3: Carbon yield of AR90MP and heat-treated samples at 1 000 °C under nitrogen, at 10°C.min^{-1}

Sample ID	Carbon yield (%)
AR90MP	32
90MP380	61
90MP400	66
90MP420	77
90MP450	90
90MP500	96

Table A4: Carbon yield of ARSP and heat-treated samples at 1 000 °C under nitrogen, at 10 °C.min^{-1}

Sample ID	Carbon yield (%)
ARSP	9
SP380	56
SP400	64
SP420	82
SP450	89
SP500	89

Table A5: Mass changes in MP during heat treatment under nitrogen, at 10 °C.min^{-1}

Sample ID	Mass (g) before HTT	Mass (g) after HTT	Yield (%)	Volatiles released (%)
90MP380	2.24	1.43	63.38	37
90MP400	2.77	1.57	56.68	43
90MP420	2.37	1.30	54.85	45
90MP450	2.34	1.12	47.86	52
90MP500	2.39	0.92	38.49	62

Table A6: Mass changes in SP during heat treatment under nitrogen, at 10 °C.min^{-1}

Sample ID	Mass (g) before HTT	Mass (g) after HTT	Yield (%)	Volatiles released (%)
SP380	2.44	0.81	33.2	67
SP400	2.23	0.54	24.22	76
SP420	2.11	0.43	20.38	80
SP450	2.51	0.35	13.94	86
SP500	2.35	0.24	10.21	90

Table A7: Mass changes in AOP9 during heat treatment under nitrogen, at 10 °C.min^{-1}

Sample ID	Mass (g) before HTT	Mass (g) after HTT	Yield %)	Volatiles released (%)
AOP9, 380	2.04	1.71	83.38	17
AOP9, 400	2.31	1.90	82.23	18
AOP9, 420	2.22	1.78	80.02	20
AOP9, 450	2.33	1.78	76.39	24
AOP9, 500	2.24	1.66	74.12	26

Table A8: Mass changes in AOP10 during heat treatment under nitrogen, at 10 °C.min^{-1}

Sample ID	Mass (g) before HTT	Mass (g) after HTT	Yield (%)	Volatiles released (%)
AOP10, 380	2.51	2.24	89.24	11
AOP10, 400	2.19	1.94	88.58	11
AOP10, 420	2.41	2.10	87.14	12
AOP10, 450	2.25	1.92	85.33	15
AOP10, 500	2.42	1.94	80.17	20

Table A9: **Values of glass transition temperature (Tg), softening point (Ts), mass loss onset temperature (T_{onset}) and mass loss endset temperature (T_{endset}) of the as-received and heat-treated materials**

Sample ID	T_{onset}	T_{endset}	Tg	Ts	Tmax
AR90MP	260	520	32	74	376
90MP380	318	553	56	84	519
90MP 400	400	541	74	99	520
90MP 420	440	565	114	127	515
90MP 450	450	682	185	259	522
90MP 500	520	887	N/A	362	586

Sample ID	T_{onset}	T_{endset}	Tg	Ts	Tmax
ARSP	210	475	4	7	336
SP380	430	552	31	105	460
SP400	430	583	49	151	462
SP420	450	718	91	162	505
SP450	510	883	N/A	167	591
SP500	520	889	N/A	222	591

Sample ID	T_{onset}	T_{endset}	Tg	Ts	Tmax
ARAOP, 10	230	630	95	218	459
AOP10, 380	435	682	145	282	515
AOP10, 400	462	707	152	295	531
AOP10, 420	493	737	180	339	558
AOP10, 450	548	808	201	353	594
AOP10, 500	571	842	N/A	364	744

Sample ID	T_{onset}	T_{endset}	Tg	Ts	Tmax
ARAOP9	225	649	89	179	275
AOP9, 380	469	689	150	213	524
AOP9, 400	450	717	160	249	526
AOP9, 420	471	804	174	352	559
AOP9, 450	500	807	189	354	561
AOP9, 500	543	825	N/A	361	600

Table A10: Correlation coefficients obtained from the graph of the glass transition temperature and softening point

Sample ID	Correlation coefficient
90MP	0.9609
AOP9	0.7399
AOP10	0.9907
SP	0.7789